Technical Report Documentation Page

1. Report No. Research Report RC-1484	2. Government Accession No.	3. MDOT Project Manager Roger Till
4. Title and Subtitle High Performance Material for Rapid Durable Repair of Bridges and Structures		5. Report Date December 20, 2006
7. Author(s) Victor C. Li (Principal Investigator), Mo Li and Michael Lepech		6. Performing Organization Code
9. Performing Organization Name and Address The Advanced Civil Engineering Material Research Laboratory Department of Civil and Environmental Engineering University of Michigan, Ann Arbor, MI 48109-2125, U. S. A		8. Performing Org Report No. UM-06-10
12. Sponsoring Agency Name and Address Michigan Department of Transportation Construction and Technology Division P.O. Box 30049 Lansing, MI 48909		10. Work Unit No. (TRAIS) 11. Contract Number: Master Contract #03-0026 11(a). Authorization Number: Work Auth #4
15. Supplementary Notes		13. Type of Report & Period Covered Oct. 13, 2004 – Oct. 13, 2006 14. Sponsoring Agency Code

16. Abstract

The research presented herein describes the development of High Early Strength Engineered Cementitious Composites (HES-ECC) under the guidance of micromechanical models for concrete bridges & structures repair applications. HES-ECC can achieve high early age compressive strength of around 3400 psi at 4h, 5000 psi at 6h, 6000 psi at 24h, and high late age compressive strength of around 7000 psi at 7d, 8000 psi at 28d, and 8200 psi at 60d. It also has high tensile strain capacity of more than 3% and toughness indicated by multiple micro-cracking behavior under uniaxial tensile loading. Besides material durability, HES-ECC can greatly improve durability and load carrying capacity of a simulated layered repair system. Experimental study showed that when subject to monotonic flexural loading, HES-ECC layered repair system exhibited 100% increased load carrying capacity, and 10 times the deformation capacity compared with HES-Concrete layered repair system. When under the same level of fatigue flexural loading, HES-ECC layered repair system showed significantly prolonged service life. In addition, the high ductility of HES-ECC relieved shrinkage induced stresses in the HES-ECC repair layer and at the HES-ECC/concrete interface, thereby suppressing large repair surface cracks and interface delamination.

Based on the findings within, the larger scale batching of HES-ECC is applicable by using traditional concrete gravity mixers. The overall mixing of HES-ECC material can proceed smoothly and result in a fresh material which is homogeneous, flowable, and rheologically stable. Testing of hardened mechanical properties of HES-ECC showed that the early age and late age compressive strength and tensile strain capacity were similar to those mixes made in a laboratory size Hobart mixer, and continued to meet all of the targets set forth when developing this material. In this report, the results of larger scale batching (1, 3 and 6 cubic feet) and demonstration are summarized and recommendations are made along with material specifications, mix design and batching sequences for large scale mixing of HES-ECC.

Overall, this project successfully developed a HES-ECC material which is high-early-strength, durable and can be easily applied. This HES-ECC material can be suitable for a wide range of concrete repair applications in transportation infrastructures with significantly shortened down time, greatly improved durability and reduced future maintenance.

17. Key Words HES-ECC, Concrete repair, Strain-hardening, High early strength, Durabiity, Crack width control, Shrinkage, Fatigue	18. Distribution Statement No restrictions. This document is available to the public through the Michigan Department of Transportation.

19. Security Classification (report) Unclassified	20. Security Classification (Page) Unclassified	21. No of Pages	22. Price

Final Report

On

High Performance Material for Rapid Durable Repair of Bridges and Structures

By

Victor C. Li (Principal Investigator), Mo Li and Michael Lepech

The Advanced Civil Engineering Materials Research Laboratory

Department of Civil and Environmental Engineering

University of Michigan, Ann Arbor, MI 48109-2125, U. S. A.

Submitted to

Michigan Department of Transportation

December 20, 2006

Research Sponsor: Michigan Department of Transportation

MDOT Project Manager: Roger Till

Award Reference Number: MDOT Contract No. 2003-0026 Work Authorization #4

Contract Period: October 13, 2004 – October 13, 2006

DISCLAIMER

The contents of this report reflect the views of the authors, who are responsible for the facts and accuracy of the information presented herein. This document is disseminated under the sponsorship of the Michigan Department of Transportation, in the interest of information exchange. The Michigan Department of Transportation assumes no liability for the contents or use thereof.

ACKNOWLEDGEMENTS

The presented research has been sponsored by the Michigan Department of Transportation, which is gratefully acknowledged. The authors thank the Michigan DOT project manager Roger Till and the other members of the MDOT research Advisory Panel for their useful comments, discussions and support.

Table of Contents

1. INTRODUCTION

1.1 Background

A large number of existing concrete structures worldwide, including previously repaired ones, are presently suffering deterioration or distress (Vaysburd et al, 2004). A recent project managed by the Michigan Department of Transportation (MDOT) studied the condition of Michigan's Prestressed Concrete (PC) bridges, and revealed that while most were in fair or better than fair condition, older bridges were showing signs of deterioration, particularly at the ends of I-beam structures (Figure 1.1) (Ahlborn et al, 2002). Cracks and delamination in the prestressed beams could be caused by concrete shrinkage, improper curing of the concrete, water leakage and flow of deicing chemicals from the deck joints, loss of prestress, or inadequate procedure used to prestress the beams. The PC bridges, together with the other deteriorating concrete structures, are in urgent need of repairing or retrofitting, which should address underlying concrete deterioration problems and protect concrete from aggressive environment in the long term. Ultimately, repairs should last.

There is an increasing demand for durable high early strength or rapid hardening concrete materials in repair and retrofit practices where minimum traffic disruption is preferred. For instance, highway transportation authorities often require the repair job to be completed in 6-8 hours at night such that the lane can be re-opened to traffic the next morning. This requires the repair material to gain strength fast enough at the early age. In the past two decades, intensive experimental investigations carried out by both academic and industrial groups have led to successful formulation of concrete mixes that can attain sufficient compressive and flexural strengths at very early age. With various early strength development rates, these concrete mixes obtain high early strength by using either proprietary rapid hardening cements (Seehra et al., 1993; Knofel and Wang, 1994; Whiting and Nagi, 1994; Sprinkel, 1998; Balaguru and Bhatt, 2000) or normal Portland cement together with accelerating admixtures (Parker and Shoemaker, 1990; Kurtz et al., 1997; Anderson et al., 2003).

However, structural repairs based on these traditional concrete mixes are often perceived to lack both early age performance and long-term durability due to the inherent brittleness and susceptibility to fracture of the repair material. It has been estimated that

almost half of all concrete repairs fail in field (Mather and Warner, 2003). Premature deterioration is more common in repair sites where high early strength concrete is used [Soroushian and Ravanbakhsh, 1999]. Early age cracking can be widely observed, which is associated with the internal stresses caused by higher internal temperature related to the rapid strength gain, early age shrinkage, high elastic modulus, and lack of curing time. Reduced freeze-thaw resistance and corresponding disintegration were also found in some high early strength concrete mixes (Whiting and Nigi, 1994). Cracking and disintegration can expedite the penetration of chlorides, oxygen, moisture, alkali or sulphates into the repaired system and accelerate further deterioration. Furthermore, the loss of structural integrity impairs load transfer between the repair and the concrete substrate. As a result, the repaired structure with unsatisfactory performance and unexpectedly short life must be further maintained or repaired again, which leads to significantly increased service life cost.

A number of recent studies have indicated that Engineered Cementitious Composites (ECC) show promise in serving as excellent repair materials for concrete structures. ECC is a special type of high performance fiber reinforced cementitious composites (HPFRCC) featuring significant tensile ductility and moderate fiber volume fraction (typically 2%). The design of ECC is guided by micromechanics models, which provide quantitative links between composite mechanical behavior and the properties of the individual phases, i.e., fiber, matrix and interface (Li, 1998). Utilizing the models, the desired high tensile ductility, which is achieved by strain-hardening and multiple cracking, is converted to a set of constraints on individual component properties. These components, i.e. the fiber, the matrix and the interface, are then synergistically tailored to meet the constraints. The high ductility of ECC, achieved by its multiple micro-cracking behavior, is the foremost repair material property to ensure the durability of repaired concrete bridges and structures (Lim and Li, 1997; Wang et al 1997; Weimann and Li, 2003; Li, 2004; Lepech et al, 2004).

Based on the above discussion, high early strength and good ductility are most desirable repair material properties. Conventional ECC mix uses Type I ordinary Portland cement (OPC), which shows relatively slow strength development. Therefore,

a new version of ECC with high early strength is needed to be developed for various concrete repair applications.

Figure 1.1: Illustration of durability problems in prestressed concrete structures (Photographs courtesy of Roger Till, Ahlborn et al, MDOT report, 2002)

1.2 Goal and Impact

The goal of this research is to develop a high early strength engineered cementitious composite (HES-ECC) that is suitable for a wide range of concrete repair applications in transportation infrastructures. To achieve this goal a number of requirements must be met. These include designing the material based on micromechanics to achieve the target early strength and large tensile strain capacity, and experimentally documenting these properties. Shrinkage properties including free shrinkage deformation and restrained shrinkage cracking must also be tested and documented, since shrinkage is the foremost factor which can cause repair early age cracking and initiate the deterioration process. Additionally, layered repair system using the HES-ECC as the repair layer and old concrete as the substrate must be investigated for its durability in term of repair cracking and repair/old interface delamination under restrained shrinkage. Furthermore, a similar layered repair system must be tested under monotonic/fatigue loading conditions for its behavior in terms of reflective cracking, interface delamination, load carrying capacity, deformation capacity, and fatigue life. By this means, the performance of HES-ECC repair can be justified under both environmental loading and mechanical loading conditions. Finally, the laboratory mixing quantities and batching procedures of HES-ECC must be scaled up and proven effective in typical construction site equipment, i.e. gravity mixers. The ultimate goal of this research project is to provide MDOT an engineered material that contributes to fast repairs that last.

This research program directly addresses the needs of MDOT as specified in the 11/30/99 MDOT document entitled “Strategic Research Program for the Next Five Years – Bridges and Structures”. Specifically, this research program addresses item 7 (High performance concrete including, but not limited to high durability, early strength gain, low permeability, and low shrinkage), item 23 (Develop rapid repair and replacement construction procedures that have less impact on the traveling public), and item 24 (Investigate the viability of high performance materials to be used in bridges and highway structures for more efficient designs) of this document. The high early strength,

ductile ECC material is expected to significantly improve the durability of service life of existing concrete bridges and structures.

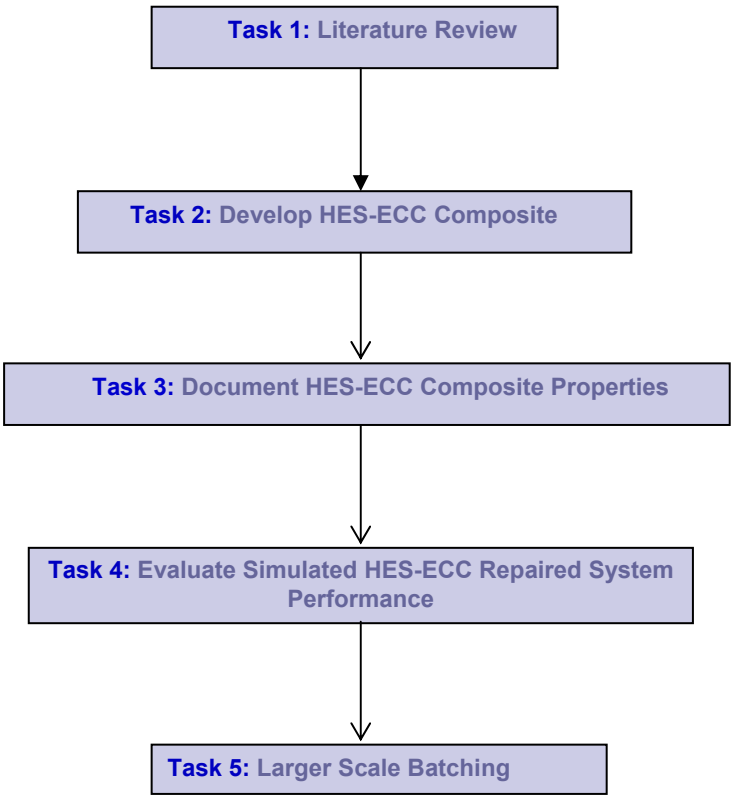

Figure 1.2: Overall research plan flow chart

1.3 Overview

This project is divided into 5 tasks as shown in the overall research plan flow chart (Figure 1.2). In section 2, literature review (task 1) was made on the requirements of high early strength by FWHA and various DOTs in the US, currently used methods to obtain concrete material high early strength, and ECC design philosophy and criteria. In section 3, target HES-ECC properties were set based on the literature review in section 2, and MDOT requirements for repair applications. Then the HES-ECC material was designed to meet the target compressive strength, tensile strain capacity, and workability requirements (task 2). In section 4, task 3 was carried out to document composites properties of the developed HES-ECC material. Extensive experimental work was

conducted to measure HES-ECC compressive strength, flexural strength, tensile strength, tensile strain capacity, shrinkage strain, and restrained shrinkage cracking from the age of 4 hour to 60 days. In section 5, performance of a simulated HES-ECC repaired system was investigated under both environmental (shrinkage) and mechanical (monotonic bending, fatigue bending) loading conditions, and compared with HES-Concrete and HES-FRC (High Early Strength Fiber Reinforced Concrete) repaired systems (task 4). In section 6, larger scale batching of HES-ECC was done using a gravity mixer with a capacity of about 9 cubic feet (task 5). Batch sizes of 1, 3 and 6 cubic feet were adopted, and specimens made from these batches were tested for their compressive and tensile properties. Documentation on quality control and construction specification were included.

2. LITERATURE REVIEW (TASK 1)

2.1 High Early Strength Requirements

Repair material strength gain rate at the early age determines when the repaired structure can be opened to traffic. Different repair applications may have different strength requirements at different ages. For example, large deck patches are typically given a 24-hour curing; small deck patches generally use fast setting mortar to open traffic after a number of hours; and for prestressed concrete beam ends repairs, both the early age strength and the 28 days strength are normally specified. To be suitable for various repair applications, the HES-ECC developed must meet the minimum strength requirements at both the early and late ages.

The requirements of high early strength in terms of compressive strength and/or flexural strength of various DOTs in the US were reviewed. Currently, there is no existing standard for minimum high early strength requirements. The California Department of Transportation (Caltrans) specifies a minimum flexural strength of 400 psi prior to opening to highway traffic for full depth highway pavement repairs (Concrete Construction, 2001). The 400 psi requirement is based on pavement design and the experience that the durability and life expectancy of the repaired pavement may be jeopardized if the slab is subjected to traffic prior to obtaining this strength. The New

Jersey State Department of Transportation specified a minimum compressive strength of 3000 psi in 6 hours, and a minimum flexural strength of 350 psi in 6 hours, for the "Fast-tract mix" developed in mid-90's (Kurtz et al., 1997). The Michigan Department of Transportation (MDOT) specifies the physical requirements for prepackaged hydraulic fast-set materials for use in structural concrete repairs, and the procedure to be followed by producers in order to have their products included on MDOT's Qualified Products List (MDOT QA/QC, 2003). In this document, minimum compressive strengths of 2000 psi in 2 hours, 2500 psi in 4 hours, and 4500 psi in 28 days are required. The 28 days strength needs to be higher for prestressed concrete applications.

Moreover, Parker et al (1991) suggested a minimum 2000psi compressive strength for road patching repair, which was considered sufficient to prevent cracking, abrasion, deformation and raveling when initially opened to traffic. A national research program report [Zia et al., 1991] on high performance concretes designates three categories based on strength: (a) very early strength, (b) high early strength, and (c) very high strength. The very early strength concretes have strength of at least 3,000 psi within 4 hours after placement. And the high early strength concretes have a compressive strength of at least 5,000 psi within 24 hours. In addition, FHWA Manual of Practice: Materials and Procedures for Rapid Repair of Partial-Depth Spalls in Concrete Pavements (FHWA, 1999) recommends for Rapid-setting Cementitious Concrete a minimum compressive strength of 1000 psi at 3 hours, 3000 psi at 24 hours, and initial set time of 15 minutes.

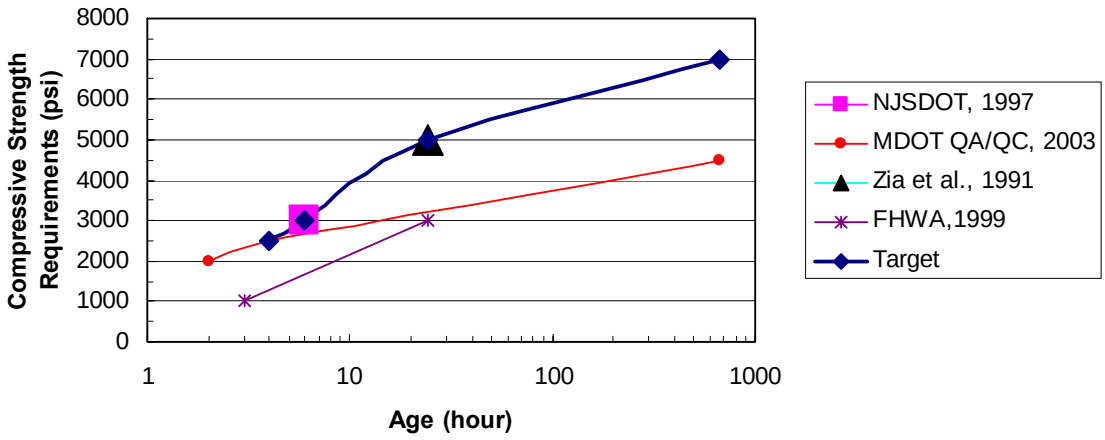

Figure 2.1: Compressive strength requirements at different ages

The compressive strength requirements at different ages by various DOTs and FHWA are summarized in Figure 2.1. The target compressive strengths set for this research project, with details discussed in Section 3.1, is also plotted on this figure.

2.2 Current Methods to Obtain High Early Strength

In current repair applications, high early strength is mostly attained by using traditional concrete ingredients and concreting practices, although sometimes special materials or techniques are needed. Depending on the age at which the specified strength must be achieved and on application conditions, high early strength is normally achieved by using one or a combination of the following:

a) Type III Portland Cement
b) Proprietary rapid hardening cements
c) High cement content
d) Low water-cementing materials ratio
e) Chemical admixtures (accelerator, superplasticizer, retarder, etc.)
f) Silica fume (or other supplementary cementing materials)
g) Insulation to retain heat of hydration
h) Higher freshly mixed concrete temperature
i) Higher curing temperature
j) Steam or autoclave curing

Type III Portland Cement is widely used in construction where a more rapid rate of strength gain is desirable. Type III Portland Cement and Type I Ordinary Portland Cement (OPC) are both normal Portland cement and their compositions are the same from the same manufacturer. The strength gain of normal Portland cement is mainly contributed by the hydration of Tricalcium Silicate (C_3S) and Dicalcium Silicate (C_2S), which produces a calcium silicate hydrate (C-S-H). By grinding the cement more finely compared with Type I cement (2637 ft^2/lb vs. 1806 ft^2/lb), the resultant increased surface area that will be in contact with water means faster hydration and more rapid development of strength. By this means, Type III cement can develop strength much faster than Type I cement within the first 3-8 hours. The amount of strength gain of

Type III cement over the first 24 hours is about double that of Type I cement (Neville and Brooks, 1987).

Proprietary rapid hardening cements such as magnesium phosphate based cement, gypsum-based cement and calcium aluminate cement have also been used to obtain very high early strength in some concrete mixes (Seehra et al., 1993; Knofel and Wang, 1994; Whiting and Nagi, 1994; Sprinkel, 1998; Balaguru and Bhatt, 2000). However, many proprietary rapid hardening cements often perform unpredictably under various job conditions. For example, magnesium phosphate based cement is extremely sensitive to water content, and its strength can be severely reduced by very small amount of extra water (Smith et al., 1991); concrete containing gypsum-based cement may lose durability in freezing weather or when exposed to moisture (Stingley, 1977), and the presence of sulfates in its mixture may promote embedded steel corrosion (Smith et al., 1991); calcium aluminate cement may lose strength at high curing temperature due to a chemical conversion (FWHA, 1999). Furthermore, most commercially available proprietary rapid-hardening cements are expensive compared with Type III cement. Due to the unpredictable performance and higher cost, proprietary rapid-hardening cements will not be considered in this research project unless HES-ECC based on Type III cement fails to achieve the target strengths.

Chemical admixtures play a key role in producing high early strength concrete mixtures that meet strength and workability criteria. Water-reducing admixtures increase early strength by lowering the quantity of water required while increasing the workability for appropriate concrete placement and finishing techniques. It disperses the cement, providing more efficient cement hydration, thus increasing strength at later ages as well. Accelerating admixtures aid early strength development and reduce initial setting times by increasing the rate of hydration. Hydration controlling admixtures allow time for transportation of the concrete from the ready-mix plant to the jobsite, and provide time for adequate placement and finishing. The detail information on various chemical admixtures and their potential effects on material performance are reviewed in this section:

(a) Water-reducing admixtures

A water-reducing admixture can effectively lower the water/cement ratio by reducing the water required to attain a given slump. Consequently, it improves the strength and impermeability of the cement matrix. The strength increase can be observed in as early as one day if excessive retardation does not occur (Collepardi, 1984). Furthermore, since the cement is dispersed and a more uniform microstructure is developed, the compressive strength can be as much as 25% greater than that achieved by the decrease in w/c alone (Malhotra et al., 1989),

Water-reducing admixtures are often observed to increase the rate of shrinkage and creep of concrete, depending on the cement type and the particular admixture. However, after 90 days of drying, there is little difference in shrinkage compared to a control concrete (Nmai et al., 1998; Ramachandran et al., 1998). The shrinkage properties of the developed HES-ECC and related durability issues will be investigated in the subsequent research tasks.

(b) Accelerating admixtures:

Accelerating admixtures accelerate the normal strength development and processes of setting and strength development. Regular accelerators are used to speed construction by permitting earlier attainment of sufficient strength to allow removal of formwork and to carry construction loads. Quick-setting admixtures provide setting times of only a few minutes. They are generally used in shotcreting applications and for emergency repair in general where very rapid development of rigidity is required. Accelerators are also beneficial during winter concreting because it can partially overcome the slower rate of hydration due to low temperatures and shorten the period for which protection against freezing is required (Edmeades and Hewlett, 1998, Mindess et al., 2002).

Accelerating admixtures can be divided into three groups: (1) soluble inorganic salts, (2) soluble organic compounds, and (3) miscellaneous solid materials (ACI Committee 212, 1991). Many soluble inorganic salts can accelerate the setting and hardening of concrete to some degree, calcium salts generally being the most effective. Soluble carbonates, aluminates, fluorides, and ferric salts have quick-setting properties

and they are commonly used in shotcreting applications. Calcium chloride is the most widely used because it is the most cost effective, while giving more acceleration at a particular rate of addition than other accelerators (Ramachandran, 1986). However, the use of calcium chloride will increase the rate of corrosion of metals embedded in concrete. The ACI Building Code places limits on the chloride content of concrete that preclude its use for both prestressed and reinforced concrete. Chloride-free accelerators should be used in such cases.

Organic compounds for most commercial uses include triethanolamine, calcium formate, and calcium (Rear and Chin, 1990). These compounds accelerate the hydration of tricalcium aluminate and produce more ettringite at early age. The reaction of triethanolamine with Portland cement is complex. Although listed as an accelerator, it can cause retardation or flash setting, depending on the amount used (Hewlett and Young, 1989).

Solid materials are not often used for acceleration. Calcium fluoroaluminate or calcium sulfoaluminate can be used as admixtures to obtain rapid-hardening characteristics. Additions of calcium aluminate cements cause Portland cements to set rapidly, and concrete can be "seeded" by adding fully hydrated cement that has been finely ground during mixing to cause more rapid hydration. Finely divided carbonates (calcium or magnesium), silicate minerals, and silicas are reported to decrease setting times (Ramachandran, 1984; Rixom and Mailvaganam , 1986; Rear and Chin, 1990; Mindess et al., 2002).

Although accelerating admixtures can be expected to increase early strength, the increase diminishes with time, and later strengths (at 28 days or more) are likely to be lower than the strength of concretes without an accelerating admixture (Ramachandran, 1984). This reduction in later strength is more pronounced when the initial accelerating effects are large.

Accelerating admixtures may also increase the rate of drying shrinkage and creep, although the ultimate values are not affected (Rixom and Mailvaganam, 1986). The early shrinkage leads to high tensile stresses in restrained repair material, resulting in cracking or interface delamination.

2.3 Engineered Cementitious Composites (ECC) Design Philosophy and Criteria

2.3.1 ECC Design Philosophy

The design philosophy of ECC follows the Integrated Structures and Materials Design Approach (ISMD) (Li & Fisher, 2002). ISMD is illustrated as a merging of two approaches, the Performance Driven Design Approach (PDDA) (Li, 1992), and the Performance Based Design Code approach (PBDC). Figure 2.2 showing the concept of ISMD contains two triangles, one of which involves structural mechanics and the other one involves micromechanics. Material properties serve as a connection between two triangles.

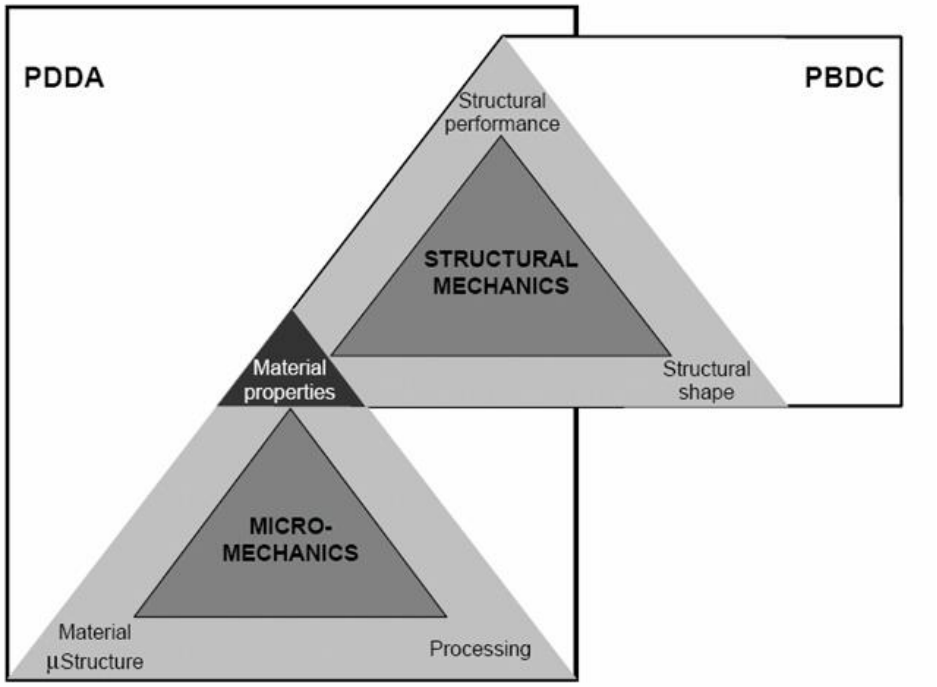

Figure 2.2: Integrated structures and material design (ISMD) (Li & Fischer, 2002)

In the upper triangle, performance based design approach is illustrated as the concept, with structural mechanics serving as the tool. Performance based design approach has been introduced into current structural design code, particularly in the US and in Japan, which shifts from traditional prescriptive structural design approach. Without specifying prescriptive requirements in structural material and shape, the PBDC

approach specifies structural performance objectives, in terms of functionality, repairability, life-safety, or collapse prevention under different specified loading levels (SEAOC, 1995). Structural engineers use structural mechanics as an analytical tool to decide the structural shape and the required properties of building materials to achieve a desired structural performance, such as load carrying capacity, flexibility, and durability. The decided material properties can be material strength, elastic modulus, strain capacity, toughness, and maximum crack width, and etc. After the required material properties are decided, the design procedure then goes down to the lower triangle.

In the lower triangle, material engineers use micromechanics as an analytic tool to tailor the material microstructure and processing, and design the material to have the desirable material properties. Performance driven design approach contains the lower triangle and part of the upper triangle. In this approach, the target structural performance is decided firstly, and then the important material properties are identified. The material microstructure, material processing, and material properties are related and tailored to meet the target material property requirements. Micromechanics models serve as powerful analytical tools to provide constituent guidance in material tailoring. This method switches material development from empirical combinations of material constituents to systematic "engineered" approach. For ECC development, these material constituents are characterized by the fiber, matrix, and interface properties, with each phase described by a set of parameters. Micromechanics models relate these parameters to create desirable ECC material properties, and to satisfy the target structural requirements.

The success of this approach has been demonstrated by the design of several versions of ECC with different functionalities. This design philosophy of ECC distinguishes it from traditional Fiber Reinforced Concrete (FRC) and other High Performance Fiber Reinforced Cementitious Composites (HPFRCC) materials. Most HPFRCC attains strain hardening behavior with high fiber volume fractions (5% and up). In contrast, ECC uses only a small fiber volume fraction (~2%) to achieve high ductility, strain hardening behavior and high toughness by optimizing the material composition through micromechanics. For design of ECC to be successful, the quantitative link

between material microstructure, and composite properties, provided by micromechanics, is critical.

The ISMD approach is adopted in this research project to tailor ECC with high early strength as well as high strain capacity for making rapid and durable repair of bridges and structures.

2.3.2 ECC design criteria

ECC contains three main phases in its microstructure: (a) fiber; (b) matrix; and (c) fiber/matrix interface. Each phase can be characterized by several micro-parameters (Table 2.1) (Kanda and Li, 1998; Lin and Li, 1998). These micro-parameters can be tailored based on micromechanical models so as to control the failure mode, the ultimate tensile strength and strain, and the pre-failure micro-cracking width of the composite.

Table 2.1: Three phases of ECC microstructure and corresponding micro-parameters

Phase	Micro-parameters
Fiber	Length L_f, Diameter d_f, Volume Fraction V_f Tensile Strength σ_f, Elastic Modulus E_f
Matrix	Fracture Toughness K_m, Elastic Modulus E_m, Initial Flaw Size Distribution a_0
Fiber/Matrix Interface	Chemical Bond G_d , Frictional Bond τ_0, Slip Hardening Property β, Snubbing Coefficient f'

The condition for multiple-cracking and pseudo strain-hardening behavior of ECC is that the steady state cracking criteria can be satisfied. The criteria requires the crack tip toughness J_{tip} to be less than the complementary energy J'_b calculated from the bridging stress σ vs. crack opening δ curve (Figure 2.3) [Marshall and Cox, 1988; Li, 1993].

$$J_b^{'} = \sigma_0 \delta_0 - \int_0^{\delta_0} \sigma(\delta) d\delta \geq J_{tip} \tag{2.1}$$

$$J_{tip} = \frac{K_m}{E_m} \tag{2.2}$$

where,

J_{tip} = crack tip toughness

J'_b = complimentary energy calculated from the bridging stress σ vs. crack opening δ curve (Figure 2.3) (Marshall and Cox, 1988; Li, 1993)

σ_0 = maximum fiber bridging stress

δ_0 = crack opening corresponding to the maximum fiber bridging stress σ_0

σ_{ss} = steady state cracking stress

δ_{ss} = crack opening corresponding to the steady state cracking stress σ_{ss}

K_m = matrix toughness

E_m = matrix elastic modulus

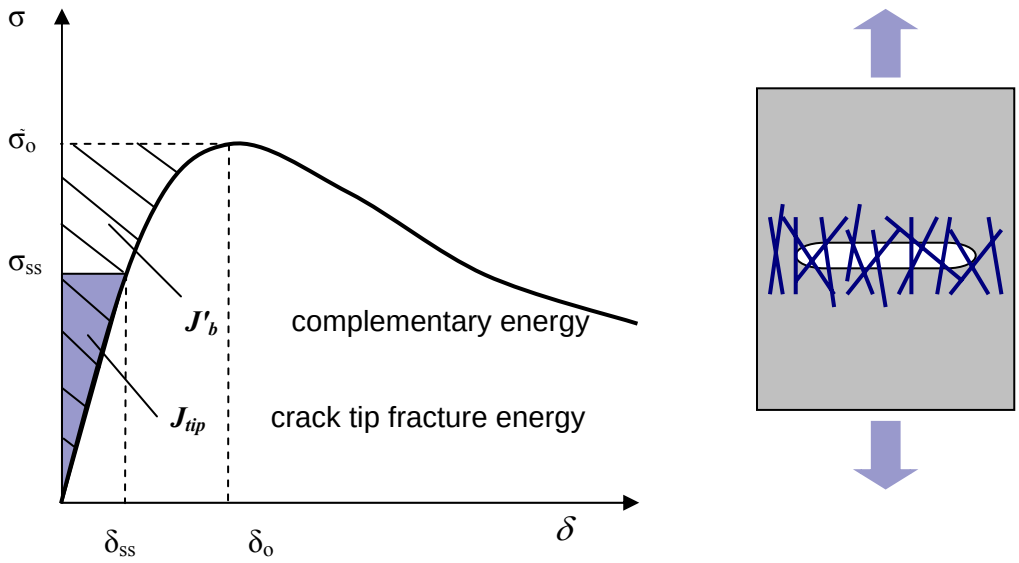

Figure 2.3: A typical $\sigma \sim \delta$ curve for strain hardening composite. The hatched area represents the complementary energy J'_b. The shaded area represents the crack tip toughness J_{tip}.

Related to the shape of the $\sigma \sim \delta$ curve, the complementary energy J'_b reflects fiber properties and fiber/matrix interface properties. For example, if the fiber/interface properties are the same, higher fiber bridging stress indicates higher peak value of the $\sigma \sim \delta$ curve and higher complementary energy J'_b. On the other hand, lowering the

fiber/matrix interface bond may also increase the complementary energy J'_b since δ_0 will shift to the right on the curve because the fiber bridging stiffness is reduced.

The crack tip toughness J_{tip} reflects matrix properties. It is determined by the matrix toughness K_m and matrix Young's Modulus E_m. Lower matrix toughness and higher matrix Young's Modulus allows for lower value of J_{tip}, which is favorable for pseudo strain hardening to occur.

Another condition for pseudo strain-hardening is that the tensile first cracking strength σ_{fc} must not exceed the maximum bridging stress σ_0 (Li and Leung, 1992; Li and Wu, 1992),

$$\sigma_{fc} < \sigma_0 \tag{2.3}$$

where,

σ_{fc} = matrix tensile first cracking strength. It is the tensile stress when the first crack happens. σ_{fc} is determined by the matrix fracture toughness K_m and the maximum size of the initial flaws existing in the matrix max[a_0]

σ_0 = maximum fiber bridging strength

Satisfaction of both equation (2.1) and (2.3) is necessary to achieve ECC strain hardening behavior. Otherwise, tension softening behavior like normal Fiber Reinforced Concrete (FRC) occurs.

The steady state cracking criteria ensures the occurrence of multiple cracking. However, it is not directly related to the density of multiple cracking, which is closely related to the ultimate strain capacity the material can achieve. It is the matrix pre-existing flaw size distribution, together with the matrix fracture toughness, that determines the number of cracks which can be developed before the maximum fiber bridging stress (i.e. the peak value of $\sigma \sim \delta$ curve) is reached. The maximum fiber bridging stress imposes a lower bound of critical flaw size c_{mc} such that only those flaws larger than c_{mc} can be activated and contribute to multiple cracking. To ensure the development of saturated multiple cracking and obtain high material strain capacity, the size distribution of pre-existing flaws in matrix needs to be optimized. Ideally, as illustrated in Figure 3.4, a narrow distribution above critical size c_{mc} is desired, which

may lead to a prolonged yielding plateau on the ECC stress-strain curve (Wang and Li, 2004). Both smaller and larger flaws should be avoided, because the former cannot activate cracking and the latter will deteriorate homogeneity of fiber distribution and the workability of the composites.

From the conditions for strain-hardening and multiple cracking saturation, it is evident that high material strain capacity requires high J'_b, low J_{tip} and sufficient number of pre-existing flaws larger than c_{mc}. In conventional ECC, sufficient margin between J'_b and J_{tip} exists (Li et al., 2002), allowing for a large number of cracks to occur. In HES-ECC to be developed, it is expected that the margin between J'_b and J_{tip} is small, or even that J_{tip} may exceed J'_b. This is because of the rapidly increased fracture toughness of the HES-ECC matrix. Consequently, few cracks can be developed and the strain capacity of the composite may be low. To solve this problem and tailor the composites to have required strain capacity, artificial flaws with prescribed size distribution can be introduced to the matrix, which can be activated before the maximum fiber bridging stress is reached (Figure 2.4). By this means, the composites can achieve saturated multiple cracks and the corresponding high strain capacity.

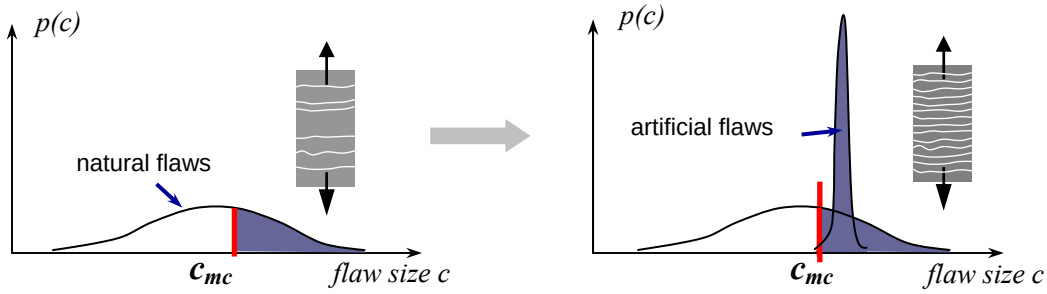

Figure 2.4: Optimization scheme for pre-existing flaw size distribution in matrix: (a) natural flaw size distribution with random nature inherent from processing; (b) artificial flaws larger than critical size c_{mc} imposed to ensure saturation of multiple-cracking (Wang and Li, 2004).

3. HES-ECC COMPOSITES DEVELOPMENT (TASK 2)

3.1 Target HES-ECC Properties

The objective of this research project at the material development stage is to add high early strength functionality to the normal ECC material, while guaranteeing good workability and high material tensile strain capacity (ductility) at different ages. The developed HES-ECC material should be competent for making rapid and durable repair of various concrete structures.

The target HES-ECC properties are specified as below referring to FHWA and DOTs specifications reviewed in section 2.1:

Compressive strength: > 2500 psi at 4 hr
> 3000 psi at 6 hr
> 5000 psi at 24 hr
> 7000 psi at 28 d

Tensile strain capacity: > 2% after 4 hours

Initial setting time: > 15 minutes

The minimum compressive strength of 2500 psi at 4 hr and 3000 psi at 6 hr enables the repaired bridge or structure to be opened to traffic within 4-6 hours after placement. Consequently a fast repair can be done at night, and then opened to traffic the next morning. The early age strength gain rate within 24 hours is considered to be sufficient for repair jobs in heavy traffic areas. The minimum compressive strength of 7000 psi at 28 days should be adequate for prestressed concrete applications. A minimum 2% tensile strain capacity of the HES-ECC is targeted for normal service conditions. A minimum 15 minutes working time is necessary for repair handling and placement.

3.2 HES-ECC Design Strategy

Four approaches have been used in this research project to achieve rapid strength development at early ages:

a) Replace Type I cement with Type III cement
b) Add admixtures, especially accelerator
c) Lower water/cement ratio

d) Eliminate fly ash

Traditional ECC is based on Type I cement binder. By changing Type I cement to Type III cement, together with adding accelerator, the strength within 24 hours was expected to increase by 100-200% according to the experience with high early strength concrete. Other types of admixtures, such as superplasticizer and stabilizer, were included when workability needs to be controlled. Traditional ECC mix also contains high content of fly ash and water, which adversely affects early strength development. Therefore, the water/cement ratio was lowered and fly ash was eliminated from the HES-ECC composition. In sum, the matrix mix proportion was re-designed.

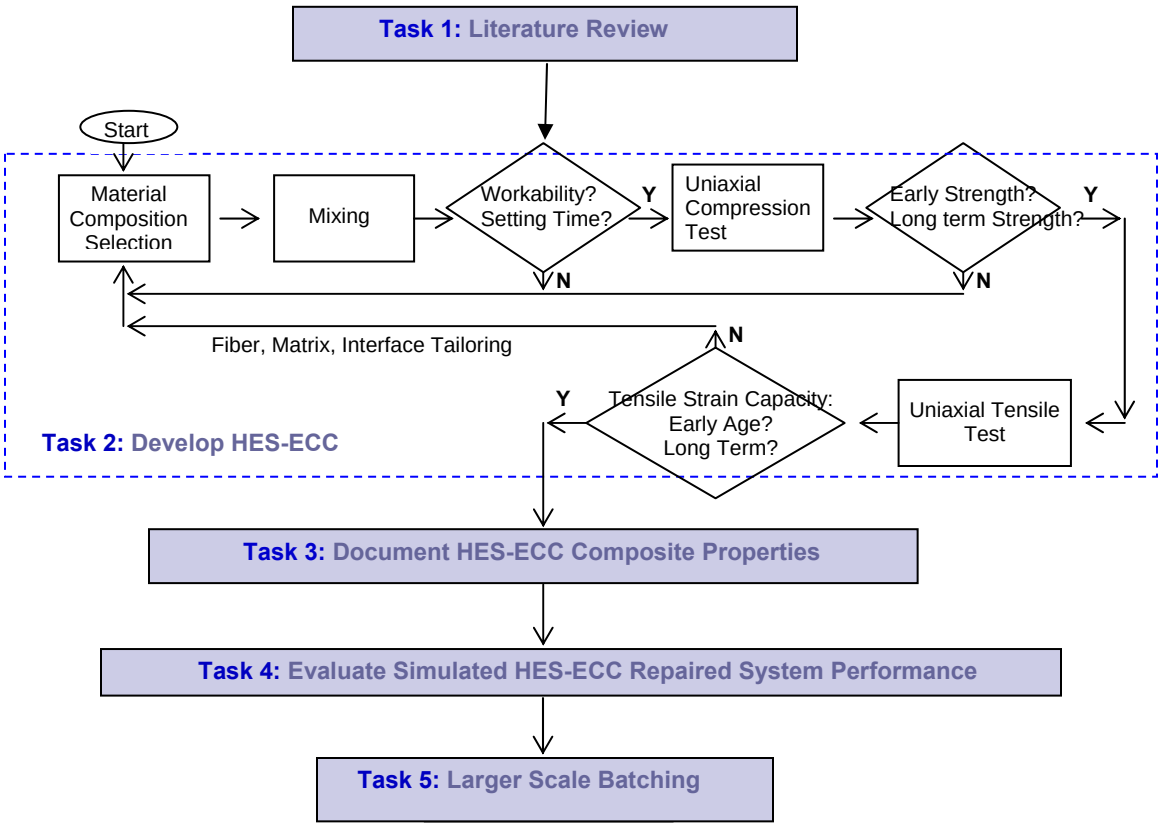

Figure 3.1: Detailed research plan flow chart – Task 2: Develop HES-ECC

The detailed research plan flow chart for the Task 2 (Develop HES-ECC) is shown in the dashed box of Figure 3.1. The initial tentative HES-ECC mixes with different mixing proportions were firstly mixed and cast to check workability and setting time. If good workability could be achieved and the setting time requirement was satisfied, the mixes were further tested for compressive strength development. The

promising mix satisfying the target compressive strengths at different ages were afterwards tested for its tensile strain capacity.

Since changing mixing proportion would change both ECC matrix properties and matrix/fiber interface properties, it was expected that the tensile strain capacity of the initially selected HES-ECC mix would be sacrificed. However, ECC is a "designable material", and the target strain capacity could be regained by tailoring the micromechanical parameters based on the theoretical model briefly introduced in section 2.3. Matrix toughness test and single fiber pullout test were conducted to measure the time-dependent development of matrix properties and fiber/matrix interface properties, which gave corresponding information for material tailoring purpose.

Once the target strengths, strain capacity and workability had been achieved, HES-ECC composite was successfully developed.

3.3 Initial Material Composition Selection Based on Strength Requirements

3.3.1 Motivation and Objectives

Initial composite tests in uniaxial compression were conducted on various mixes with different mixing proportions. The purpose is to narrow the choice of binder systems which can satisfy the target high early strength requirements. The selected mix will be further tailored to obtain the other target performances, i.e. workability and tensile strain capacity.

3.3.2 Materials

The investigated Mix Proportions and material details are summarized in Table 3.1 and 3.2. Two types of cements were investigated. Type III Portland cement has the same composition as Type I Ordinary Portland Cement (OPC), except that it is finely ground. Fly ash is an integrated part of conventional ECC. It is eliminated from some of the mixes to obtain more rapid strength development. Fine silica sand is the main aggregate in ECC with the maximum particle size of 270 μm, and the average particle size of 110 μm. Polystyrene (PS) bead is the other type of aggregate which has very weak bond with cementitious matrix so that it behaves as artificial flaws under tensile loading. As the uniaxial tensile test (Section 3.4, 3.5) show that the initially selected

mix could not meet the target tensile strain capacity requirements, the polystyrene beads were deliberately introduced to the mix for controlling initial flaw size and distribution at the material tailoring stage, so that the material can develop multiple micro-cracks on its strain hardening stage.

The accelerating admixture used in this research project was Pozzolith ® NC 534 (NC534, from Master Builders, Inc.). The accelerating species in NC534 are calcium nitrate and sodium thiocyanate. The recommended maximum effective dosage of NC534 is 4 wt% to cement.

Superplasticizer is necessary to achieve sound workability when the mixing composition has low water/cement ratio. The superplasticizer used in this research project was Glenium® 3200 HES (GL3200, from Master Builders Inc.). GL3200 is a late generation superplasticizer with powerful dispersion capacity at low w/c. It can provide more complete hydration of cement particles and hence result in stronger accelerating effect. It demands less dosage compared with other types of superplasticizer, such as melamine formaldehyde based ML330, to achieve the same workability due to combined forces of electrostatic and steric repulsion.

The fiber used in this research project is REC15 PVA fiber from Kuraray Co., Japan. This fiber has been micromechanically tailored for ECC applications with the highest performance to price ratio in the market of High Performance Fiber Reinforced Cementitious Composites (HPFRCC). The properties of REC15 fiber are listed in Table 3.3.

3.3.3 Experimental Program

Each of the compositions was mixed in a Hobart type mixer with 0.42-cubic-foot capacity. Solid ingredients, including cement, sand and fly ash if applicable were first mixed for approximately 1 min. Then water was slowly added and mixed for another 3 min. Next, superplasticizer was added into the mixer. Once a consistent mixture was reached, fiber was slowly added. Accelerating admixture, if used, was added after fiber and just before casting. The whole mixing procedure for each batch generally took 10-15 minutes. After mixing, the mixture was cast into molds with moderate vibration applied. The molds were covered with plastic sheets and cured in air at room

temperature (60-70°F). Specimens were demolded for testing after 24h, or 3h if applicable.

Compressive testing was conducted according to ASTM C39 "Standard Test Method for Compressive Strength of Cylindrical Concrete Specimens" on standard 3" × 6" cylinders. The ends of the specimens were capped with sulfur compound and tested on a FORNEY F50 compression test system. Test began at 4 hours after casting or when adequate strength had developed. The age of the specimen is recorded as the time elapse from finish casting to test. Three specimens were tested for each test series.

Table 3.1: List of materials used

Category	**Product Name**	**Manufacturer**	**Chemical Composition**	**Particle Size**
Cementitous Material	Portland cement Type I	LaFarge Co., USA	Ordinary Portland Cement (OPC)	Blaine Surface area: 3300 cm^2/g
	Portland cement Type III	Holcim Co., USA	Finely ground OPC	Blaine Surface area: 5000 cm^2/g
	Normal fly ash	Boral Material Tech. Inc., USA	ASTM C618 class F	Mean size: 10-20 μm
Accelerating Admxture	Pozzolith® NC 534	Master Builders, Inc., USA	Calcium nitrate <43% Sodium thiocyanate <5%	Specific weight: 1.39g/ml
Aggregate	Silica sand F110	U.S. Silica Co.	Silica	Mean size: 110 μm, max. size 250 μm
	PS beads	Dow Chemical Co., USA	Polystyrene	Size: 4mm, Density: 1.4g/cm^3
Superplasticizer	Daracem® ML330	W. R. Grace & Co., USA	Melamine formaldehyde sulfonate	Specific weight: 1.18 g/ml
	Glenium® 3200HES	Master Builders, Inc. USA	Polycarboxylate based	Specific weight: 1.05 g/ml
Hydration Control	Delvo® Stabilizer	Master Builders, Inc. USA		
Fiber	REC15	Kuraray, Co, Japan	Polyvinyl alcohol (PVA) fiber	

Table 3.2: Mixing proportions for initial uniaxial compressive test

Mix	Cement	Silica Sand	Fly Ash	Water	Admixtures	Fiber V_f(%)
1	Type I 1.0	0.8	1.2	0.53	GL3200 0.75%	2.0
2	Type III 1.0	0.8	1.2	0.53	GL3200 0.75%	2.0
3	Type III 1.0	1.0	-	0.53	-	2.0
4	Type III 1.0	1.0	-	0.45	GL3200 0.35%	2.0
5	Type III 1.0	1.0	-	0.33	GL3200 0.75%	2.0
6	Type III 1.0	1.0	-	0.33	GL3200 0.75% + NC534 4.0%	2.0

Table 3.3: Properties of REC 15 PVA fiber from Kuraray, Co, Japan

Fiber Type	Nominal Strength (ksi)	Fiber Diameter (in)	Fiber Length (in)	Young's Modulus (GPa)	Elongation (%)
REC15	234.961	1.535×10^{-3}	0.472	6207.614	6.0

3.3.4 Results and Discussions

The compressive strength development of various mixes is summarized in Table 3.4, and plotted in Figure 3.2 to Figure 3.5. Three specimens were tested for each test series and the average values were plotted.

Table 3.4: Compressive strength of trial mixes at different ages

Age (Hour)	Compressive Strength (psi)					
	Mix 1			Mix 2		
4				492	498	522
5				1023	1190	1360
6				2502	2722	2777
10				3530	3705	4099
12	2578	2600	2654	4176	4410	4683
24	3187	3278	3543	5136	5578	5594
48	4515	4682	4727	6034	6175	6493
72	5925	6420	6800	6453	6793	7013
144	8106	8398	8733	7986	8203	8369
672	9100	9507	9675	8664	8994	9534

Table 3.4: Compressive strength of trial mixes at different ages

Age (Hour)	Compressive Strength (psi)								
	Mix 3			Mix 4			Mix 5		
4				254	280	291	675	732	769
5				754	760	778	1286	1476	1698
6				857	855	913	3354	3781	3830
7				1412	1623	1861	4396	4512	4581
8	202	270	362	2034	2210	2485	4760	4938	5183
9	465	490	590	2692	2898	2906	4798	5220	5559
10	586	680	792	2723	2902	3063	5411	5467	5656
12	1412	1587	1792	3098	3232	3312	5320	5622	5940
24	2373	2563	2783	4244	4388	4466	6080	6312	6448
48	3601	3700	3898	4612	4794	4946	6951	7282	7523
72	3592	3874	4075	4800	4962	5034	7633	8024	8144
96	3726	3912	4065	5166	5278	5462	7791	8006	8178
120	4001	4150	4164	5395	5580	5780	8160	8327	8445
144	3928	4223	4443	5823	6232	6314	8097	8394	8702
168	4012	4267	4321	6193	6334	6535	8257	8510	8905
336	4105	4307	4449	6690	6840	6960	8692	9034	9251
480	4232	4398	4297	6960	7144	7196	9038	9324	9355
672	4213	4401	4616	6901	7113	7346	9127	9480	9675

Age (Hour)	Compressive Strength (psi)					
	Mix 6 (w/ sulation)			Mix 6 (w/o nsulation)		
2.7				1802	1816	1821
3	1100	1120	1261	3083	3195	3294
4	2523	2596	2606	3857	4081	4245
5	4151	4304	4598	4982	5012	5017
6	4791	4971	5032	5552	5823	5943
7	5050	5274	5427	5736	5923	6050
8	5383	5598	5771	5866	6022	6169
9	5701	5834	5870	6063	6287	6447
10	5730	5798	5964	6166	6361	6618
12	5789	5961	6133	6494	6503	6540
24	6457	6621	6894	6635	6967	7327
48	6906	7156	7259	7396	7514	7716
72	7516	7680	7865	7716	8183	8380
96	7675	7845	8107	7932	8203	8449
120	7895	8003	8120	8147	8292	8319
144	7878	8102	8256	8189	8492	8556
168	8267	8422	8548	8296	8482	8546
336	8674	8803	8847	8626	8698	8783
480	8806	9025	9190	9089	9170	9284
672	8937	9139	9336	9048	9236	9476

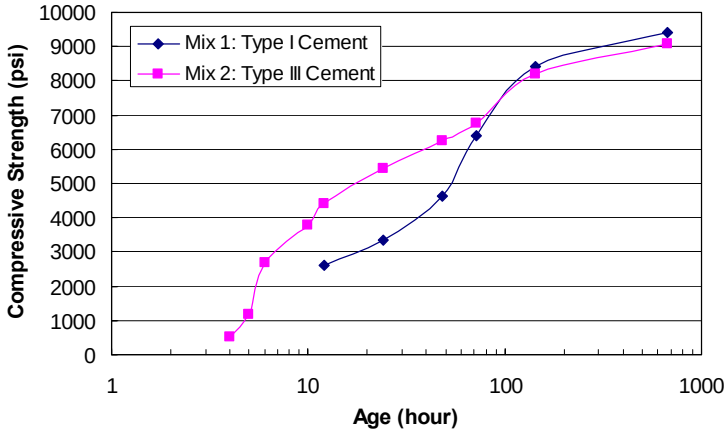

Figure 3.2: Effect of cement type on compressive strength development

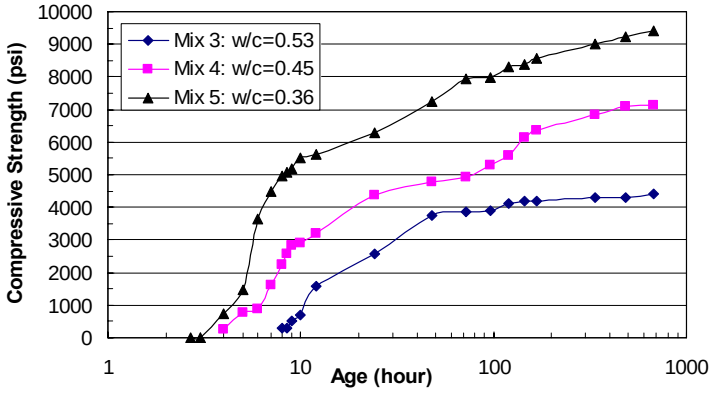

Figure 3.3: Effect of w/c ratio on compressive strength development

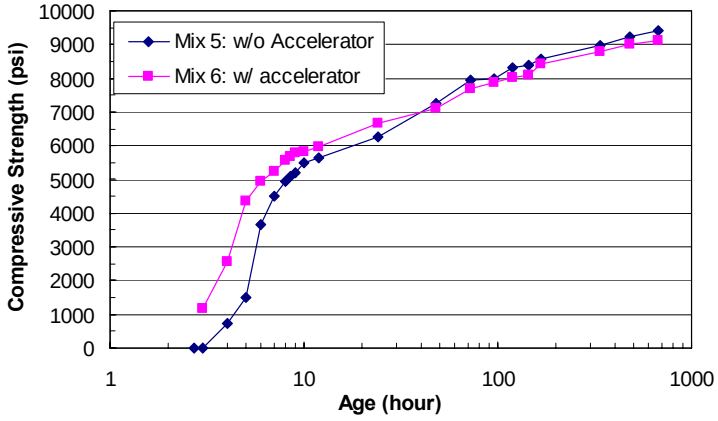

Figure 3.4: Effect of accelerator on compressive strength development

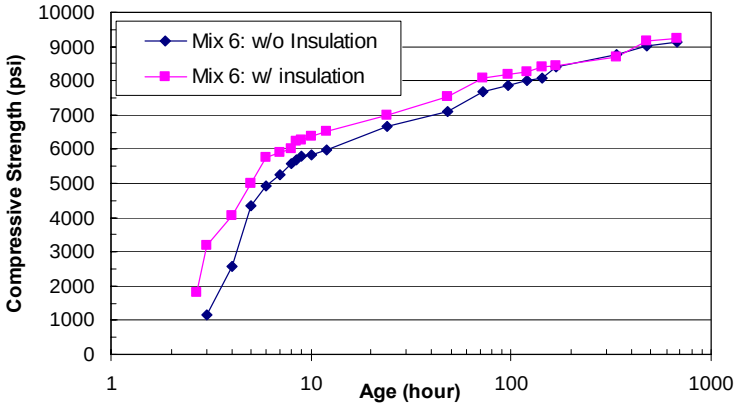

Figure 3.5: Effect of curing condition on compressive strength development

By changing Type I cement to Type III in the mixing proportion of conventional ECC (Mix 1), the early age compressive strength gain rate was greatly improved (Figure 3.2), although the long term compressive strength exhibited little difference. However, the Mix 2 containing Type III cement still could not achieve the target high early strength. Its compressive strength was about 500 psi at 4h, far below the target 2500 psi at 4h. The 6h and 24h compressive strength requirements also could not be satisfied. This low early strength could be due to the presence of high content of fly ash. Therefore, in the following mixes, fly ash was eliminated from the mixing proportions.

Figure 3.3 shows the effect of water/cement ratio on the compressive strength development. By reducing w/c from 0.53 to 0.33, the compressive strength at 28 d doubled, and the early age strength was improved significantly. It indicates that reducing w/c ratio is a very effective way to increase both early age compressive strength and 28 d compressive strength.

To further improve strength development within the first 24 hours, additional accelerators were incorporated (Mix 6). As shown in Figure 3.4, use of NC534 at dosage of 4.0% can reduce the age to reach 2500 psi strength from 6 hour to 4 hours, which already met the target 2500psi at 4h. The 6h, 24h, and 28d compressive strengths were measured as 4931psi, 6657psi and 9137psi respectively, which also satisfied the strength requirements.

Curing condition was found to have significant influence on the strength gain rate at early ages. As shown in Figure 3.5, same Mix 6 developed strength much faster in the first 12 hours under insulated condition where the specimens were stored in plastic container with insulation foam. The target 2500psi at 4h compressive strength could be achieved as early as 3 hours. This can be explained by the temperature controlled hydration rate of C_3S and formation of C-S-H. It should also be noted that compressive strength was measured using relatively small cylinders (3"×6") in this experimental program. For field applications, the effect of curing condition is expected to be lower where hydration heat can be better preserved due to the large material volume.

Furthermore, Mix 6 remained workable within 20 minutes, which was considered sufficient for repair jobs. For the larger scale mixing when longer working time is desired, hydration control agent can be used to retard the hydration process and retain the workability. Delvo ® stabilizer from Master Builders has been tested to work well for this purpose in Task 5: HES-ECC larger scale batching (Section 6).

As a conclusion, Mix 6 was the initially selected mix proportion which satisfied the strength and workability requirements.

3.4 Initial Composite Test in Uniaxial Tension – Early Age and Long Term

3.4.1 Motivation and Objectives

Initial composite tests in uniaxial tension were conducted on the selected mixing proportion (Mix 6) which satisfies the high early strength criteria. The purpose was to evaluate the tensile strain capacity of the selected mix at both early age and long term. If the target strain capacity could not be satisfied, the mix needed to be further tailored to meet the requirements.

3.4.2 Experimental Program

Uniaxial tension testing was performed on ECC coupon specimen measuring 9”×3”×0.5”. After demolded, aluminum plates were glued at the both ends of the coupon specimen to facilitate gripping (Figure 3.6). Tests were conducted on an MTS machine with 5.62kip capacity under displacement control at rate of 1.97×10^{-4}in/s.

Two external LVDTs (Linear Variable Displacement Transducers) were attached to the specimen surface with a gage length of 4" to measure the displacement. Specimens were demolded at 4 hours, cured in air, and tested at different ages from 4 hours to 28 days.

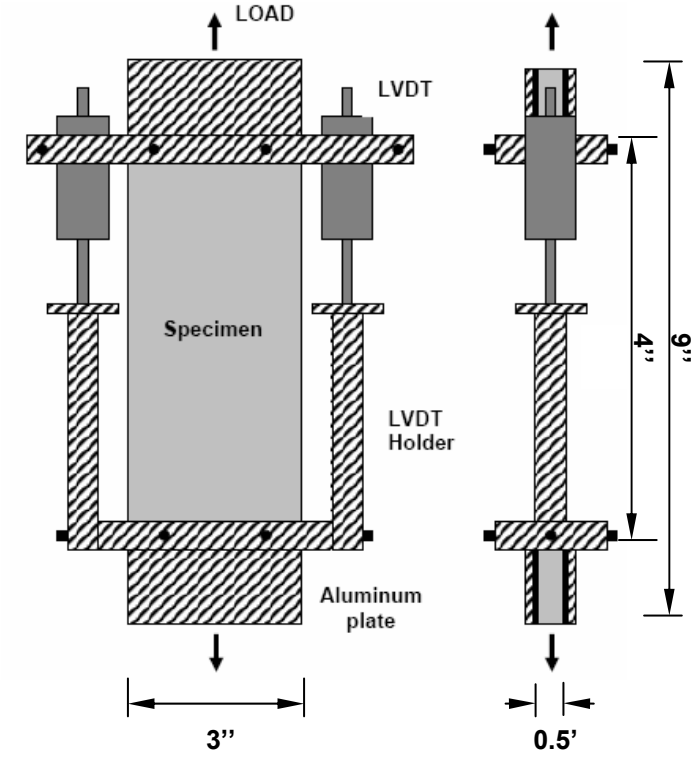

Figure 3.6: Uniaxial tensile test set-up

3.4.3 Results and Discussions

Initial tensile test on the selected mix shows rapid strain capacity decrease with age, accompanied by increase of the first cracking strength (Figure 3.7). At 4h after casting, the material has already shown satisfactory ECC behavior with a strain capacity of above 4%. The strain-capacity slightly decreases to 3% at 24h, which still meets the minimum 2% tensile strain capacity requirement. However, the strain capacity continues decreasing to about 1.2% at 3 days and retains only 1% after 7 days.

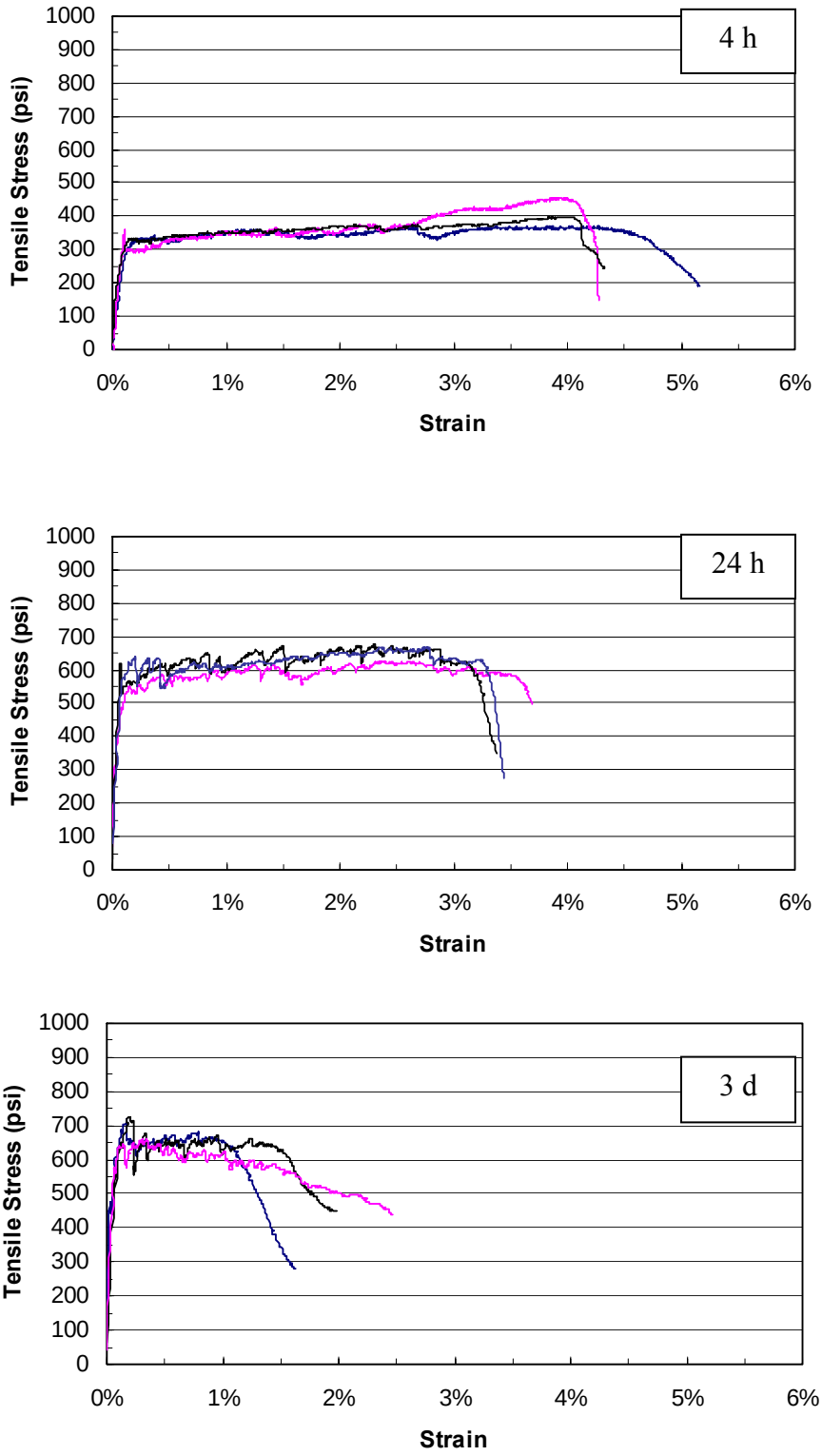

Figure 3.7: Age-dependent tensile stress vs. strain curve of Mix 6

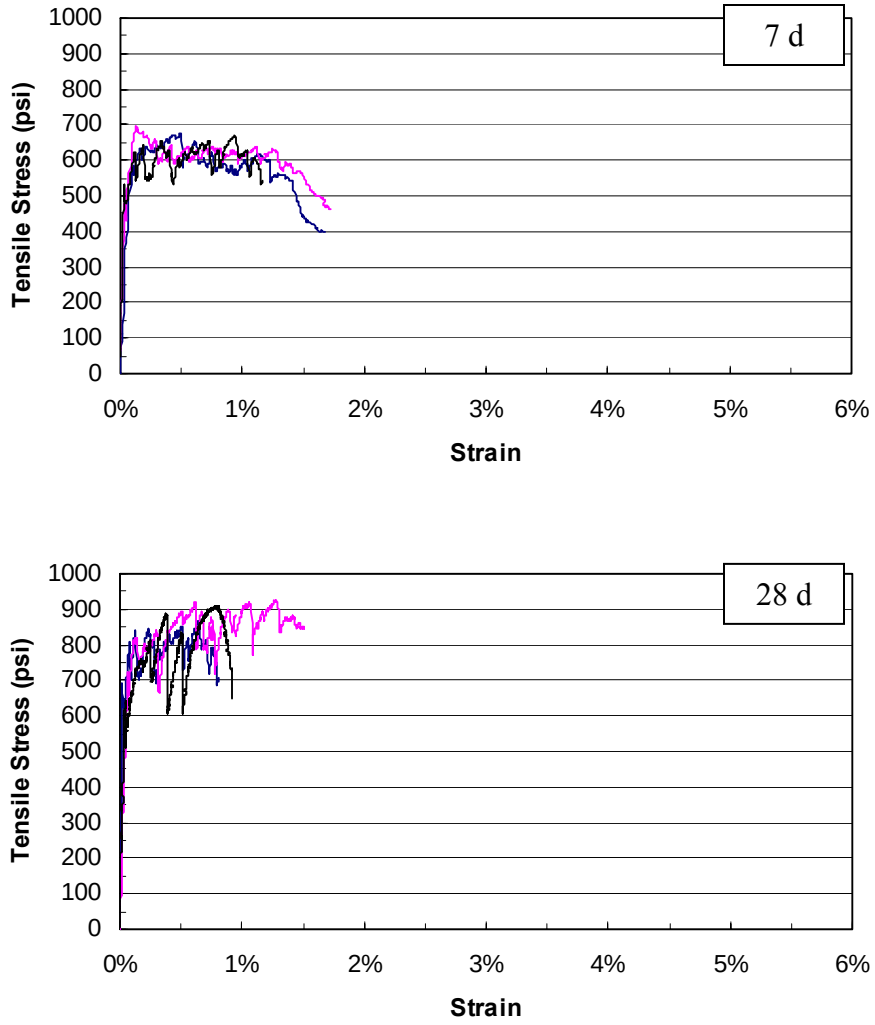

Figure 3.7: Age-dependent tensile stress vs. strain curve of Mix 6

3.5 HES-ECC Tailoring for Ductility

3.5.1 Motivation and Objectives

The initially selected HES-ECC mix (Mix 6) could not meet the tensile strain capacity requirements after 24h, although the target compressive strengths have been achieved. Consequently, the initial selected HES-ECC mix needed to be further tailored to regain the target strain capacity (>2% after 4h). The objective was to finally develop a HES-ECC material which meets all the compressive strength, setting time and tensile strength capacity requirements.

3.5.2 Experimental Program

To understand how the HES-ECC matrix toughness changed with time, matrix toughness testing was conducted through testing similar to ASTM E399 "Standard Test Method for Plane-Strain Fracture Toughness of Metallic Materials". The ASTM E399 allows one to use different geometry specimens, such as bending specimens and compact tension specimens, to measure the K_m value. The bending specimen should have a straight–through initial notch as shown in Figure 3.8.

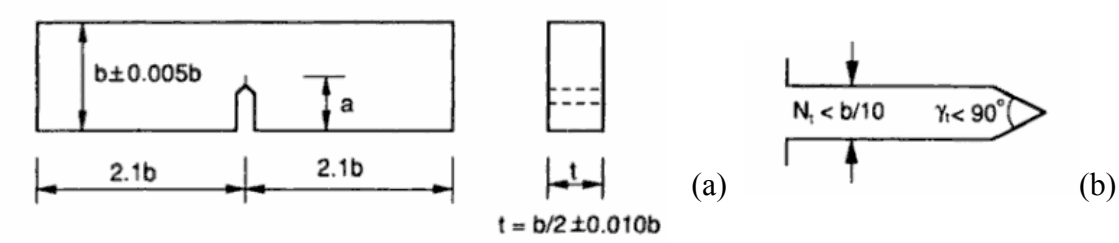

Figure 3.8: Three-point bending specimen specified by ASTM E399: (a) specimen geometry and (b) machine notch geometry

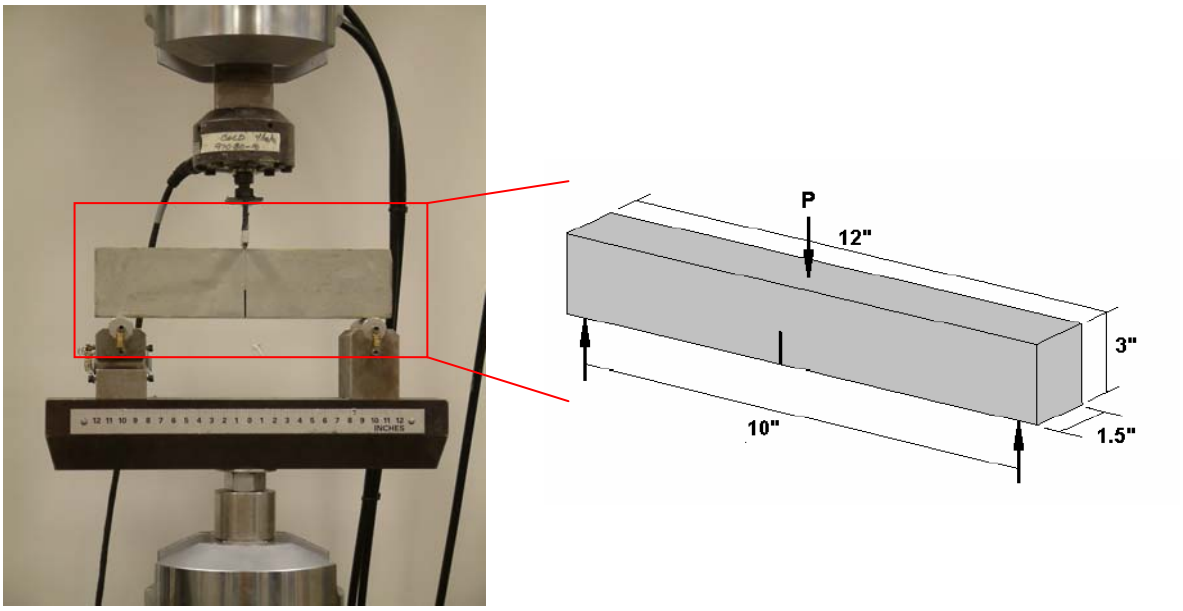

Figure 3.9: Matrix fracture toughness test set-up

Notched prism specimens were prepared from HES-ECC mortar (HES-ECC material without fibers) with dimensions of 12"×3"×1.5". A single notch with width of 0.06" was cut using a diamond saw before testing at the midspan to a depth of 40% of prism depth (Figure 3.9). Notched specimens were tested beginning at 4 hours in three-point bending to determine the fracture toughness $K_{m.}$ Three specimens were tested for each test series.

To understand the age-dependent development of the fiber/matrix interface bond properties, single fiber pull-out tests were conducted to characterize the fiber/matrix bond properties, including the chemical bond, frictional bond, and slip-hardening properties as a function of age. Single fiber pull-out tests were conducted on small-scale prismatic specimens approximately 0.4"×0.2"×0.02". A single fiber was aligned and embedded into the center of the initially selected HES-ECC mortal prism with an embedment length of 0.02" (Figure 3.10). The load versus displacement curve was obtained through quasi-static testing and used to calculate necessary micromechanical properties for overall composite design and evaluation. Testing began at 4 hours after demolding and at least three specimens were tested for each series.

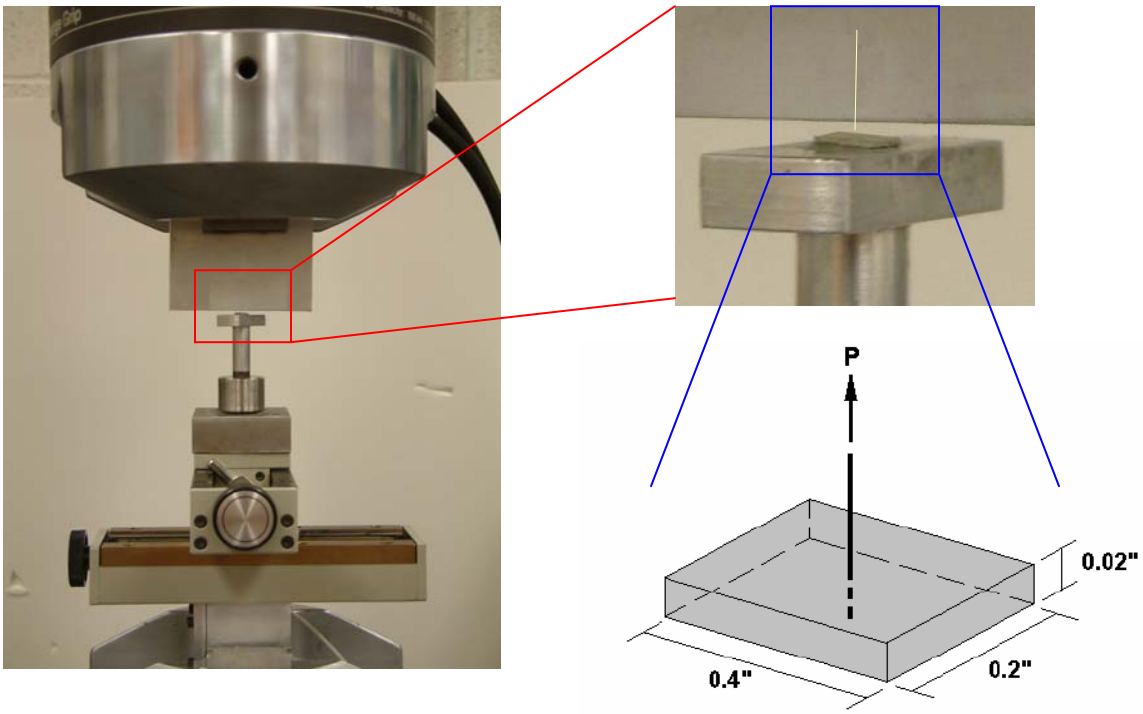

Figure 3.10: Single fiber pull-out test set-up

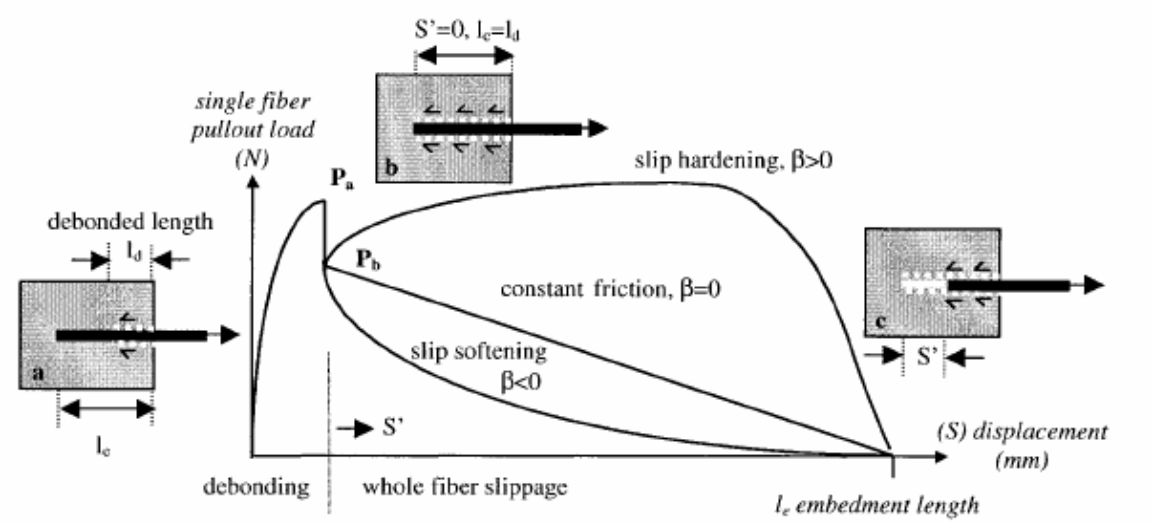

Figure 3.11: General profile of a single fiber pullout curve

The general profile of a single fiber pullout curve can be decomposed into three major regimes (Figure 3.11) (Redon et al., 2001). Initially, a stable fiber debonding process occurs along the fiber/matrix interface (Fig 3.11 (a)). The load resisted by the fiber is increasing up to P_a. The fiber embedded end, $l = l_e$, does not move. The debond length, l_d, increases towards $l_d = l_e$. The displacements correspond only to the elastic stretching of the debonded fiber segment and of the fiber-free length. Then the load decreases from P_a to P_b. If the load drop is significant, it reveals that the chemical bond between the fiber and the matrix was broken. The chemical debonding energy value, Gd, is calculated from the P_a to P_b difference, shown in (3.1)

$$G_d = \frac{2(P_a - P_b)^2}{\pi^2 E_f d_f^3} \tag{3.1}$$

where *Ef* = fiber axial Young's modulus; and *df* = fiber diameter (Li et al., 1998).

In the case of nonchemically bonded fibers, such as steel or polyethylene fibers, P_a would be close or equal to P_b. At point P_b, the embedded fiber end is just debonded (Figure 3.11 (b)). From the P_b value, one calculates the frictional bond strength τ_0 at the onset of fiber slippage (*S*' = 0 at P_b)

$$\tau_0 = \frac{P_b}{\pi d_f l_e} \tag{3.2}$$

Finally, in the slippage regime, the fiber load is resisted by frictional forces (Figure 3.11 (c)). The fiber can undergo sliding with slip hardening, constant friction or slip-softening effect, characterized by the coefficient b, which is, respectively, positive, zero or negative (Lin and Li, 1997). Slip-hardening occurs often with polymer fibers. Because they are less hard than the surrounding matrix, they are damaged and a jamming effect can take place inside the matrix. This leads to an increasing load resisting fiber pullout. This phenomenon can be very beneficial as long as the fiber tensile strength is not exceeded. Conversely, constant friction or slip-softening are often observed when the fiber hardness is higher than that of the surrounding matrix. The β value is calculated from the initial (*S*' approaching 0) slope of the P versus S' curve and using

$$\beta = (d_f / l_f)[1/\tau_0 \pi d_f)(\Delta P / \Delta S')\big|_{S'->0} + 1] \tag{3.3}$$

3.5.3 Results and Discussion

The deterioration in the strain capacity of HES-ECC can be attributed to the continuing increase of both matrix toughness and matrix/fiber interface bond strength, as a function of age. Age dependent values of matrix toughness K_m were measured from the notched beam bending test and plotted in Figure 3.12. Age dependent values of matrix/fiber interface chemical bond G_d, frictional bond τ_0 and slip hardening coefficient β were calculated from the load versus displacement curve measured from single fiber pullout tests, and were plotted in Figure 3.13, 3.14, 3.15.

It can be seen that matrix toughness K_m kept increasing with time, and saturated after about 3 days. The development of K_m is fastest at early age. The development of interface chemical bond G_d and frictional bond τ_0 remained relatively slow at the first 48 hours, accelerated considerably after 48 hours, and finally reached saturation after 7 days. Compared with K_m, the development of interface bonding strength was much lower at the early age until about 3 days.

It was the difference between the development rates of matrix toughness and matrix/fiber interface bonding that resulted in the quick change of the J_b'/J_{tip} ratio (J_b'/J_{tip} dropped from 41.2 at 3h to 7.9 at 24h). The age dependent development of J_b'/J_{tip} ratio is plotted in Figure 3.16. At the early ages, the fiber/matrix interface bonding was very low so that fibers were often pulled out instead of rupture, resulting in relatively high

complementary energy J_b'. At the same time, the value of J_{tip} was relatively low due to a lower K_m at early ages. Consequently, the high J_b'/J_{tip} ratio corresponded to high tensile strain capacity at the early age, i.e. at >3% at 5 h and 24 h. After 48 hours, the rapid increase in the interface bonding strength resulted in more and more fiber rupture instead of pulling-out. Reflecting on the micromechanical property, the fiber rupture before pull out led to a diminishing complementary energy J_b'. This was accompanied by an increasing J_{tip} corresponding to increased matrix toughness K_m. Therefore, the J_b'/J_{tip} ratio kept decreasing after 48 hours, leading to the deteriorated tensile strain capacity. Good correspondence can be found between the age dependent development of tensile strain capacity and J_b'/J_{tip} ratio.

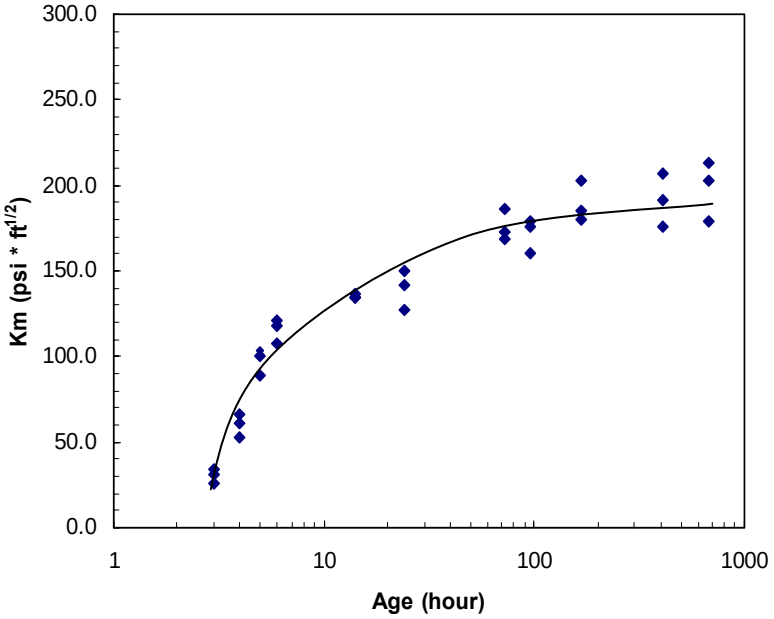

Figure 3.12: Age dependency of matrix fracture toughness

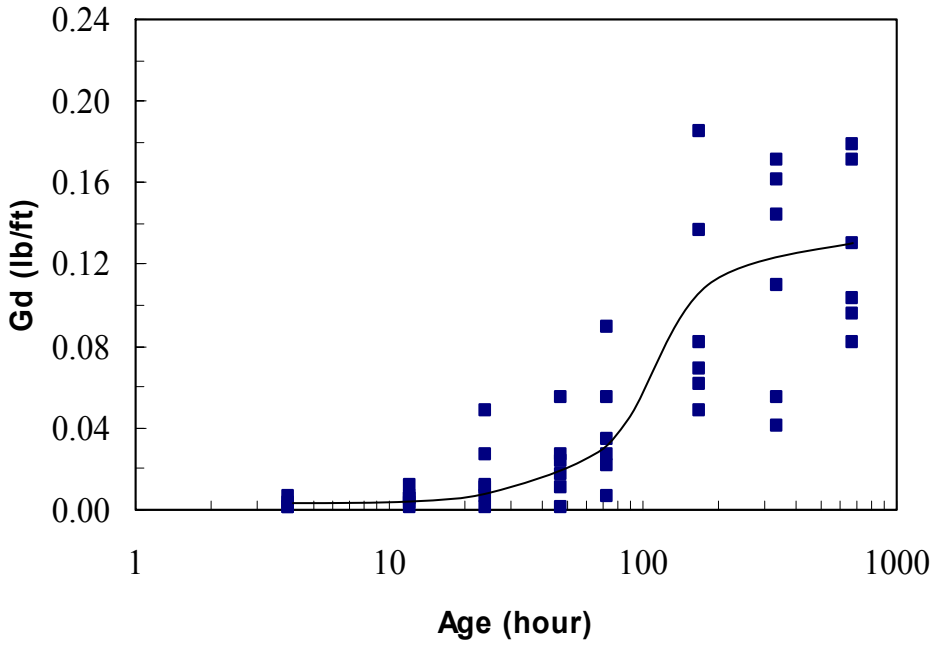

Figure 3.13: Age dependency of matrix/fiber interface chemical bond

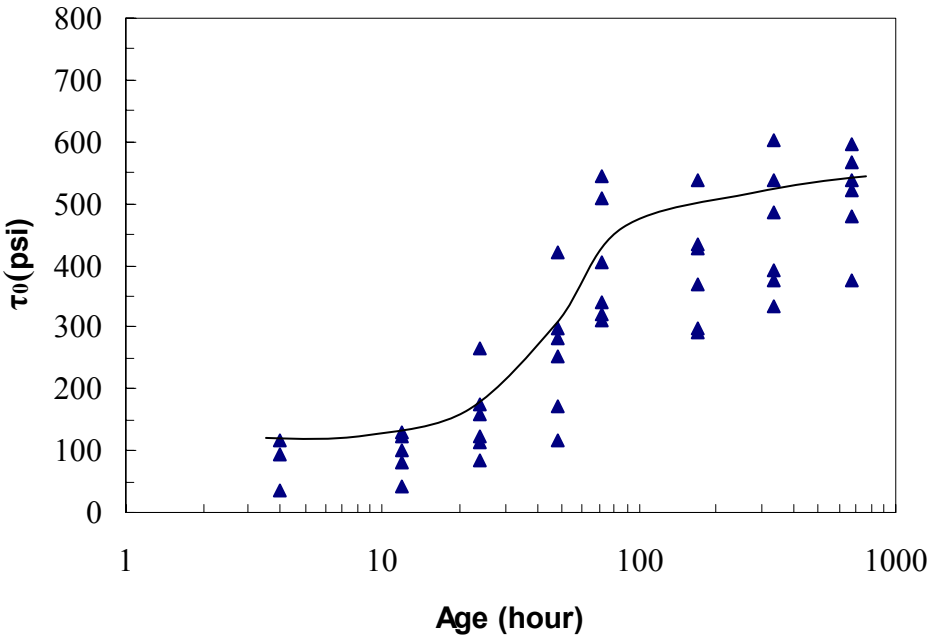

Figure 3.14: Age dependency of matrix/fiber interface frictional stress

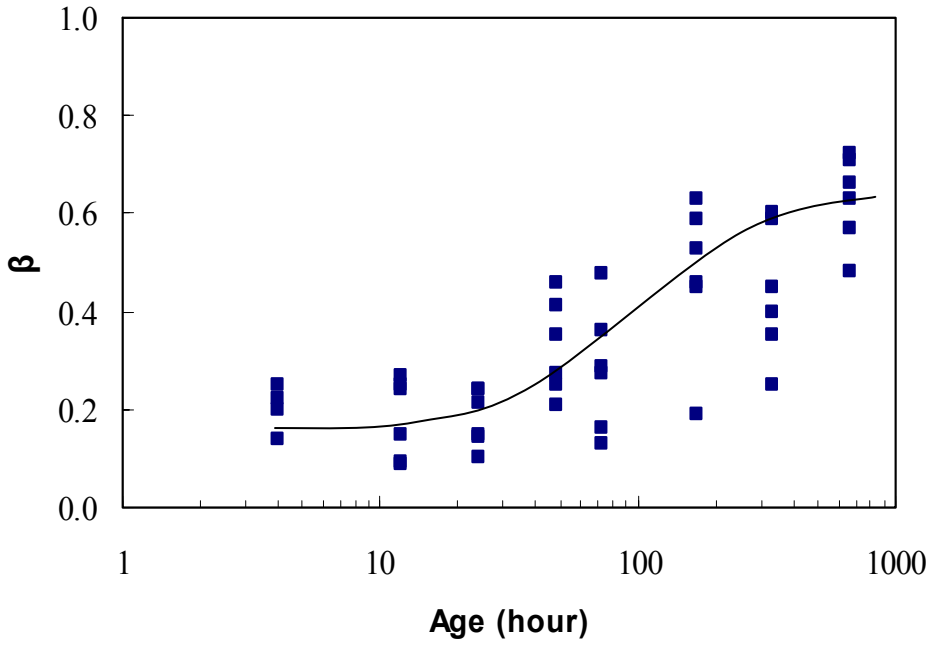

Figure 3.15: Age dependency of slip hardening coefficient

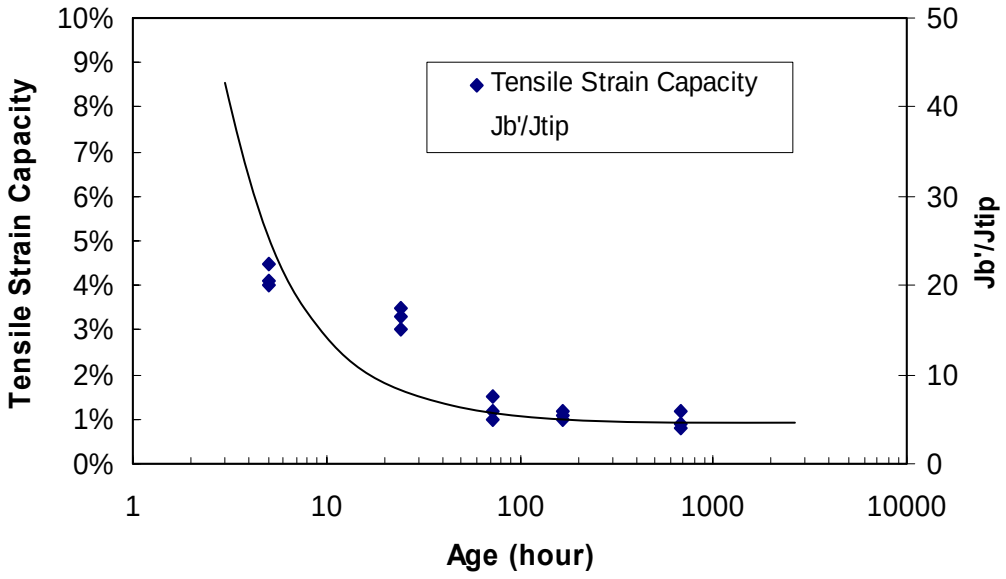

Figure 3.16: Evolution of tensile strain capacity and J_b'/J_{tip} ratio with age (Mix 6)

3.5.4 HES-ECC Material Tailoring Using Artificial Flaws

One approach to regain the HES-ECC tensile strain capacity is to introduce artificial flaws into the HES-ECC matrix, as discussed in Section 2.3.2. Polystyrene (PS) beads with a size of 0.157in were added as artificial flaws at a dosage of 5% by volume (Figure 3.16). Having cylinder shape with sharp edges and extremely weak bond with the surrounding cement binder, these PS beads can serve as crack initiators. The modified mixing proportion of HES-ECC (Mix 7) is the same as Mix 6 except the presence of additional PS beads (Table 3.4).

Figure 3.17 shows the tensile stress-strain curves of Mix 7 at age of 4h, 24h, 3d, 7d, 28d and 50d. Figure 3.18 compares tensile strain capacity of Mix 6 and Mix 7 at different ages. Significantly improved tensile strain capacity can be seen in Mix 7 at late ages after 24h. The strain capacity remains about 4% after 50d (Figure 3.17), as the saturation of micromechanical properties has been reached at about 7d, suggesting that the strain capacity can be retained in a long term. The first cracking strength of Mix 7 increases with age and stabilizes after around 7d, which is consistent with the development trend of matrix toughness K_m (Figure 3.11).

The introduction of PS beads exhibits little effect on the early compressive strength gain rate, although it greatly improves the multiple cracking behavior in tension. Figure 3.19 compares the compressive strength development of Mix 6 and Mix 7. The strength gain at the first 6 hours of the both mixes have no big difference, while at late ages Mix 7 exhibits lower compressive strength than Mix 6.

In summary, Mix 7 satisfies the strength requirements, workability requirement, and tensile strain capacity requirements at both early and late ages.

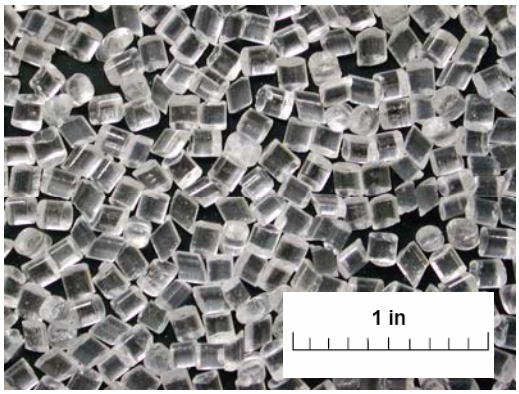

Figure 3.17: Aggregates used as artificial flaws: Polystyrene (PS) beads

Table 3.4: Mixing proportion of HES-ECC before / after adding artificial flaws

Mix	Cement	Silica Sand	Fly Ash	Water	Other Aggregates	Admixtures (wt% of cement)	Fiber V_f(%)
6	Type III 1.0	1.0	-	0.33	-	GL3200 0.75% + NC534 4.0%	2.0
7	Type III 1.0	1.0	-	0.33	PS Beads 0.064	GL3200 0.75% + NC534 4.0%	2.0

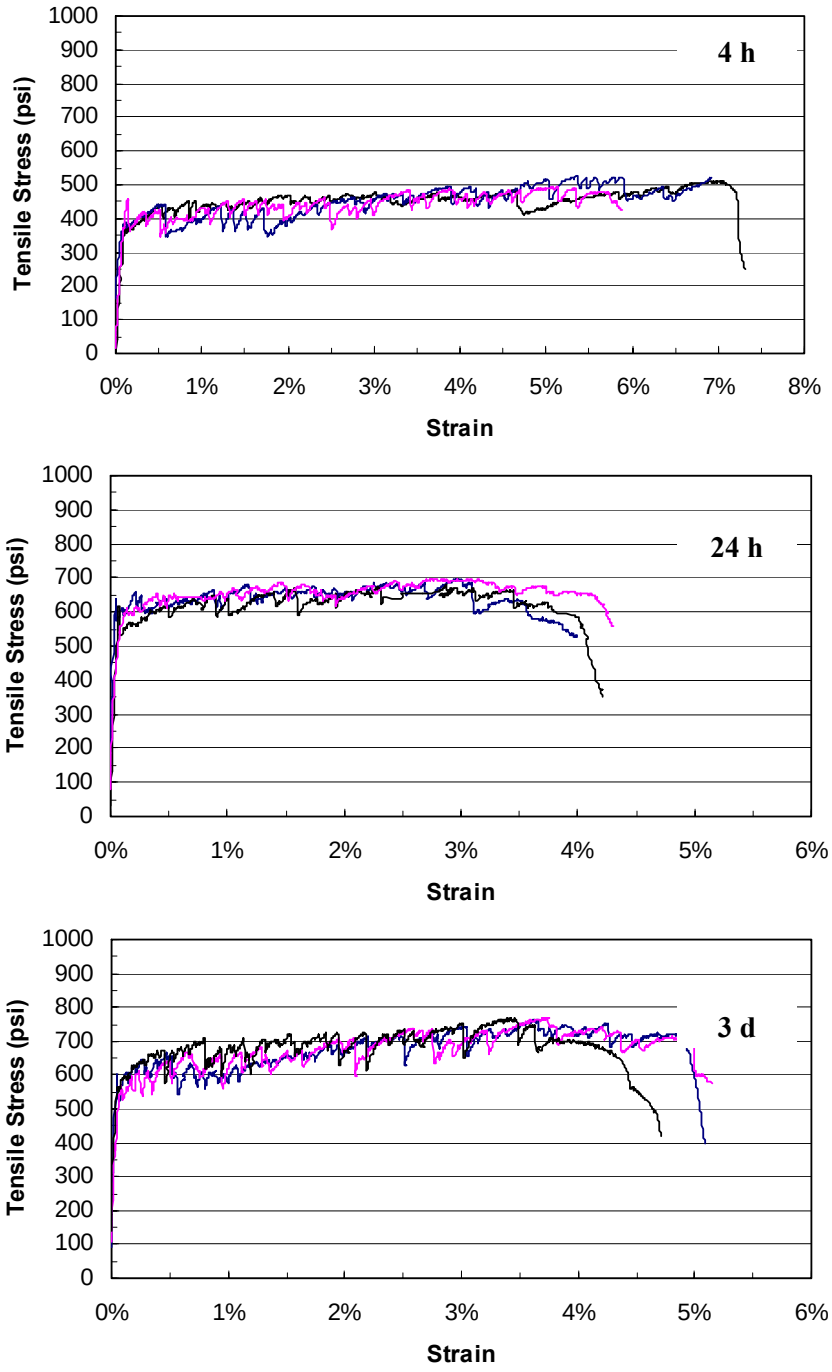

Figure 3.18: Age dependent tensile stress vs. strain curve of Mix 7

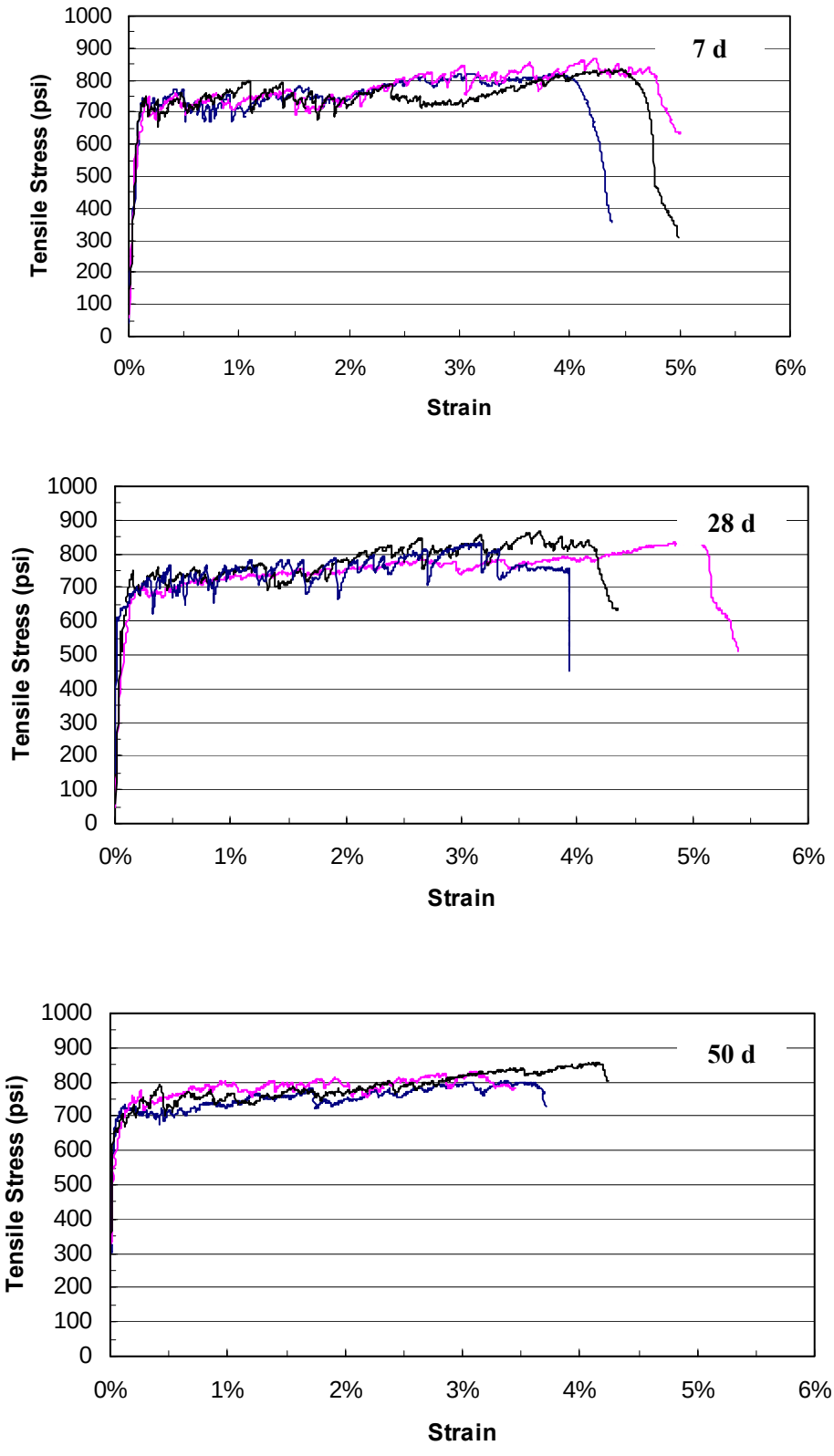

Figure 3.18: Age dependent tensile stress vs. strain curve of Mix 7

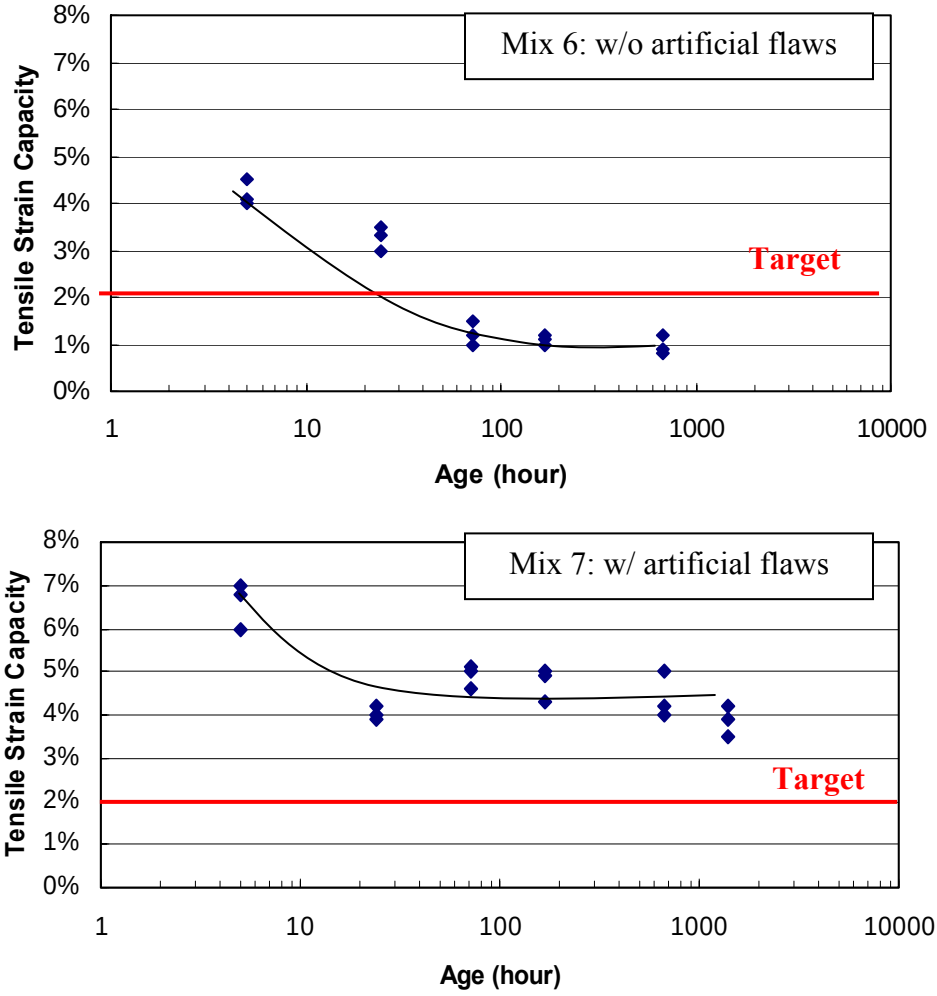

Figure 3.19: Age dependency of tensile strain capacity before (Mix 6) and after (Mix 7) adding artificial flaws

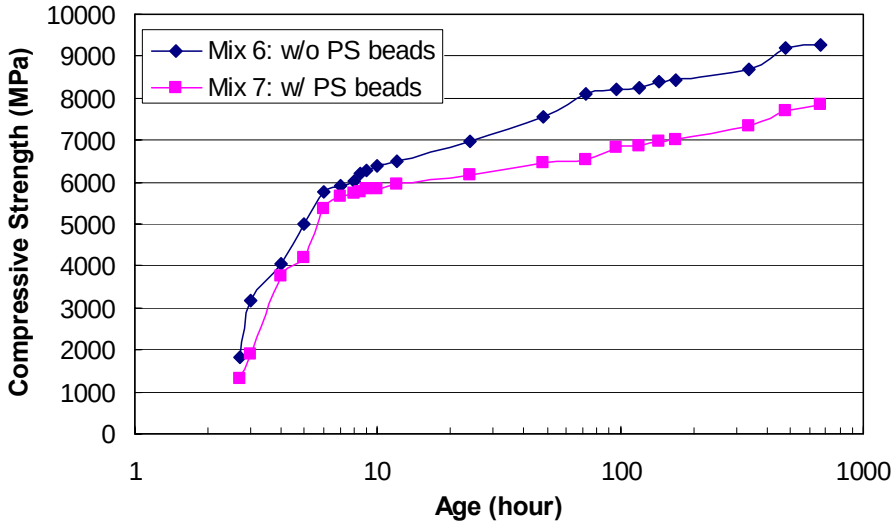

Figure 3.20: Effect of PS beads on compressive strength development

4. HES-ECC COMPOSITE PERFORMANCE DETERMINATION (TASK 3)

High Early Strength ECC (HES-ECC) has been developed under the guidance of micromechanical models in Section 3. The material can achieve the target compressive strength and tensile strain capacity at both early and late ages. The material mix proportion is summarized in Table 4.1.

Table 4.1: Mix proportion of high early strength ECC materials

HES-ECC Mix Design Parameter	Value (lb/yard^3)
Portland Cement, Type III	1547.37
Silica sand, F110	1547.37
Water	507.54
Poly-vinyl-alcohol Fiber	44.01
Polystyrene Beads	99.09
Superplasticizer, Glenium® 3200HES	11.61
Accelerating Admixture, Pozzolith® NC 534	61.83
Hydrating Control Admixture, Delvo® Stabilizer	Optional

In this section research was focused on detailed determination of HES-ECC composite performance. Extensive experimental work was done to investigate HES-ECC age-dependent properties under uniaxial tension, uniaxial compression, flexure, free shrinkage and restrained shrinkage. These properties were documented and reported here. The detailed research plan flow chart for the material properties documentation part is shown in Figure 4.1.

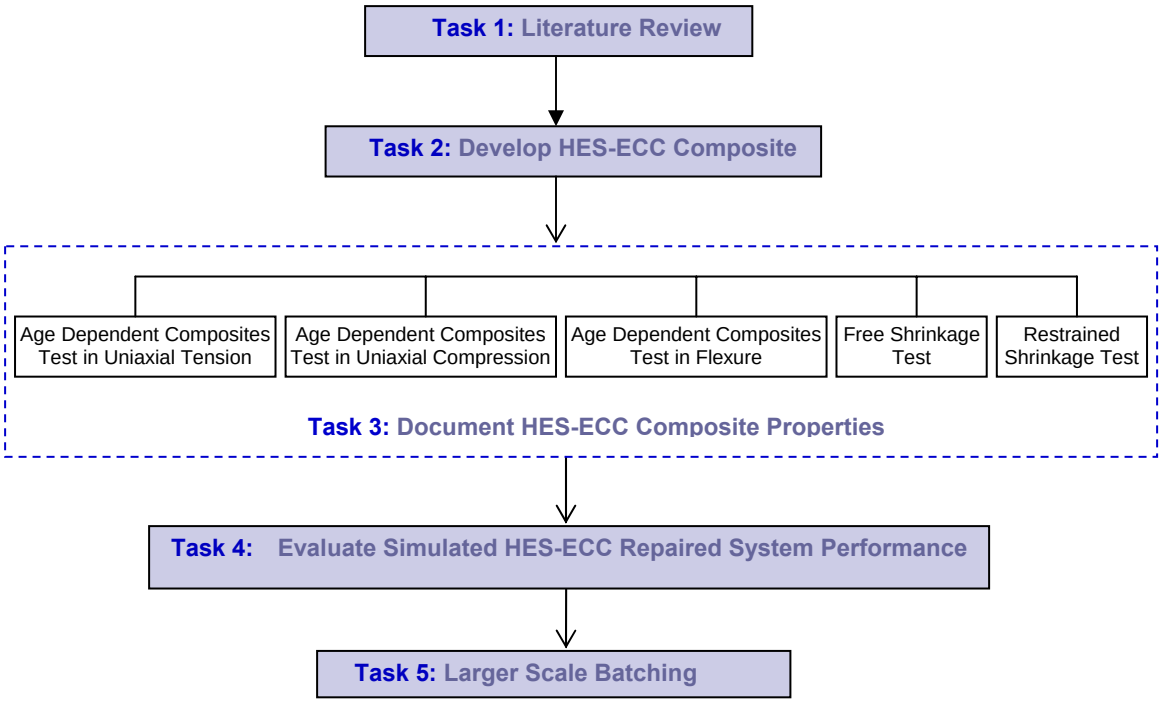

Figure 4.1: Detailed research plan flow chart – stage 2: HES-ECC composite properties documentation

4.1 Age Dependent Composite Test in Uniaxial Tension (Task 3a)

4.1.1 Motivation and Objectives

Repair material tensile ductility has been gradually recognized as the most critical property for achieving repair durability. Repair material with high tensile strain capacity and low Young's modulus can exhibit remarkable deformation compatibility with concrete substrate structure and thus prevent cracking. HES-ECC can achieve exceptionally high tensile strain capacity by developing multiple micro-cracks. These micro-cracks are not "real cracks" in the mechanical sense because they are very tiny and keep carrying increasing load after formation. Tensile strain capacity of HES-ECC material is mainly related to how many micro-cracks can be formed in the hardening stage before failure. Besides tensile strain capacity, evaluation of the crack width of these micro-cracks is also necessary because crack width determines the repair's

resistance to the ingress of water, chloride and other chemical agents which may cause durability problems.

In this task, age dependent composite tests in uniaxial tension were conducted on the developed HES-ECC mix. This task established a database of HES-ECC uniaxial tensile properties. The age-dependent development of its tensile strength, tensile strain capacity, crack width and crack pattern, as well as Young's Modulus were evaluated and documented.

4.1.2 Experimental Program

HES-ECC material was mixed in a Hobart type mixer with 0.424 cubic feet capacity. All of the mixing work in this section followed the procedure below:

1) Mix cement and sand for approximately 1 minute;
2) Add water slowly and continue mixing for 1-2 minutes;
3) Add superplasticizer and continue mixing for 1-2 minutes until a consistent mixture is reached;
4) Add fibers slowly and mix for 2 minutes until fibers are well distributed;
5) Add PS beads and mix for 1-2 minutes
6) Add hydration control admixture and mix for 1 minute, if casting will be performed after 15 minutes or longer time;
7) Add accelerator before casting and mix for 1 minute.

The whole mixing procedure for each batch normally took 10-15 minutes. After mixing, the mixture was cast into molds with moderate vibration applied. The molds were then covered with plastic sheets and cured in air at room temperature (60-70°F). Specimens were demolded and began testing after 4h.

Figure 4.2: Uniaxial tensile test setup

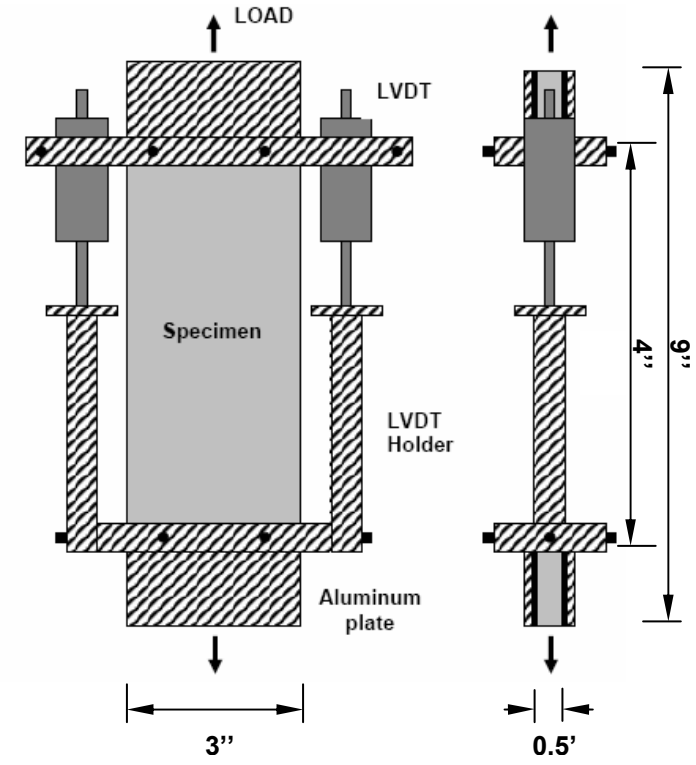

Figure 4.3: Dimensions of tensile test specimen

Uniaxial tensile tests were conducted to characterize the tensile behavior of the HES-ECC material. Direct uniaxial tensile test is considered the most convincing method to evaluate material strain-hardening behavior (Stang, 2003), since some quasi-brittle Fiber Reinforced Concrete (FRC) can also show apparent hardening behavior under flexural loading. Figure 4.2 and Figure 4.3 show the uniaxial tensile test setup and specimen dimensions. HES-ECC coupon specimen is 9" in length, 3" in width and 0.5" in thickness. Before testing, aluminum plates were glued to both ends of the coupon specimen to facilitate gripping. Tests were conducted on an MTS machine with 5.62kip capacity under displacement control at rate of 1.97×10^{-4}in/s. Two external LVDTs (Linear Variable Displacement Transducer) were attached to the specimen surface with a gage length of 4" to measure the displacement. Specimens were demolded at 4h, cured in air, and tested at different ages from 4h to 60d. Ten to fourteen specimens were tested at each age.

4.1.3 Results and Discussion

HES-ECC material exhibits significant tensile strain hardening behavior. Its typical tensile stress - strain curves at ages from 4h to 60d are shown in Figure 4.4. Figure 4.5 - 4.7 plot the age-dependent development of HES-ECC tensile properties. The strain capacity exceeds 5% at 4h, decreases a little to 4% at 3d, and retains an average 3.5% after 7d until 60d (Figure 4.5). The tensile strength increase rapidly during the first 24 hours, from 501 psi at 4h to 680 psi at 24h respectively, and continue increasing at a smaller slope at late ages to 839 psi until age of 60 days (Figure 4.6). The age-dependent development of HES-ECC tensile strength and strain capacity is due to the maturing of the composite matrix and fiber/matrix interface properties.

Young's modulus (E) of HES-ECC was determined from its tensile stress-strain curve. From each curve, E was defined as the slope of the line drawn between the starting point and the point corresponding to a strain of 0.015%. The 0.015% tensile strain is an approximate elastic strain capacity of ECC material (Li, 2004). The age dependency of HES-ECC Young's modulus is plotted in Figure 4.7. It can be seen that Young's modulus of HES-ECC increases with ages from 1900 ksi at 4h to 3452 ksi at 60d, which is lower than that of concrete material due to the absence of coarse aggregates

in the HES-ECC mix. The tensile properties of HES-ECC, including Young's modulus, tensile strength and strain capacity at different ages are summarized in Table 4.2. First cracking strength of HES-ECC can be hardly defined from the tensile stress-strain curve, and therefore it is not reported here.

Introduction of small volume proportion of PS particles into HES-ECC mix facilitates this material to develop saturated multiple micro-cracks under tensile loading, resulting in a high tensile strain capacity of the material. Figure 4.8 shows typical cracking pattern of tensile specimens tested at 4h, 24h, 3d and 28d. Epoxy glue was spread on the surfaces of the specimens before taking pictures for better revealing the cracking pattern. Near saturated multiple micro-cracks were observed at all the ages, with crack width below 2.76×10^{-3} in. It should be noted that crack width at the very early age – 4h is as low as around 0.39×10^{-3} in, which can be attributed to the relatively low matrix toughness, but rapidly developed interface bonding at the early age, so that saturated cracks form with very tight crack width.

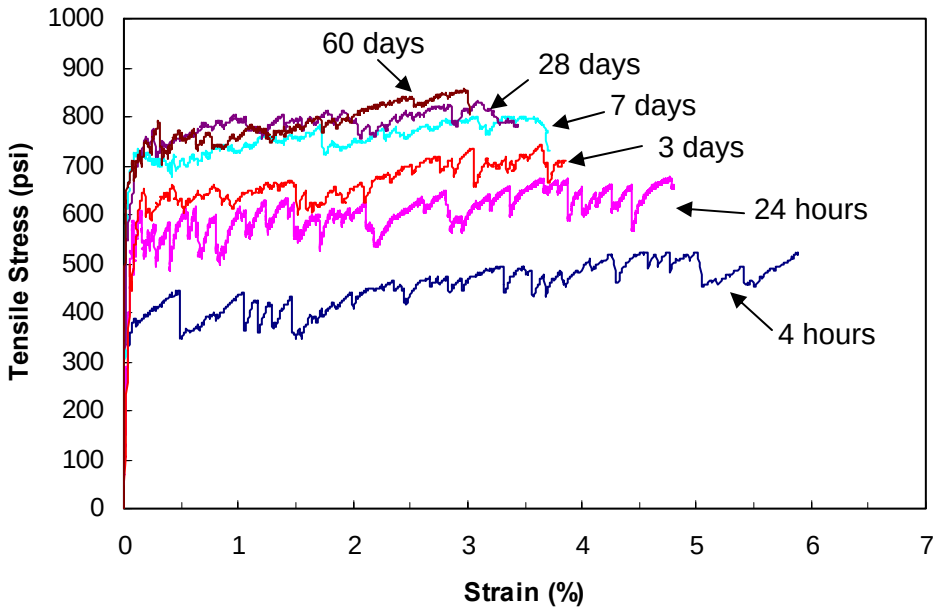

Figure 4.4: HES-ECC tensile stress-strain curve at different age

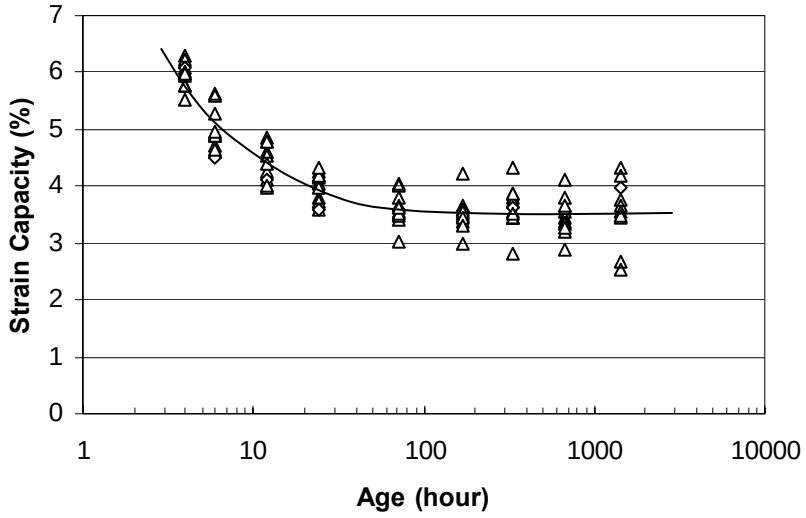

Figure 4.5: HES-ECC tensile strain capacity development with age

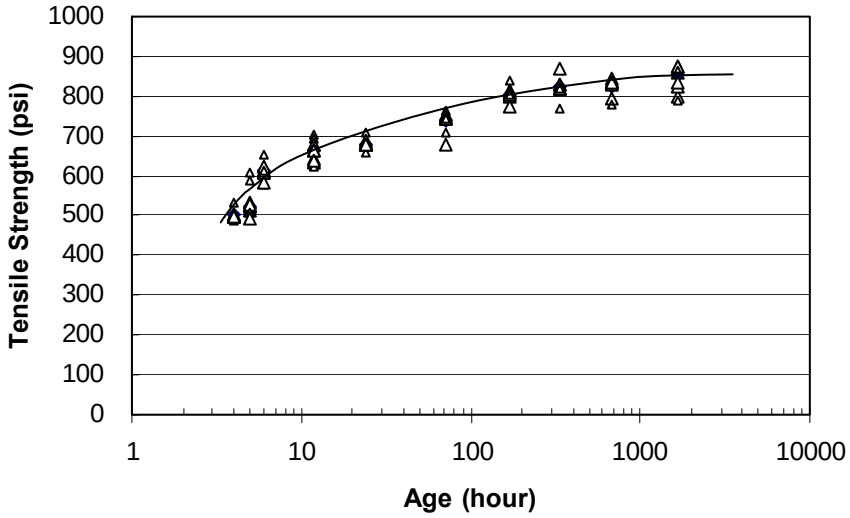

Figure 4.6: HES-ECC tensile strength development with age

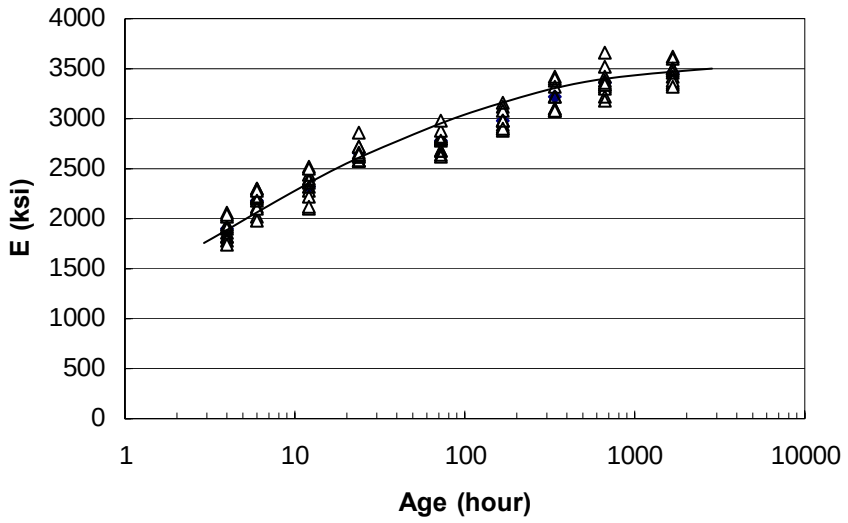

Figure 4.7: HES-ECC Young's modulus (E) development with age

Table 4.2: HES-ECC tensile properties at different ages (mean ± standard deviation)

Age	Young's Modulus (ksi)	Ultimate Strength (psi)	Strain Capacity (%)
4 h	1900.12 ± 111.44	501.23 ± 11.64	5.97 ± 0.22
6 h	2173.37 ± 114.11	610.41 ± 19.42	4.97 ± 0.38
12 h	2328.26 ± 147.29	662.27 ± 25.18	4.41 ± 0.33
24 h	2654.19 ± 84.87	680.35 ± 11.50	3.99 ± 0.27
3 d	2770.22 ± 116.91	738.32 ± 23.62	3.61 ± 0.28
7 d	2986.32 ± 100.90	806.82 ± 16.42	3.52 ± 0.29
14 d	3216.27 ± 147.47	823.42 ± 23.01	3.64 ± 0.37
28 d	3364.88 ± 139.77	823.19 ± 20.39	3.47 ± 0.62
60 d	3451.90 ± 103.45	839.27 ± 28.11	3.52 ± 0.57

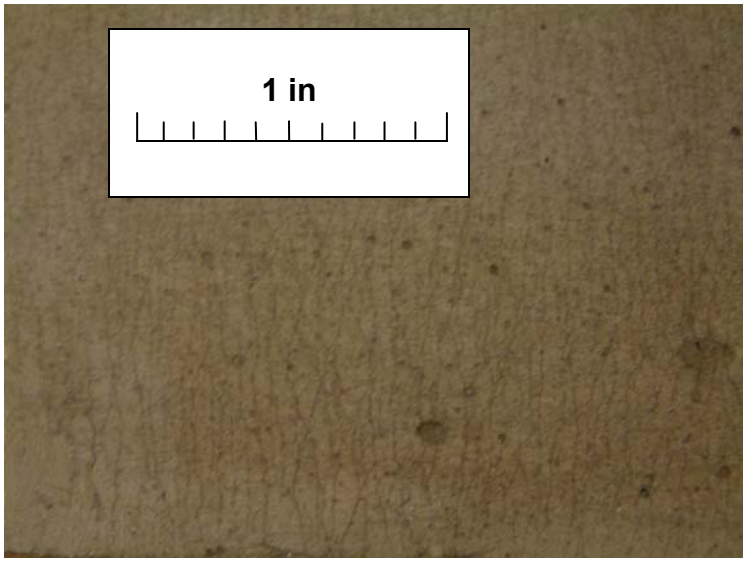

4h: crack width around 0.39×10^{-3} in

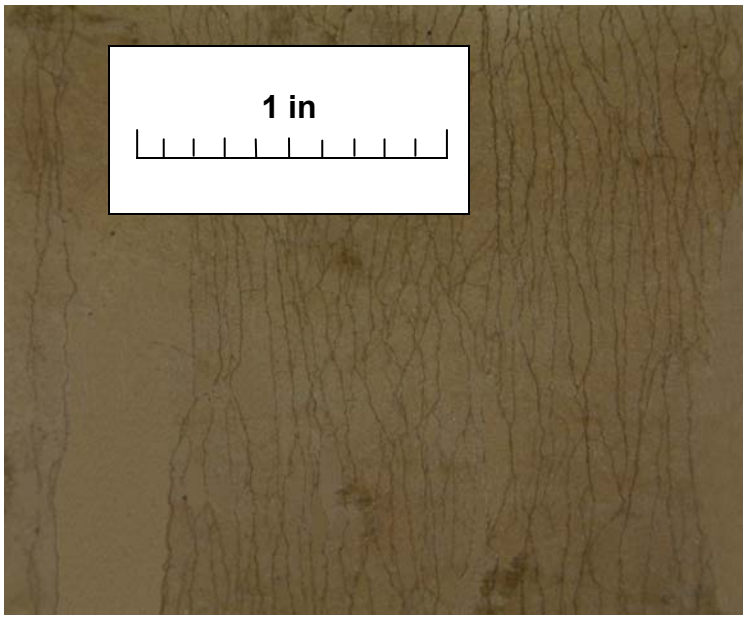

24h: crack width $1.18\times10^{-3} \sim 2.36\times10^{-3}$ in

Figure 4.8: HES-ECC multiple micro-cracking pattern at different ages

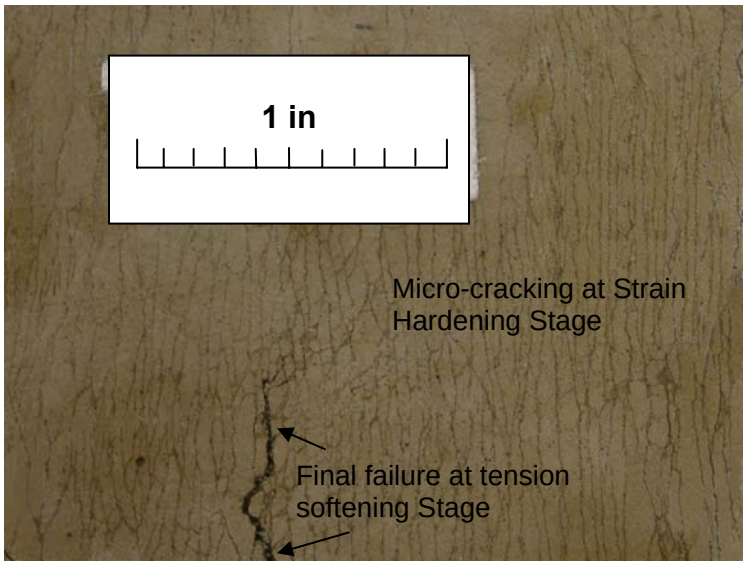

3d: crack width $0.79 \times 10^{-3} \sim 1.97 \times 10^{-3}$ in

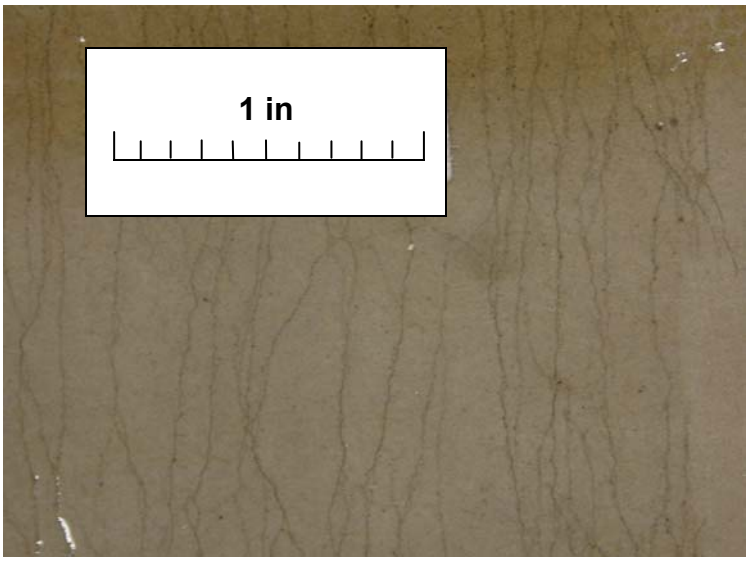

28d: crack width $1.18 \times 10^{-3} \sim 2.76 \times 10^{-3}$ in

Figure 4.8: HES-ECC multiple micro-cracking pattern at different ages

4.2 Age Dependent Composite Test in Uniaxial Compression (Task 3b)

4.2.1 Motivation and Objectives

How fast the HES-ECC as a repair material can gain its compressive strength at early ages determines how early the repaired structure can be re-opened to traffic. Age dependent composite tests in uniaxial compression were conducted on the HES-ECC mix. The purpose was to establish a database of HES-ECC compressive properties at both early and late ages.

4.2.2 Experimental Program

Compressive testing was conducted on a FORNEY F50 compressive test system with standard 3" × 6" cylinders, according to ASTM C39 "Standard Test Method for Compressive Strength of Cylindrical Concrete Specimens." The test set-up is shown in Figure 4.9. The ends of the specimens were capped with sulfur compound before testing. Tests began at 4 hours after casting. Specimens were demolded at 4h, cured in air, and tested at different ages from 4h to 60d. Ten to fourteen specimens were tested at each age.

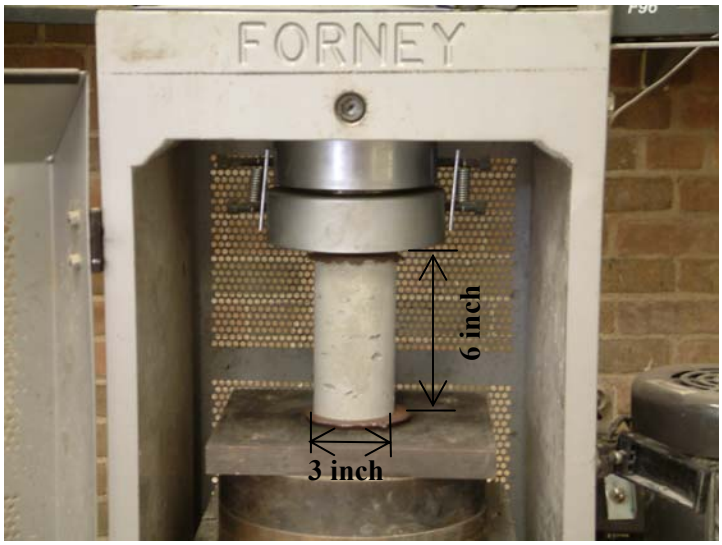

Figure 4.9: Uniaxial compressive test setup

4.2.3 Results and Discussion

It should be mentioned that a few standard 4" × 8" cylinders made of HES-ECC were also tested for comparison purpose. No difference in compressive strength exceeding the standard deviation was observed between the standard 3" × 6" and 4" × 8" cylinders.

Table 4.3: HES-ECC compressive properties at different ages

(mean ± standard deviation)

Age (h)	Compressive Strength (psi)
3h	1424.82 ± 81.54
4 h	3422.16 ± 203.33
6 h	4963.22 ± 181.51
12 h	5367.54 ± 266.43
24 h	6129.62 ± 201.55
3 d	6482.65 ± 343.99
7 d	6884.56 ± 274.83
14 d	7366.43 ± 344.71
28 d	8062.90 ± 315.03
60 d	8233.13 ± 250.08

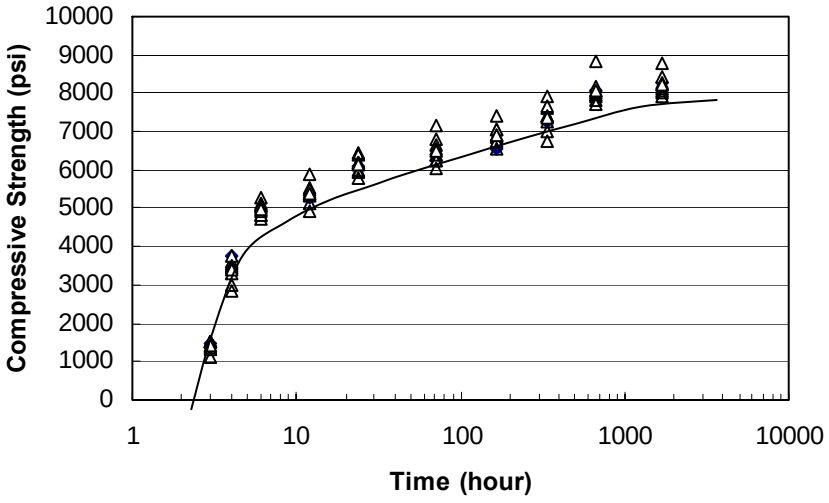

Figure 4.10: HES-ECC compressive strength development with ages

Figure 4.10 and Table 4.3 summarize HES-ECC compressive strength development at different specimen ages. The comparison between the compressive

strength development with the requirements by DOTs and FHWA is shown in Figure 4.11. Because of the high cement content, use of Type III Portland cement and accelerator, the HES-ECC material can gain compressive strength of 3422.16 ± 203.33 psi (mean ± standard deviation) in the first 4 hours and 4963.22 ± 181.51 at the age of 6 hours. Similar as the developing trend of tensile strength, the compressive strength of HES-ECC develops fastest during the first 24 hours, reaching 6129.62 ± 201.55 psi. The increasing trend slows down at later ages and arrives at 8062.90 ± 315.03 psi at the age of 28d, and 8233.13 ± 250.08 psi at the age of 60d. Furthermore, the HES-ECC cylinder specimens exhibited very ductile failure mode under the compressive loading with the final failure plane normally at 45° angle. In contrast, high early strength concrete (HES-Concrete) cylinder specimens were made and tested to have suddenly explosive failure due to the inherent high brittleness of this material.

It should be noted that the variation in the compressive strength of HES-ECC is lower than that for concrete. Coefficient of Variation (COV) is defined as the ratio of standard deviation to the mean value for a group of data. For HES-ECC, its COV of compressive strength is normally below 0.05 at ages from 4h to 60d. However for concrete, its COV of compressive strength can be as high as 0.112 calculated from the whole test data set. The higher variation in concrete compressive strength may come from the variation of coarse aggregates in concrete mix, and the brittle failure mode of concrete material under compressive loading.

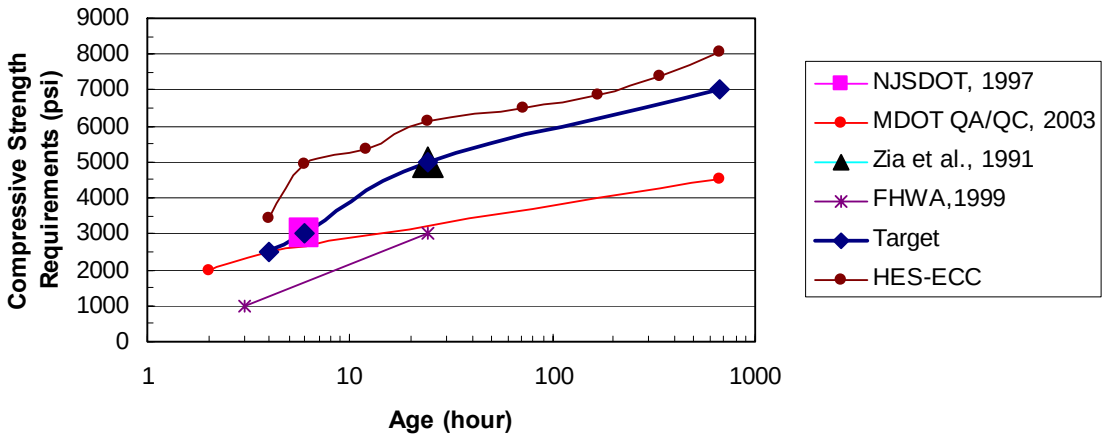

Figure 4.11: Compressive strength development of HES-ECC compared with requirements by DOTs and FHWA

4.3 Age Dependent Composite Test in Flexure (Task 3c)

4.3.1 Motivation and Objectives

Minimum flexural strength of repair material, besides its compressive strength, is usually specified by engineers as the requirements for the time before opening to traffic. The New Jersy State Department of Transportation specified target flexual strength of 350 psi in 6 hours to the "Fast-track mix" developed in mid-90's (Kurtz et al., 1997). The California State Department of Transportation (Caltran) requires a minimum flexual strength of 400 psi prior to opening to traffic for full depth pavement repair (Concrete Construction, 2001). FHWA Manual of Practice: Materials and Procedures for Rapid Repair of Partial-Depth Spalls in Concrete Pavement (FHWA, 1999) recommends minimum flexural strength of 450 psi according to ASTM C78 for Rapid-setting Cementitious Concretes.

For high early strength concrete, the flexural strength requirement is more stringent than the corresponding compressive strength requirement because of the material's brittle nature. In contrast, ECC material features very high flexural strength, or modulus of rupture (MOR) attributed to its high ductility and strain hardening behavior. The flexural strength of ECC normally approaches three times of the matrix flexural strength. It was expected that once HES-ECC has met the compressive strength requirements and tensile ductility requirements, the flexural strength target can be easily achieved.

In this task, age dependent composite test in flexure was conducted on the developed HES-ECC material. This task established a database of flexural properties of HES-ECC mix. HES-ECC flexural stress-deformation curve and material flexural strength / MOR at different ages were evaluated and documented.

4.3.2 Experimental Program

Testing procedures followed ASTM C78 "Standard Test Method for Flexural Strength of Concrete (Third-point bending)." The third-point bending test set-up and specimen dimensions are shown in Figure 4.12 and Figure 4.13. Each beam specimen measures 16 in (length) × 3 in (width) ×4 in (depth). The specimen has a test span length of 12'. Specimens were demolded at 4h, cured in air, and tested at different ages

from 4h to 60d. The air-curing condition was different from which specified in ASTM C78, and it was intended to simulate the curing condition in field applications, where the repair was expected to be exposed to air and open to traffic in 4 hours. Five specimens were tested at each age.

Figure 4.12: Third-point bending test setup

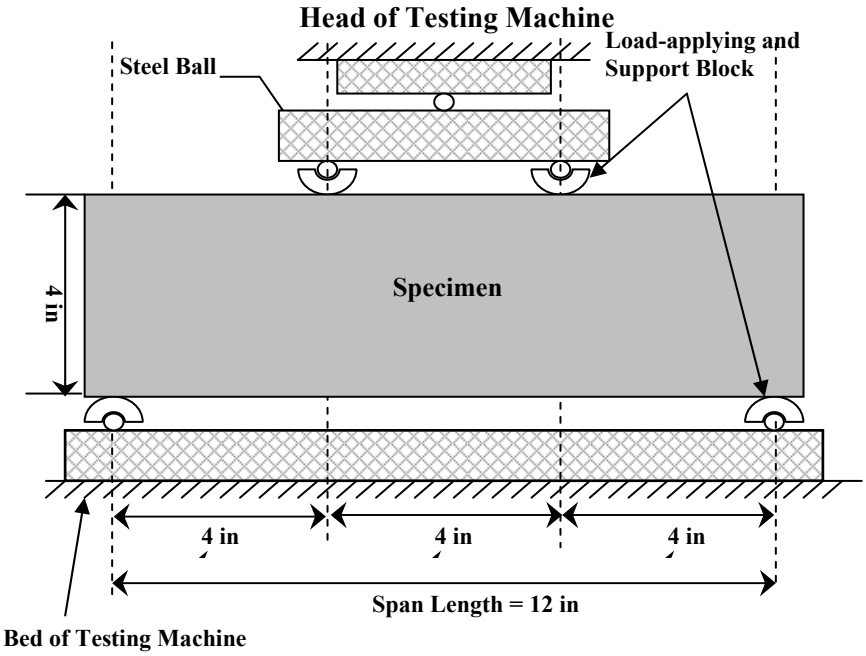

Figure 4.13: Dimensions of third-point bending test specimen

4.3.3 Results and Discussion

The flexural responses of HES-ECC at ages of 4h, 24h, and 28d are shown in Figure 4.14. Significant deflection hardening behavior was observed after the age of 4h. Both first cracking strength and ultimate flexual strength increased rapidly during the first 24 hours, and the increasing trend slowed down at late ages till 28 days. At the same time, specimen flexural ductility (deflection upon failure) decreased at the very early age, but approached constant after around 3 days and the composite demonstrated sufficient ductility at late ages. The flexural strength of HES-ECC is about 1500psi at age of 4h, which is significant higher than the all the target specifications in the documents described in section 4.3.1 . At later age, the flexural strength stabilizes at 2187.64 ± 49.87, which exceeds twice the normal values of high strength concrete.

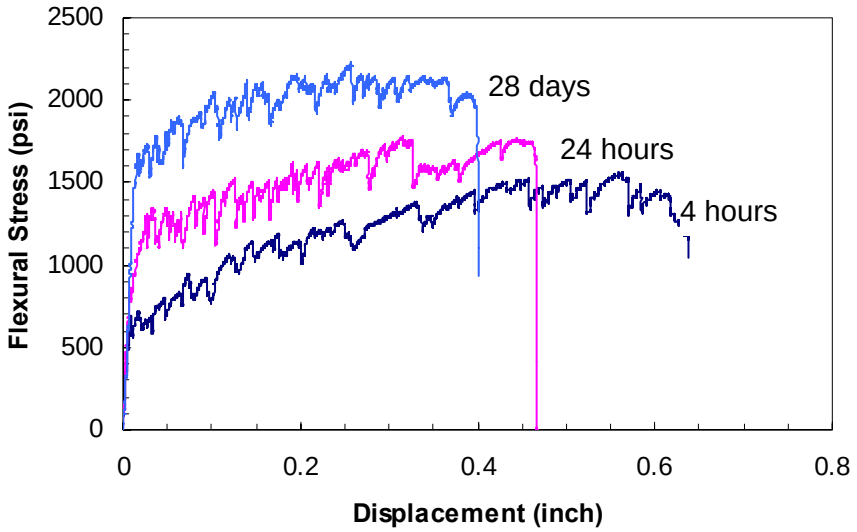

Figure 4.14: HES-ECC flexural strength / MOR – displacement curve at different ages

Table 4.4: HES-ECC flexural properties at different ages (mean ± standard deviation)

Age (h)	Flexural Strength / MOR (psi)	Deflection at Failure (in)
4 h	1422.19 ± 34.22	0.58 ± 0.02
6 h	1598.67 ± 51.94	0.61 ± 0.02
24 h	1655.54 ± 29.78	0.49 ± 0.02
3 d	1879.63± 50.79	0.42 ± 0.02
7 d	1965.28 ± 62.61	0.39 ± 0.01
28 d	2187.64 ± 49.87	0.38 ± 0.02

4.4 Free Shrinkage Test (Task 3d)

4.4.1 Motivation and Objectives

When repair material is bonded to the concrete structure, restrained volume change of the repair material due to drying shrinkage can induce early age repair cracking. The early age cracking is the insidious cause of many repair pathologies. It can introduce chloride, oxygen, moisture and other chemical agents into the repaired structure and cause durability problems. Therefore, the investigation of shrinkage properties of HES-ECC is of interest for repair durability concern. In this task, free shrinkage behavior of HES-ECC is determined and compared to normal ECC (M45), high early strength concrete (HES-Concrete) and normal concrete. The results can help to estimate shrinkage deformations of prospective HES-ECC repairs.

4.4.2 Experimental Program

The testing procedure followed ASTM C157 "Test Method for Length Change of Hardened Cement Mortar and Concrete" and C596 "Standard Test Method for Drying Shrinkage of Mortar Containing Portland Cement." The free drying shrinkage test set-up is shown in Figure 4.15. Twenty specimens were made and demolded after one day. After storage under water for two days the specimens were in equilibrium with 100% relative humidity. The drying shrinkage deformation of the HES-ECC specimens was then measured as a function of drying time until the hygral equilibrium was reached. Drying shrinkage of a high early strength concrete (HES-Concrete) mix was also measured as control. The drying shrinkage strain of ECC (M45) and normal concrete plotted in Figure 4.16 were adopted from (Weimann and Li, 2003).

4.4.3 Results and Discussion

The measured drying shrinkage strain as a function of the relative humidity is plotted in Figure 4.16. Five HES-ECC specimens stored at each relative humidity were measured and the average was plotted. In addition, the drying shrinkage of a HES-Concrete control mix, ECC M45, and normal concrete were also shown in Figure 4.16. The ECC M45 is a normal type I cement based ECC material, with mixing proportion the same as Mix 1 shown in Table 3.2. The drying shrinkage of HES-ECC is

found to be approximately twice of that of the HES-Concrete control mix. This was expected because of the very high cement content and lack of coarse aggregates in HES-ECC mix. HES-ECC drying shrinkage is also higher than ECC M45, also due to high cement content (no fly ash) in its mix.

It should be noted that the drying shrinkage strain of HES-ECC is approximately one magnitude lower than tensile strain capacity of this material. This suggested that when drying shrinkage of HES-ECC is restrained, the material can accommodate the shrinkage deformation of itself by forming multiple micro-cracks at its strain hardening stage.

Figure 4.15: Free drying shrinkage test setup

Table 4.5: Drying shrinkage strain as a function of relative humidity

Relative Humidity (%)	Total Drying Shrinkage Strain (%)			
	HES-ECC	HES-Concrete	ECC (M45) *	Normal Concrete *
25	0.267	0.125		
30			0.210	0.095
45	0.237	0.112		
60	0.202	0.099		
65			0.142	0.078
80	0.162	0.072		
100	0	0	0	0

* Data were adopted from (Weimann and Li, 2003)

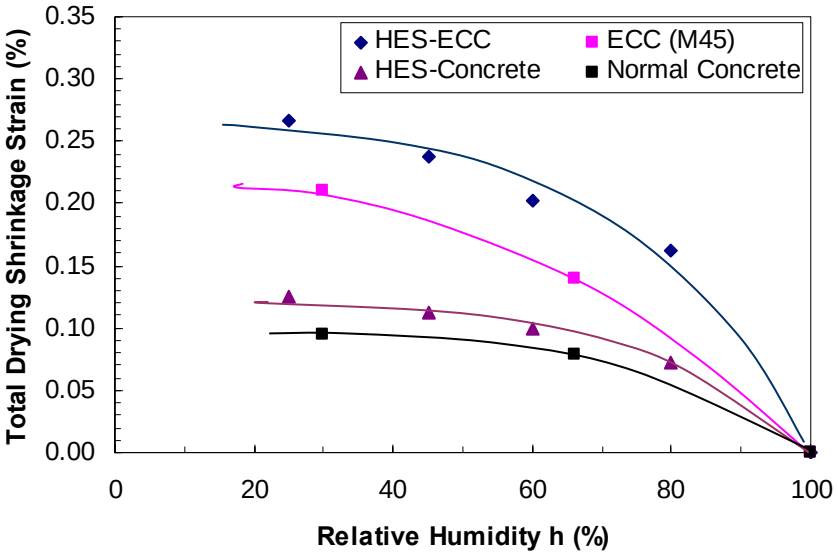

Figure 4.16: Drying shrinkage strain as a function of relative humidity

4.5 Restrained Shrinkage Test (Task 3e)

4.5.1 Motivation and Objectives

In order to achieve high early strength at very early ages when developing HES-ECC, fly ash was eliminated from the HES-ECC mix. Lack of replacement of cement with fly ash can increase drying shrinkage deformation of the HES-ECC material. In section 4.4, the free drying shrinkage test has verified that drying shrinkage strain of HES-ECC is higher than ECC M45, and greatly higher than concrete materials. The potential impact of this high free drying shrinkage deformation on durability in HES-ECC repair was investigated in this task. Specifically, restrained drying shrinkage test was conducted, which aims at establishing a database of restrained shrinkage properties of the HES-ECC. The restrained shrinkage crack pattern and crack width development with time were documented.

4.5.2 Experimental Program

Testing procedure followed AASHTO PP-34 "Standard Practice for Estimating the Crack Tendency of Concrete." The test set-up and specimen dimensions are shown in Figure 4.17. For each specimen, a layer of HES-ECC or HES-Concrete material was cast around a rigid steel ring. A plastic covered paper cylinder was used as an outer

mold during casting. The outer mold was removed 4 hours after casting, simulating time of opening to traffic. The specimen was subsequently exposed to 45±5% relative humidity. Drying shrinkage deformation of the HES-ECC layer was restrained by the steel ring, resulting in an internal radial pressure. From this, the HES-ECC layer was then subjected to a circumferential tensile stress state, which may cause cracking. The cracking pattern, crack number and crack width were measured as a function of time using a portable microscope. Measurements were taken at three different locations along each crack and the average value was plotted. Three HES-ECC specimens were investigated. Specimens made of HES-Concrete were also tested as control.

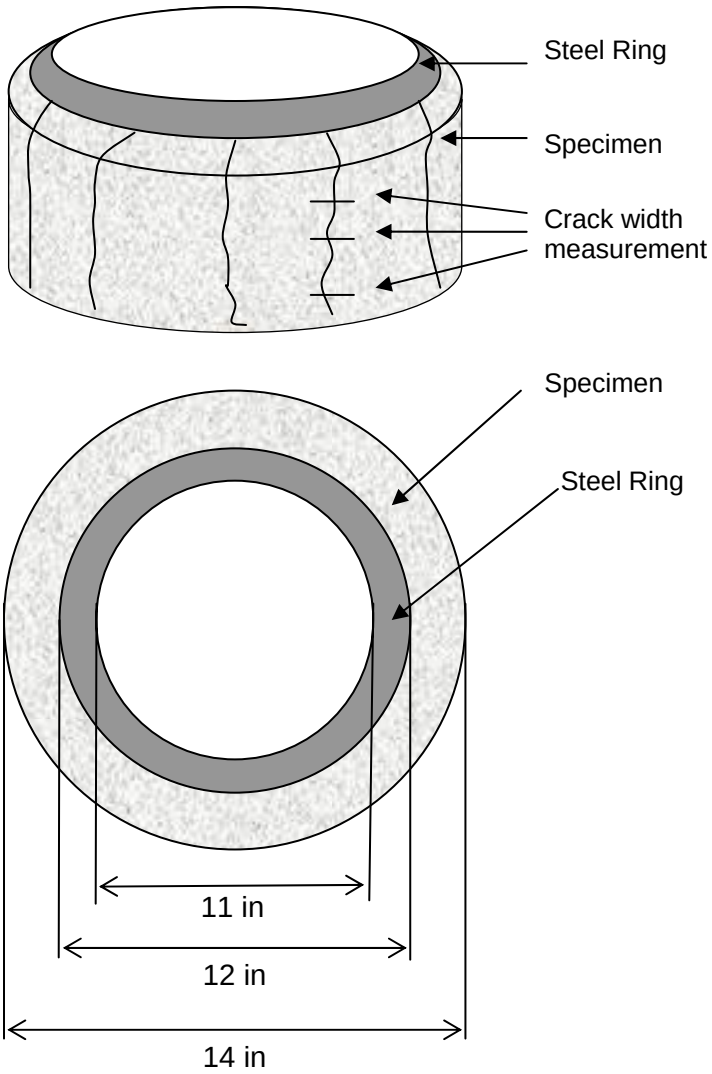

Figure 4.17: Restrained drying shrinkage test setup and dimensions

4.5.3 Results and Discussion

The crack widths due to restrained drying shrinkage for HES-ECC and HES-Concrete specimens were measured and shown in Table 4.6 and Figure 4.18. For each of the three HES-Concrete control specimens, one crack was observed with crack width of 49.3×10^{-3} in, 41.8×10^{-3} and 18.5×10^{-3} in respectively. However for each of the three HES-ECC specimens, 25, 23, and 19 cracks were formed respectively, with average crack width around 1.97×10^{-3} in, which is significantly smaller than crack width of HES-Concrete. Furthermore, the restrained shrinkage crack width of HES-Concrete kept increasing with ages, while the crack width of HES-ECC only increased a little at early age, and stabilized at later ages. Wang et al (1997) demonstrated the significance of crack width in controlling the permeability coefficient of cracked concrete. The permeability coefficient of cracked concrete was shown to decrease by seven orders of magnitude (from 10^{-4} to 10^{-11} ft/s) as crack widths decrease from 21.7×10^{-3} in to 0 in. When crack width falls below 3.94×10^{-3} in, the flow rate is similar to uncracked concrete. Hence even with a large number of surface cracks, ECC may behave like sound concrete with no cracks, by virtue of its tight crack width control.

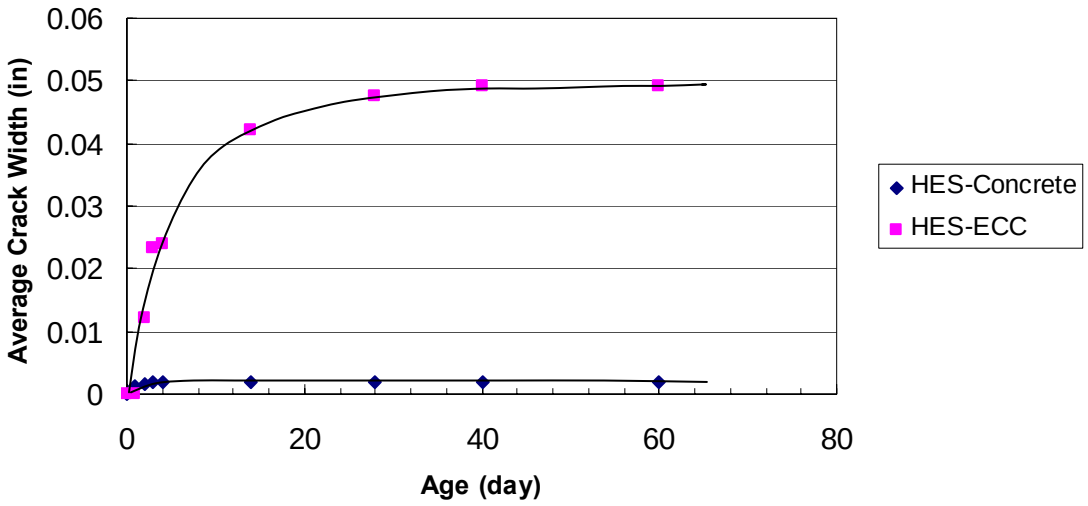

Figure 4.18: Restrained drying shrinkage crack width development with ages

Table 4.6: Restrained drying shrinkage crack width development with ages

Age (day)	Average cracking width (in)	
	HES-ECC	HES-Concrete
0	0	0
1	0.001182	0
2	0.001576	0.012214
3	0.00197	0.023246
4	0.00197	0.024034
14	0.00197	0.042158
28	0.00197	0.047674
40	0.00197	0.049250
60	0.00197	0.049250

5. HES-ECC SIMULATED REPAIR SYSTEMS (TASK 4)

High Early Strength ECC (HES-ECC) has been developed under the guidance of micromechanical models in Section 3. HES-ECC age-dependent properties under uniaxial tension, uniaxial compression, flexure, free shrinkage and restrained shrinkage were detailed measured and documented in Section 4. The material can achieve the target compressive strength and tensile strain capacity at both its early and late ages. Drying shrinkage deformation of HES-ECC is high due to the very high cement content and lack of coarse aggregates in its mix. However, under restrained drying shrinkage, HES-ECC can develop multiple micro-cracks with average crack width as low as 1.97×10^{-3} in. The high early age and late age compressive/flexural strength, large tensile strain capacity, low Young's Modulus and tight width of its multiple micro-cracks suggest the HES-ECC material as a durable material for concrete structure repair applications.

This research task focused on durability of the repaired system with HES-ECC repair material bonded to old concrete substrate. Repair surface cracking and interface delamination between the two layers under environmental and mechanical loading will be investigated. The detailed research plan flow chart for this task is shown in Figure 5.1.

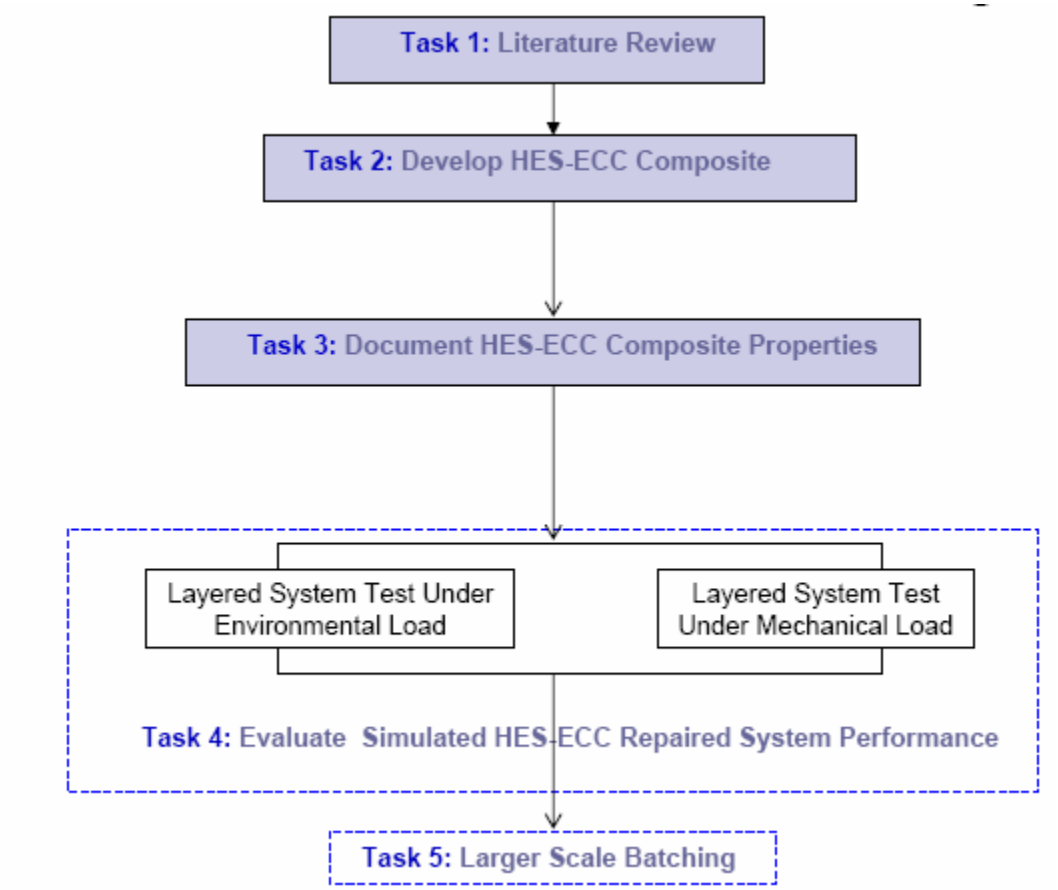

Figure 5.1: Detailed research plan flow chart – Task 4: HES-ECC simulated repaired systems

5.1 Layered System Test under Environmental Loading (Task 4a)

5.1.1 Motivation and Objectives

Concrete repair failure results from a variety of physical, chemical and mechanical processes. Generally it is the restrained volume change due to drying shrinkage or difference in thermal coefficient that induces early age repair surface cracking, or interface delamination between the repair and the old concrete. Cracking and delamination are the insidious causes of many repair pathologies. They facilitate the ingress of chlorides, oxygen, moisture, alkali or sulphates into the repaired system and accelerate further deterioration. For example, water penetrating through cracks can contribute to reinforcement corrosion or freezing-and-thawing damage. In overlay

repair applications, delamination of concrete bridge overlays from the substrate deck is one of the two primary causes of ultimate overlay failure (Kriviak, Skeet and Carter, 1995). Furthermore, the loss of structural integrity impairs load transfer between the repair and the old concrete structure. As a result, the repaired structure with unsatisfactory performance and unexpectedly short life must be repaired again, and consequently the significantly increased cost over the service life can be several times greater than the initial cost of structural design and construction.

High Early Strength Engineered Cementitious Composites (HES-ECC) is a promising repair material to improve durability of repaired concrete structures. By minimizing restrained drying shrinkage induced repair surface cracking and interface delamination between the repair layer and concrete substrate, concrete repair deterioration process can be interrupted at the beginning stage. Experiments were carried out on simulated layered repair systems under controlled humidity, and with variables of repair material type. Measurements of surface cracking and interface delamination magnitude confirm the effectiveness of simultaneously suppressing these two deterioration mechanisms when HES-ECC is used as the repair material. The experimental results will further serve as a basis for discussion of potential differences in concrete repair design between using ECC repair material and using traditional repair materials.

5.1.2 Background

In concrete repair applications, the immediate shrinkage deformation of the "new" repair material after placement is restrained by the "old" concrete substrate, which has already undergone shrinkage. Consequently, tensile stress is developed in the repair layer, and a combination of tensile and shear stress is built up along the interface between the repair and the concrete substrate. These stresses may cause repair surface cracking, and/or interface delamination as shown in Figure 5.2. Crack width and delamination magnitude determine the transport properties through the repair system, therefore they are closely related to repair durability. The detailed discussion on stress distribution and failure mechanism in a repair system undergoing drying shrinkage can be found in Wittmann and Martinola (2003).

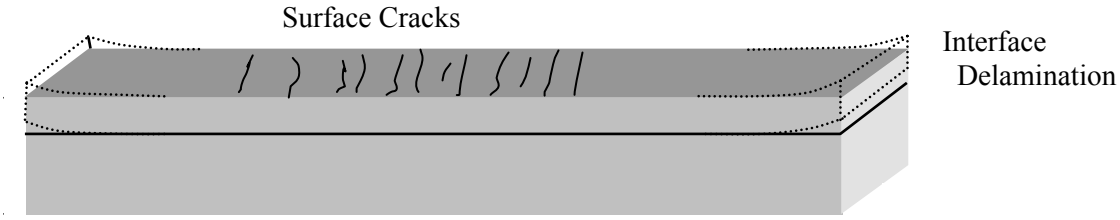

Figure 5.2: Layered repair system failure modes

Li (2004) illustrated the effect of inelastic strain capacity of cementitious material on the cracking behavior of a 2-D slab geometry of length L restrained at its ends. For brittle or quasi-brittle repair material with tension softening behavior, the cracking potential under restrained shrinkage is defined as:

$$p = (\varepsilon_{sh} - (\varepsilon_e + \varepsilon_{cp})) \tag{5.1}$$

where ε_{sh} is the material's shrinkage strain, ε_e is its elastic tensile strain capacity, and ε_{cp} is its tensile creep strain. If $p \geq 0$, one single crack forms in the repair material with crack width, w, proportional to the cracking potential p:

$$w = L((\varepsilon_{sh} - (\varepsilon_e + \varepsilon_{cp}))/(1 - L/2l_{ch})$$

$$\text{for } (\varepsilon_e + \varepsilon_{cp}) \leq \varepsilon_{sh} \leq w_c / L \tag{5.2}$$

where w is crack width, l_{ch} is Hillerborg's material characteristic length:

$$l_{ch} = EG_f / \sigma_t^2 \tag{5.3}$$

Variables E, G_f , σ_t, w_c are the material's Young's modulus, fracture energy, tensile strength, and critical crack opening. A linear tension-softening law is assumed where strength retention decreases from σ_t to 0 as the crack width opens from zero to w_c. Equation (5.2) indicates that crack width w depends on the cracking potential p, the degree of brittleness $L/2l_{ch}$, and the repair dimension L (Li, 2004). For instance, highly brittle material with relatively small characteristic lengths (l_{ch}), such as high strength concrete, is expected to exhibit more severe cracking with bigger crack width. Like other brittle or quasi-brittle materials, its crack width will increase with increasing structural dimensions.

In the case of a repair layer, the boundary conditions are different from the above. Restraint is applied at the base of the slab instead of its ends, leading to a number of

distributed cracks along the repair layer. In repair materials most of which are brittle, traction-free cracks will open with a crack width proportional to p. By the crack opening, stresses built-up at the interface can be relaxed, and the delamination values are expected to be small.

Steel fibers have been used recently in concrete repairs to control drying shrinkage and service load related cracking. For common tension-softening FRC material, shrinkage induced stresses are expected to induce surface cracking similar to normal concrete. However, since the cracks are bridged by fibers, some amount of tensile stress is still maintained in the layer. Therefore, tensile and shear stresses at the interface cannot be released by freely opening of cracks. As a result, interface delamination can be more prominent than the case of brittle repair material such as concrete and mortar.

In order to suppress both surface cracking of the repair layer and interface delamination, the repair material needs to exhibit "plastic straining" in order to accommodate its shrinkage deformation, and thus relieve the stresses built-up under restrained drying shrinkage conditions. By this means, repair cracking and interface delamination can be both minimized. Plasticity in the form of micro-crack damage has been demonstrated in HES-ECC. This material has been optimized in Task 2 (Section 3) to have large values of inelastic tensile strain capacity ε_i and tight micro-crack width at minimum fiber content. For HES-ECC, the cracking potential (Li, 2004) is modified as

$$p = (\varepsilon_{sh} - (\varepsilon_e + \varepsilon_i + \varepsilon_{cp}) \tag{5.4}$$

Figure 5.3 shows the tensile stress-strain curve of HES-ECC at different ages, with a strain capacity of more than 2.5%. This high ductility of HES-ECC is achieved by formation of many closely spaced micro-cracks. Near saturated multiple micro-cracks were observed at all the ages, with crack width below 2.76×10^{-3} in. It should be noted that crack width at the very early age of 4h is as low as around 0.39×10^{-3} in, which can be attributed to the very low matrix toughness and resulting high J_b'/J_{tip} ratio at the age of 4h. ECC's large value of ε_i gives a highly negative cracking potential p, indicating that localized fracture due to restrained shrinkage will never occur. The high tensile ductility of HES-ECC material, together with its tight crack width during

strain hardening stage, suggests HES-ECC as a promising material for durable repair jobs by minimizing repair surface cracking and interface delamination.

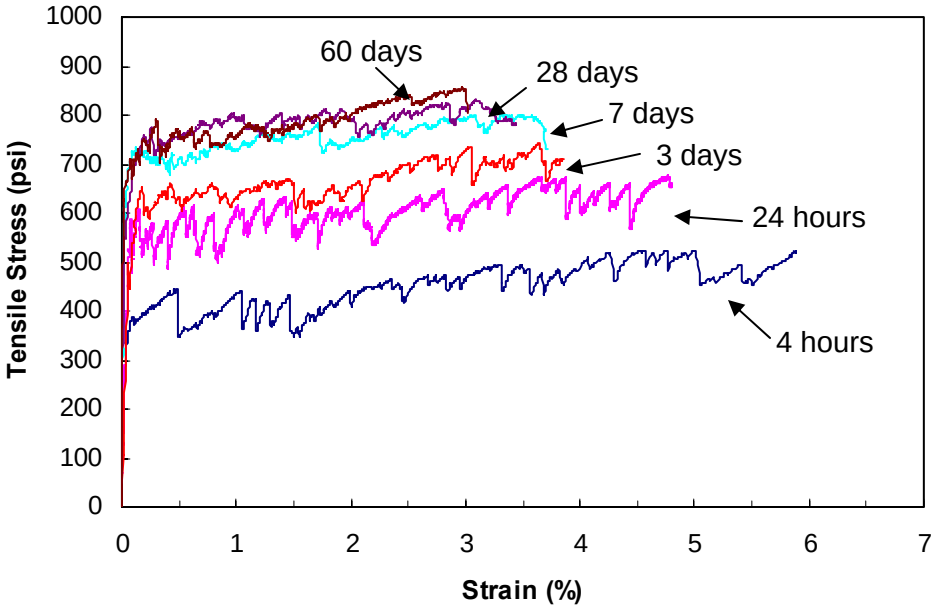

Figure 5.3: HES-ECC tensile stress-strain curve at different ages

5.1.3 Experimental Program

5.1.3.1 Materials

Three different repair materials — HES-Concrete, HES-Steel Fiber Reinforced Concrete (HES-SFRC) with tension softening stress-strain curve and HES-ECC were investigated. HES-Concrete and HES-SFRC were employed as controls since they have been used in repair applications. All of the three materials use Portland type III cement to achieve high early strength. The material mixing proportions are summarized in Table 5.2. Six specimens of each mix were tested to achieve the materials' mechanical properties in Table 5.3.

Both the HES-Concrete repair and the concrete substrate had the same material composition, except that the concrete substrate was ordinary concrete containing Portland type I cement, instead of Portland type III cement. HES-Concrete mixture, as shown in Table 5.3, consisted of coarse aggregate (CA) with 0.55 in nominal grain size, Portland type III cement (C), sand (S) and water (W). Superplasticizer (SP) was used to achieve

sound workability. Accelerating admixtures (AC) helped to accelerate the material's strength development and setting processes. HES-Concrete specimens were tested to have average compressive strength (f_c') of 7234 psi at the age of 7 days, and 7860 psi at the age of 28 days. Under tensile loading, HES-Concrete is a brittle material with sudden fracture failure.

Table 5.2: Repair materials composition

Material	**C** [(a)]	**W**	**S**	**CA**	**SP**	**AC**	**V_f**
HES-Concrete	1.0	0.4	1.3	1.3	0.005	0.04	--
HES-SFRC	1.0	0.4	1.3	1.3	0.005	0.04	0.01 [(c)]
HES-ECC (Mix 7)	1.0	0.33	1.0	0.064 [(b)]	0.0075	0.04	0.02 [(d)]

[(a)] Portland type III cement
[(b)] Polystyrene beads as coarse aggregates for HES-ECC
[(c)] Steel hooked fiber
[(d)] PVA fiber

Table 5.3: Repair materials mechanical properties

Material	**ε_u %**	**f_c' (psi)** [(a)]	**f_c' (psi)** [(a)]	**Tensile Behavior**
HES-Concrete	0.01	7234±228 (7d) 7860±345 (28d)	3803±196 (7d) 4025±221 (28d)	brittle
HES-SFRC	0.01	7462±348 (7d) 8254±290 (28d)	3725±287 (7d) 4231±189 (28d)	quasi-brittle
HES-ECC	2.5~5	6885± 275 (7d) 8063±315 (28d)	2986±101 (7d) 3365±140 (28d)	ductile

[(a)] Mean ± standard deviation

HES-SFRC mixture had the same composition with concrete mixture, except that it contained 1% (V_f, volume fraction) steel fibers. The steel fiber with length of 1.18 in and diameter of 0.02 in had smooth surface and hooked ends. The averaged 7-day and 28-day compressive strength of the HES-SFRC were 7462 psi and 8254 psi. Under tensile loading, SFRC is a quasi-brittle material with tension softening stress-strain curve. The softening part on the stress-strain curve is a result of the steel fiber's bridging effect. Both the HES-Concrete and the HES-SFRC had ultimate tensile strain capacity (ε_u) of around 0.01%.

The HES-ECC mixture was shown in Table 5.2. It comprised of Type III Portland cement (C), water (W), silica sand (S) with 3.94×10^{-3} in nominal grain size, polystyrene beads with a size of 0.157 in as coarse aggregates, superplasticizer, accelerating admixtures, and 2% (V_f) polyvinyl-alcohol (PVA) fibers. These PVA fibers (PVA-REC 15) had length of 0.472 in and diameter of 1.54×10^{-3} in. The HES-ECC material is self-consolidating before starting setting. Adjusted amount of stabilizer can be used if necessary to achieved desired setting time. The HES-ECC mixture had averaged compressive strength of 6885 psi at the age of 7 days, and 8063 psi at the age of 28 days. Its Young's modulus was averaged to be 2986 ksi at the age of 7 days, and 3365 ksi at the age of 28 days, which was lower than that of HES-Concrete (3803 ksi at 7 days; 4025 ksi at 28 days) and HES-SFRC (3725 ksi at 7 days; 4231 ksi at 28 days) due to the absence of coarse aggregates (CA) in its composition. A lower modulus repair material is desirable in limiting the tensile stress induced by restrained drying shrinkage.

Since drying shrinkage is a time-dependent process, it is necessary to evaluate the development of HES-ECC's tensile strain capacity at different ages. Direct tensile tests were conducted from material age of 4h up to 60d. The test results (Figure 5.3) show that HES-ECC's tensile strain capacity changes with age, as a result of the subtle competition between the time dependent changes of the matrix toughness and the fiber/matrix interface bond properties. However, the tensile strain hardening behavior of HES-ECC with a strain capacity larger than 2.5% can be maintained at all ages.

5.1.3.2 Specimen Configuration and Surface Preparation

In this study, layered repair systems were experimentally investigated with three different repair materials; HES-Concrete, HES-SFRC and HES-ECC. Concrete substrates were initially cast with dimensions of 63" × 4" × 4", as shown in Figure 5.4. They were moisture-cured until the age of 28 days, and then left to dry in ambient condition for an additional 150 days before the repair layers were placed. The additional 150 days were for the purpose of allowing any potential shrinkage in the substrates to occur before bonding the repairs.

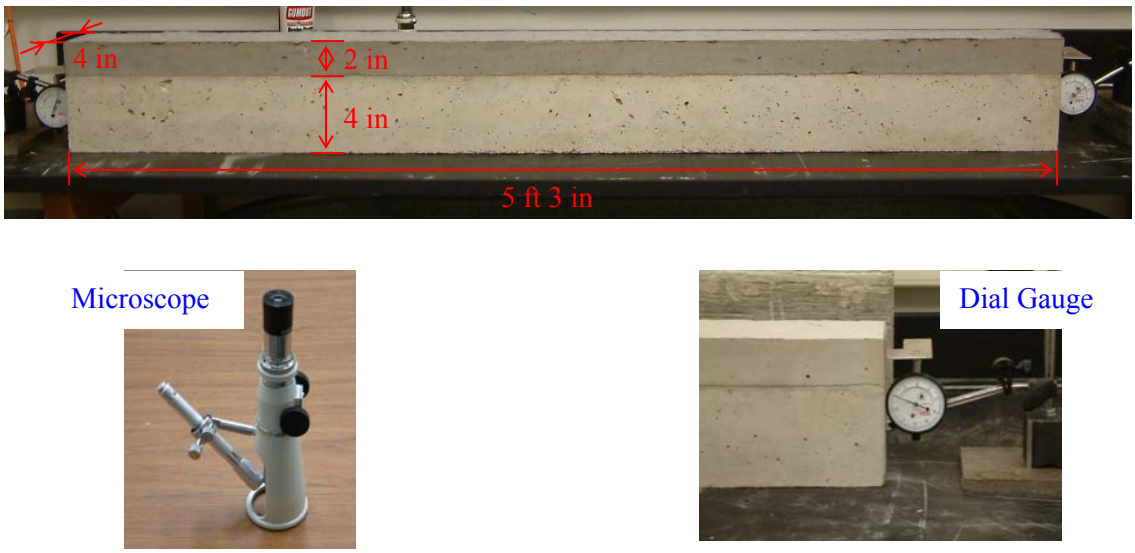

Figure 5.4: Layered repair system test set-up under restrained shrinkage

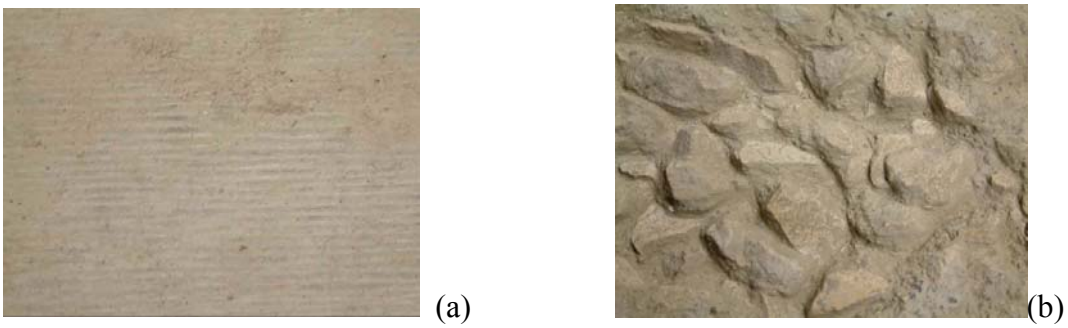

Figure 5.5: Concrete substrate surface preparation: (a) before roughened (b) roughened

The contact surfaces of the concrete substrates were roughened in fresh state using a chisel to remove slurry cement from external surfaces of coarse aggregates. The estimated roughness amplitude was 0.15 to 0.20 in, as shown in Figure 5.5. Before placing the repair layer, the substrate surface was recleaned with a brush and high-pressure air to ensure a clean bonding surface, and then it was dampened by spraying water fog on it. The moisture level of the contact surface was critical to achieve bond: Excessive moisture in a contact surface may clog the pores and prevent absorption of the repair material. On the other hand, excessively dry substrate contact surface may absorb excessive water from the repair material, resulting in undesirable excessive shrinkage. After dampening the surface, a 2-in-thick repair layer made of

each of the three repair materials was cast on the top of the concrete substrate. The repair layers were moisture cured for 6 hours and then demolded. After demolding, the layered specimens were moved into a room with ambient conditions of 60-70°F, and 35-55% RH.

For each specimen, two dial gauges (Figure 5.4) were used to record interface vertical separation distance at end locations of the specimens as a function of drying time after delamination begins. In addition, a portable microscope (Figure 5.4) was used to measure the delamination at 30 different locations along the interface, from which the delamination crack profile was derived. The microscope was also employed to observe crack pattern, crack number and crack width of the top surface of the repair layer, as a function of age. Both the delamination and the surface cracking were measured on a daily basis.

Free shrinkage tests were also carried out to characterize free shrinkage properties of the HES-Concrete, HES-SFRC and HES-ECC mixtures. The test setup was the same as shown in Figure 4.14. The free shrinkage tests specimens were from the same batch as the repair layer mix for each of the three repair materials. The tests were conducted according to ASTM C157/C157-99 and ASTM C596-01 standards, except that the storing and testing environment of the specimens was modified to be exactly the same as the layered specimens, with ambient condition of 60-70°F and 35-55% RH. The same storing and testing environment was for the purpose of relating the free shrinkage tests results to behavior of the layered specimens.

5.1.4 Experimental Results

5.1.4.1 Shrinkage of Repair Materials

Three specimens were tested for HES-ECC, HES-Concrete and HES-SFRC and the average free shrinkage strain (ε_{sh}) values were summarized in Table 5.4 and plotted in Figure 5.7. The data points show the shrinkage strain of each material at the age of 1d, 3d, 7d, 28d, and 60d. It should be noted that HES-ECC mixture had the highest shrinkage strain value because of higher cement content and absence of large coarse aggregates; HES-SFRC mixture had the lowest shrinkage strain value because of the constraint effect of steel fibers.

Table 5.4: Shrinkage strain of repair materials at different ages

Material	Free Shrinkage Strain (%)				
	1d	3d	7d	28d	60d
HES-Concrete	0.0301	0.0606	0.0815	0.1045	0.1100
HES-SFRC	0.0230	0.0442	0.0568	0.0768	0.0802
HES-ECC	0.0484	0.1500	0.1960	0.2419	0.2520

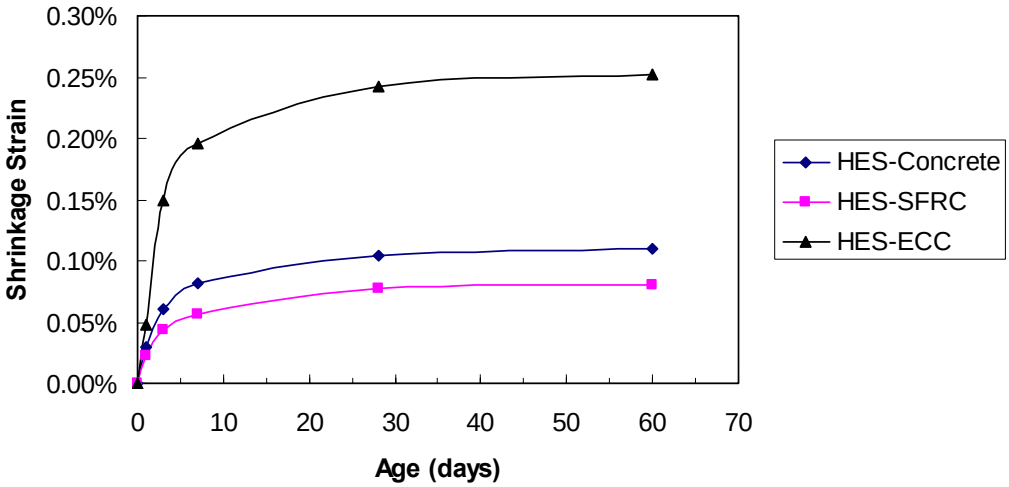

Figure 5.7: Shrinkage strain of repair materials at different ages

The cracking potential p for HES-Concrete, HES-SFRC, and HES-ECC can be estimated based on measured values of ε_{sh} and $\varepsilon_{i,}$ as shown in Table 5.5. The other parametric values (ε_e and ε_{cp}) were not measured in this study, but were adopted for estimation as the ε_e and ε_{cp} of normal concrete and SFRC from (Li, 2004). Although HES-ECC had the highest shrinkage, its negative p-value verifies that HES-ECC are on the strain hardening stage under restrained drying shrinkage, and will experience micro-cracking damage. In contrast, HES-Concrete and HES-SFRC are subjected to tensile fracturing due to their positive p-values.

Table 5.5: HES-Concrete, HES-SFRC and HES-ECC cracking potential estimation
(Properties were measured at specimen's age of 28 days.)

Properties	ε_{sh} (%)	ε_e (%)	ε_i (%)	ε_{cp} (%)	$p = \varepsilon_{sh} - (\varepsilon_e + \varepsilon_i + \varepsilon_{cp})$ (%)
HES-Concrete	0.105	0.01	0	0.02 - 0.06	0.035 - 0.075
HES-SFRC	0.077	0.01	0	0.02 - 0.06	0.007 - 0.047
HES-ECC	0.242	0.015	2.5 - 5	0.07	(-4.843) - (-2.343)

5.1.4.2 Repair Surface Cracking of Repair Layers Interface Delamination

Table 5.6 summarizes surface crack pattern, crack number and crack width of the three repaired systems respectively at the age of 60 days. Three specimens were tested for each repair material. It can be seen that when HES-Concrete was used as the repair material, 3-4 cracks localized at age of 60 days. The maximum crack width of the three specimens was 19.3 × 10^{-3} in. When HES-SFRC was used as the repair material, 1-4 localized cracks formed, and the maximum crack width of the three specimens was 11.0 × 10^{-3} in. The smaller crack width of HES-SFRC repair can be contributed by the steel fiber's bridging effect, as discussed in Section 5.1.2. It should be noted that because of a positive shrinkage cracking potential, the restrained shrinkage induced crack width for HES-Concrete or HES-SFRC repair is a structural property, which is dependent on structural dimensions.

Table 5.6: Interface delamination and surface cracking of different layered repair systems

Repair Material	Specimen Number	Delamination		Cracking	
		Height (in) ×10^{-3}	Length (in)	Number	Width (in) ×10^{-3}
HES-Concrete	(1)	3.54	6.69	3	6.30, 20.5, 14.6
	(2)	1.18	1.06	4	7.48, 13.4, 14.2, 19.3
	(3)	2.56	2.87	4	2.76, 15.0, 16.5, 17.7
HES-SFRC	(1)	12.2	12.72	2	4.33, 4.72
	(2)	10.2	11.85	4	1.97, 3.54, 4.72, 5.12
	(3)	11.8	13.46	1	11.0
HES-ECC	(1)	3.15	3.23	83	0.39 - 1.97
	(2)	1.97	1.85	109	0.39 - 2.36
	(3)	2.95	3.11	113	0.39 - 1.97

In contrast, when HES-ECC was used as the repair material, 83-113 micro-cracks were formed with the maximum crack width of 2.36 × 10^{-3} in, which was much smaller than that of HES-Concrete or HES-SFRC repair. The average crack width of HES-ECC repair was around 1.18 × 10^{-3} in. No localized fracture was observed. Since shrinkage strain of HES-ECC was less than 0.3 % (Figure 5.7), it was much below HES-ECC's tensile strain capacity of 2.5-5 %. Therefore, the restrained shrinkage cracking of HES-ECC was occurring in its strain-hardening stage, during which the material formed multiple microcracks with steady crack width. This indicates that the restrained shrinkage

crack width of HES-ECC repair is a material property, which is independent of structural dimensions. Even for larger scale repair applications with different types of restrained conditions, HES-ECC repair is still expected to exhibit tight crack width below 2.36 × 10^{-3} in.

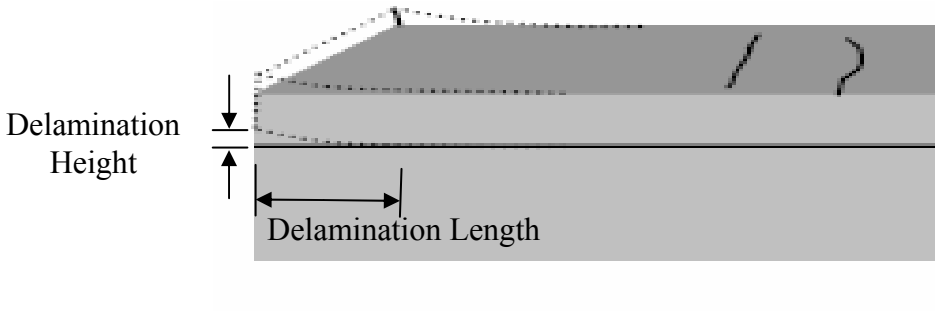

Figure 5.8: Repair interface delamination height and delamination length

The interface delamination of the 9 layered repair specimens can be found in Table 5.5. The delamination height and length were measured. As illustrated in Figure 5.8, the delamination height is the distance between the crack faces of the crack running along the repair-substrate boundary, measured at the two ends of the repaired system; the delamination length is the measured length of the delaminated section along the long axis of the specimen.

At the age of 60 days, both the HES-ECC and the HES-Concrete repaired systems exhibited relatively low delamination heights at the specimen ends, which were 3.15 × 10^{-3} in for the former and 3.54 × 10^{-3} in for the latter at the maximum. The maximum delamination length was 3.23 in for the HES-ECC repair and 6.69 in for the HES-Concrete repair at the maximum. The HES-SFRC repaired system had much larger delamination height than the HES-ECC or HES-Concrete repaired system at the age of 60 days, which is 12.2 × 10^{-3} in. Its delamination length was also larger, around 13.46 in. Figure 5.9 shows the interface delamination profiles of the three layer repair systems at different ages, which are vertical displacement/delamination of the repair layers at different locations along the repair/substrate interface. These profiles are approximately symmetric about the mid-point of the specimen, as would be expected.

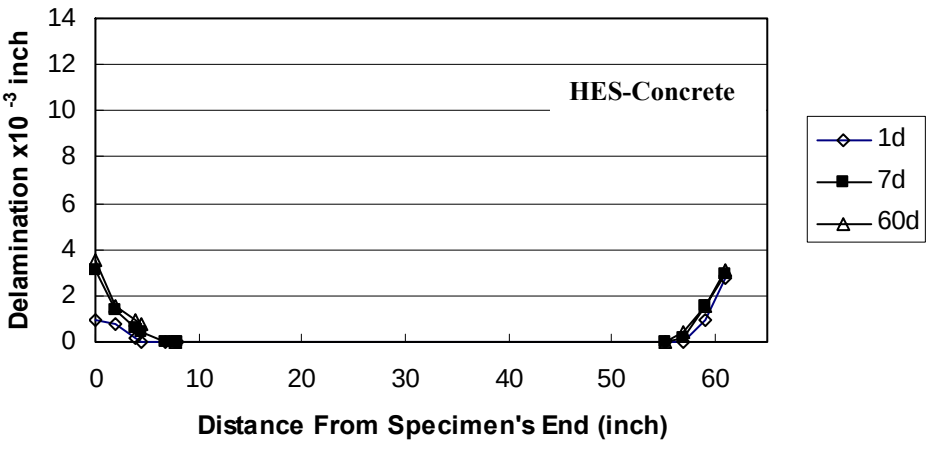

(a)

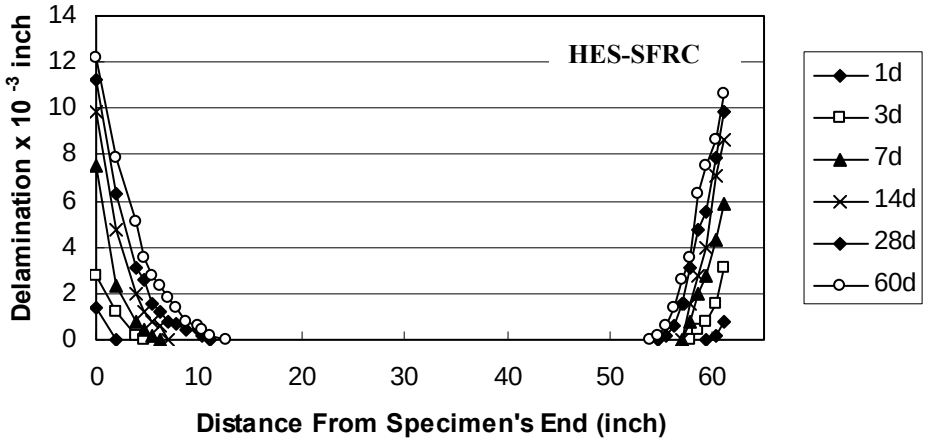

(b)

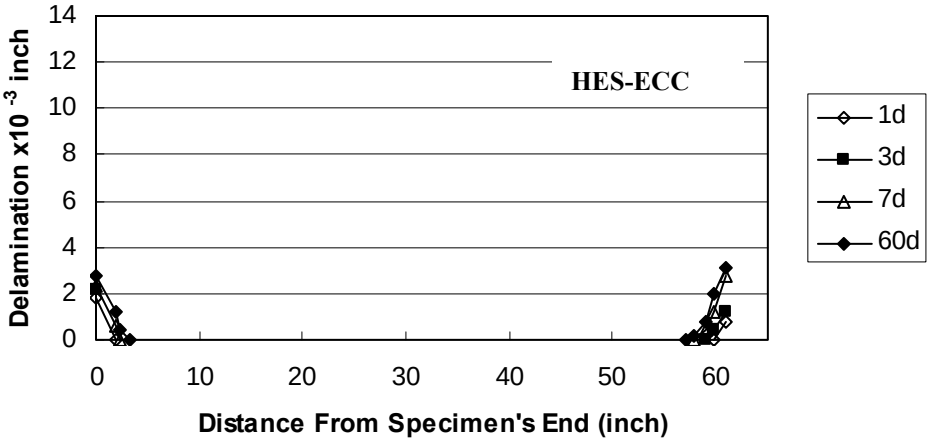

(c)

Figure 5.9: Interface delamination profile of (a) HES-Concrete (b) HES-SFRC (c) HES-ECC repaired systems

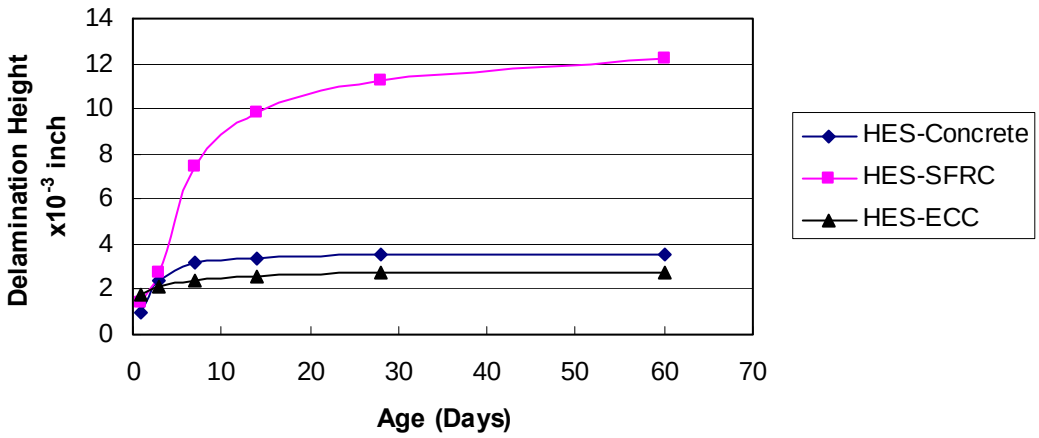

Figure 5.10: Specimen end delamination height at different ages

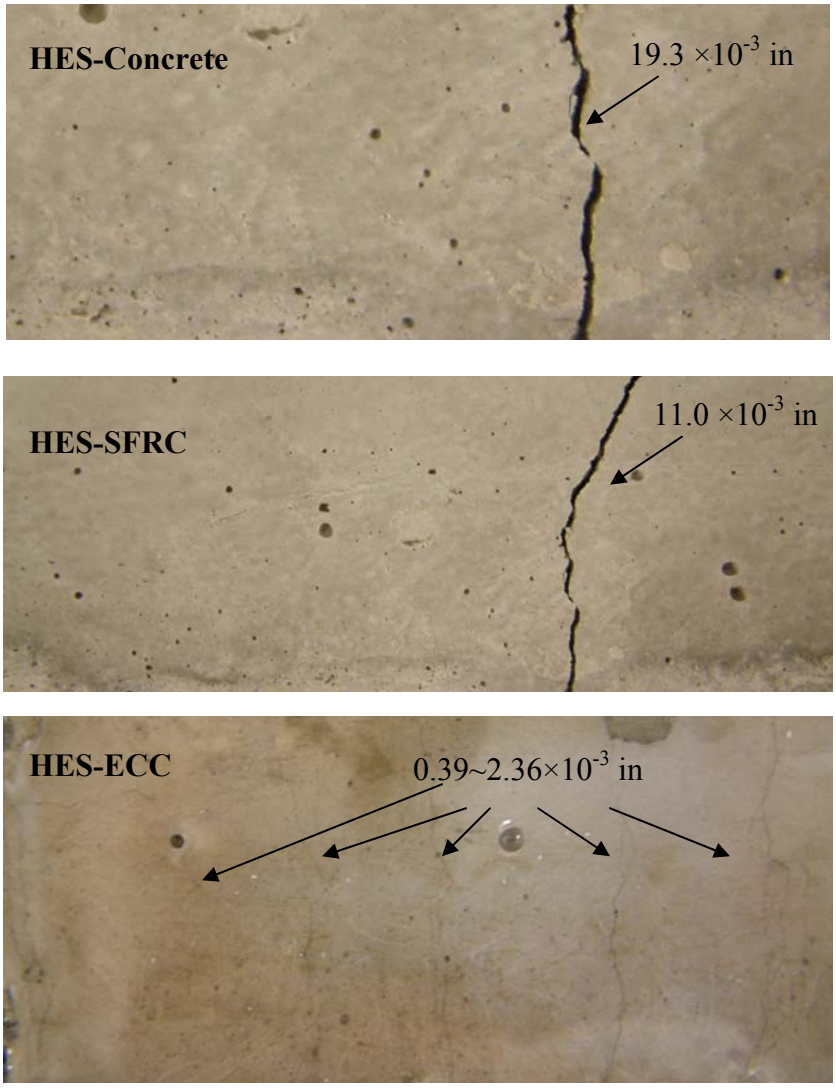

Figure 5.11: Repair surface cracking

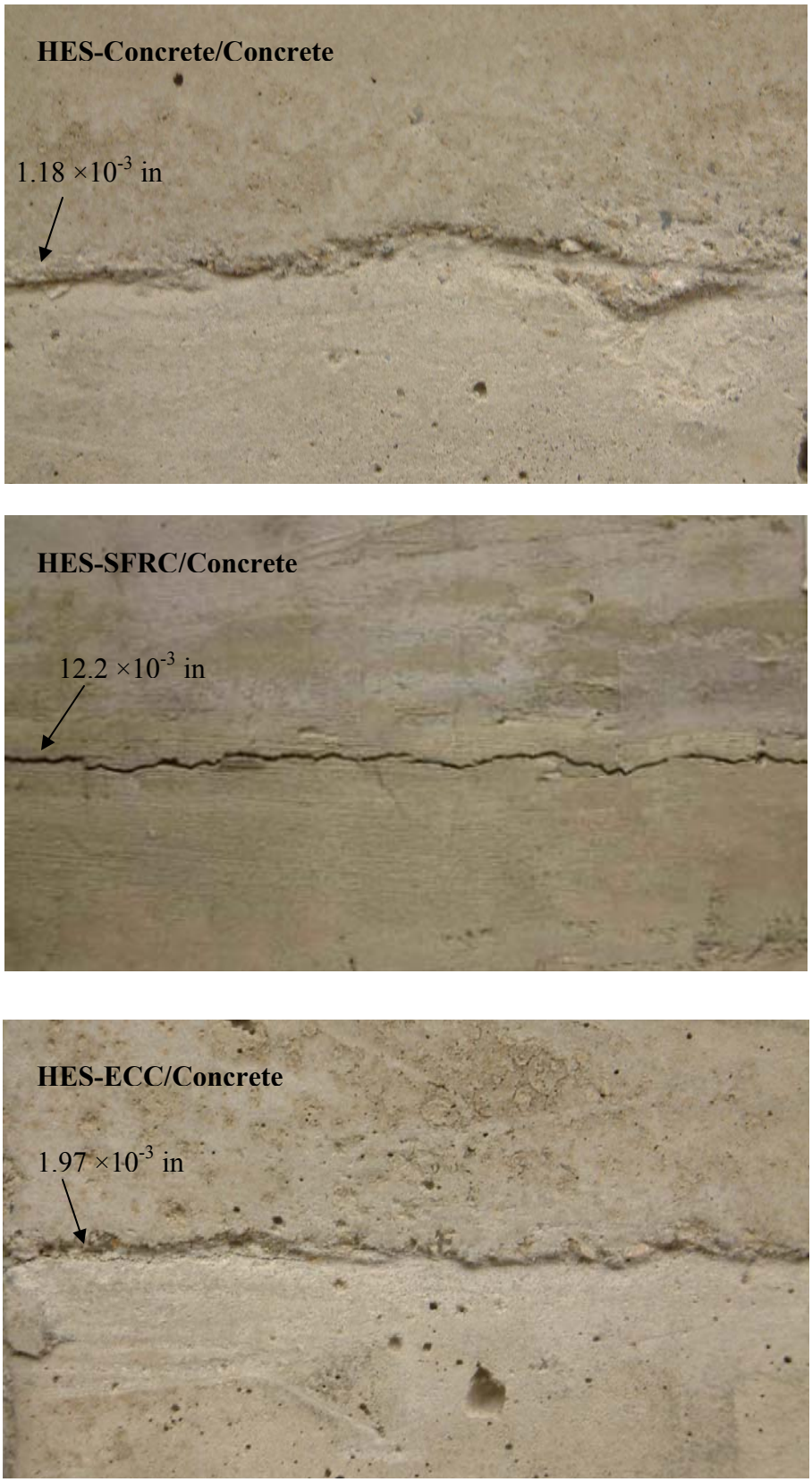

Figure 5.12: Interface delamination of layered repair systems

The interface delamination height development of the three repaired systems as a function of time is shown in Figure 5.11. It can be seen that HES-ECC and HES-Concrete repaired systems completed most of their interface delamination at very early ages – within 7 days, when cracking has happened and helped to release tensile and shear stress at the specimen interface. However for SFRC repaired system, delamination continued to evolve up to 60 days, at which time the SFRC repair material had undergone most of its shrinkage (Figure 5.7). This further confirms that the fiber-bridged cracks of HES-SFRC repair could only release part of stresses at the interface, so that delamination continued as shrinkage went on.

Figure 5.11 shows the surface cracking pattern of each type of repair layers. HES-Concrete and HES-SFRC repairs exhibited localized cracks, which were in contrast with the multiple micro-cracks of HES-ECC repair with significantly smaller crack width. Figure 5.12 shows the interface delamination height at the specimen end location of each type of repair systems. As can be seen, HES-SFRC repair exhibited interface delamination height one order of magnitude higher than HES-ECC and HES-Concrete repairs.

5.1.5 Discussion and Conclusions

Under environment with the same relative humidity and temperature, the HES-ECC repaired system exhibited the most desirable performance despite the fact that the HES-ECC's drying shrinkage strain was higher than the other two repair materials. The crack width of the HES-ECC repair and the interface delamination were both very small, which was ideal for achieving durability. Conversely, the HES-Concrete repaired system had several localized fractures with much bigger crack width. The most interesting observation is that the HES-SFRC repaired system exhibited not only relatively big crack width, but also large interface delamination height and length, although the HES-SFRC repair had the smallest shrinkage strain. The large value of crack width and interface delamination could be severe enough for introducing undesirable agents into the repaired system and resulting in a loss of durability.

The experimental results proved the concept that ductility of repair material is essential for achieving durability of repaired structures. With a negative cracking

potential p = (-4.843) to (-2.343), localized fracture was suppressed in HES-ECC. Simultaneously, the large tensile ductility of this material relaxes any potential stress build-up in the repair layer, thus minimizing the interface delamination. Tensile deformation of the HES-ECC repair layer was accomplished by forming many micro-cracks with tiny crack width. In contrast, for brittle or quasi brittle repair materials such as HES-Concrete and HES-SFRC, the way to accommodate the material's shrinkage deformation is either to crack or to delaminate from the interface, or the both. In this test, the HES-Concrete repair had strain capacity of about 0.01% (Table 5.3) and shrinkage strain of 0.105% (Figure 5.7), indicating a very large cracking potential. As a result, the shrinkage deformation of the concrete repair was accommodated by forming localized cracks and opening them. For the HES-SFRC repair, localized fractures formed because of its high cracking potential. Unlike HES-Concrete repair, these cracks were bridged by steel fibers so that they could not open freely. Therefore, the HES-SFRC repair could not accommodate all of its shrinkage deformation by only forming and opening cracks, resulting in delaminating at the interface. This explains the reason why the HES-SFRC repaired system had the most severe delamination among the three, and why the delamination continued to later ages, in contrast to the concrete or the HES-ECC repaired system.

The interaction between the repair and the old concrete structure can be a very complicated process. When shrinkage of "new" repaired material is restrained by "old" concrete substrate, there will be delicate time dependent competition between forming surface cracking and interface delamination. The contrast of repaired system behavior with HES-SFRC and HES-ECC as repair material is a direct consequence of the tension-softening vs strain-hardening properties of these two materials. These experimentally revealed effects of repair material tensile properties on the repair layer surface cracking and interface delamination behavior are consistent with those numerically predicted by Kabele (2001).

This study verified the outstanding performance of HES-ECC repaired system under restrained drying shrinkage, suggesting HES-ECC as a promising material to make durable concrete structure repairs. Under restrained shrinkage, HES-ECC developed multiple microcracks rather than several localized cracks. Unlike other brittle or quasi

brittle materials, the tight crack width of HES-ECC is a material property, which is independent of structural dimensions. This implies that with increasing structural scale, the advantage of using HES-ECC as a repair material will be even more important.

5.1.6 Implications for Repair Applications

For successful repairs with maximum life, the ACI Concrete Repair Guide ACI 546R-04 provides guidance on repair material selection, concrete substrate surface preparation and bonding methods. It also refers to ACI Concrete Building Code ACI 318-02 which recommends using shrinkage and temperature reinforcement to control cracking. These ACI recommendations or stipulations may need to be reconsidered in light of the unique properties of HES-ECC.

In Section 3.7 of ACI 546R-04, repair material with minimal shrinkage is recommended for interface integrity. Ultimate drying shrinkage of cement-based repair material is limited to below 0.2%. However, experimental results from this study reflects that cracking potential p is much more related to repair behavior under restrained drying shrinkage rather than the free drying shrinkage value. Even with ε_{sh} less than 0.1%, repairs made of HES-Concrete or HES-SFRC in this study all exhibited cracking or interface delamination to various degrees. This is because of their low strain capacity (about 0.01%) and consequent large value of cracking potential. In contrast, although ECC has ε_{sh} more than 0.2%, with a negative cracking potential p= (-4.843) to (-2.343), it suppressed localized fracture. Simultaneously, the large tensile ductility of this material relaxes any potential stress build-up in the repair layer, thus minimizing the delamination of the interface. Tensile deformation of the repair layer was accomplished by multiple micro-crack damage. The experimental results validate the concept that ductility of repair material is essential for achieving durability of repaired structures.

In addition to the above, ACI 546R-04 refers to ACI 318-02, which recommends using shrinkage and temperature reinforcement to control cracking in Section 7.12. A minimum reinforcement ratio of 0.0014 to 0.002 is specified depending on steel grade. The shrinkage and temperature reinforcement is required to be spaced not farther apart than 5 times the slab thickness, nor farther apart than 18 in. By virtue of the tight crack width control of ECC at strain-hardening stage, which is normally below 0.36×10^{-3} in,

these cracking control reinforcement may not be needed at all. The potential elimination of cracking control reinforcement removes the risks of steel corrosion and cover spalling, which are very common repair pathologies in the field. The reduction in steel reinforcement amount and repair thickness also makes the repair jobs simpler. Consequently, both construction cost and maintenance cost can be greatly reduced.

5.2 Layered System Test under Mechanical Loading (Task 4b)

5.2.1 Motivation and Background

Besides environmental loading such as shrinkage, mechanical loading can also cause repair cracking and interface delamination between the repair layer and the concrete substrate. When cracks exist in the concrete substrate, mechanical loading such as traffic loading will induce the maximum bending stress in the repair layer near to the cracks. This is because there is no load transfer through the existing cracks. Interface delamination can also happen around existing cracks due to the lack of the deformation compatibility between the two layers. Therefore, the whole delaminated section in the repair layer is subject to the maximum bending stress. Cracking happens in the repair layer when the maximum stress exceeds the repair material's tensile strength. The detailed discussion on stress distribution and failure mechanism in a repair system under mechanical loading can be found in Zhang and Li (2002).

Lim and Li (1997) discovered that ECC was most effective in trapping interface cracks and preventing repair spalling and interface delamination. The concept of interface crack trapping was experimentally demonstrated by using PE-ECC (ECC with polyethylene fibers) as the repair material. Kamada and Li (2000) investigated the influence of surface preparation on the kink-crack trapping mechanism of PE-ECC/concrete repair system. They concluded that a smooth surface of concrete substrate promoted the kink-crack mechanism in a longer delaminated zone of PE-ECC repair layer. In addition, Zhang and Li (2002) did an experimental study and theoretical analysis on a same layered repair system under both monotonic and fatigue loading, but with PVA-ECC (ECC with polyvinyl alcohol fibers) as the repair layer.

In this task, experimental study was made on the performance of a similar layered repair system under monotonic and fatigue flexural loading. Different from the

previous studies, this layered repair system involves HES-ECC as the repair layer and uses different curing conditions. The repair cracking, interface delamination, load carrying capacity and deformation carrying capacity of the repair system was investigated. Influence of concrete substrate surface preparation on the repair system's overall performance was also evaluated and reported here.

5.2.2 Experimental Program

5.2.2.1 Specimen Configuration and Loading Conditions

A layered repair system was investigated for resistance to spalling and delamination under mechanical loading, such as that induced by wheel loading. This system contains a layer of repair material cast on a substrate layer of old concrete with initial crack and little extent of interfacial delamination. The layered system was initially used by Lim and Li (1997) and Kamada and Li (2000) to simulate the reflective cracking in overlaid pavement. As shown in Figure 5.13, a vertical crack in the old concrete substrate was initially introduced to simulate already existed cracking in concrete structure. A horizontal interfacial crack between the repair layer and the substrate layer was also produced before testing to simulate an initial debonding zone above the crack location in the old concrete. The specimen was subjected to four-point bending load with load-deflection curve monitored during testing. The deflection of the specimen at the center was measured by two linear variable differential transducers (LVDTs), which were mounted on both sides at the center of the layered beam.

Both the monotonic and cyclic loading tests were conducted on a 56 kip load capacity, MTS-810 testing machine equipped for closed-loop testing. The monotonic flexural test was carried out with deformation controlled by the displacement of the actuator. The displacement was increased at a constant rate of 0.004in/min similar to ASTM C1018 "Standard Test Method for Flexural Toughness and First-Crack Strength of Fiber-Reinforced Concrete". The fatigue flexural test was conducted with load controlled using a sinusoidal waveform with a frequency of 2 Hz. It started with a ramp to the maximum load P_{max} at a rate of 22.5 lb/s followed by a sine waveform fatigue loading. The maximum load (P_{max}) is 0.9, 0.8 and 0.7 of the average load-carrying capacity of the layered repair system, which was obtained from the monotonic flexural

test results. The ratio R between the minimum and maximum load levels was constant at $R=P_{min}/P_{max}=0.1$. The test set-up is shown in Figure 5.14. Three specimens were tested for each category.

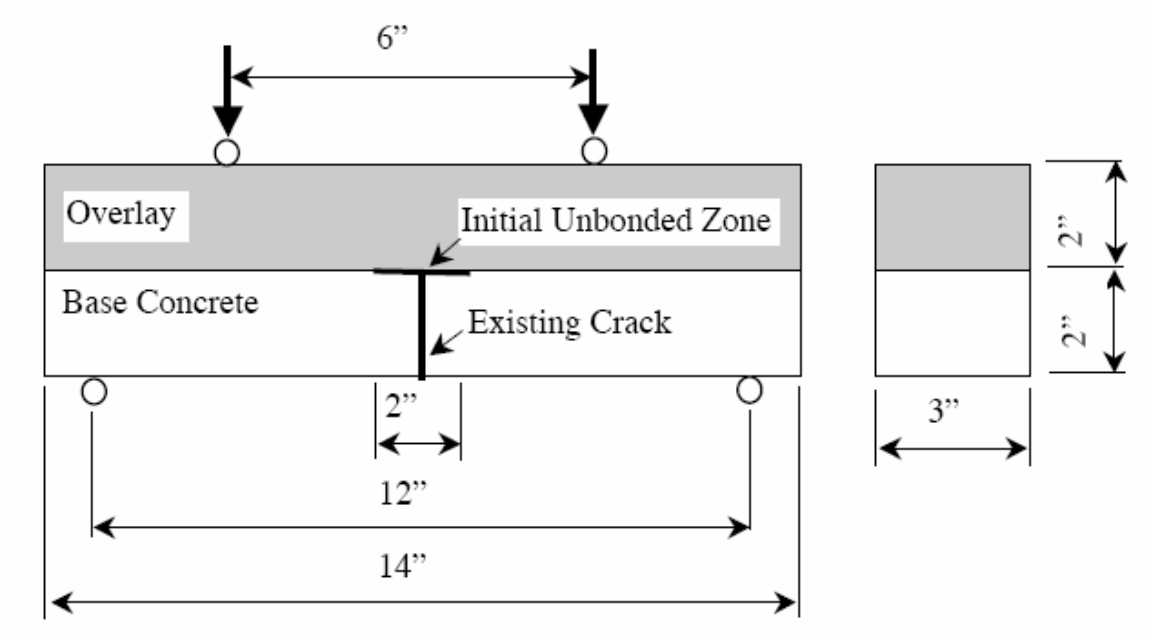

Figure 5.13: Dimensions of layered repair system under mechanical loading

Figure 5.14: Experimental set-up of layered repair system under four-point bending load

5.2.2.2 Materials and Specimen Preparation

Two different repair materials, HES-ECC and HES-Concrete，were investigated in this study. HES-Concrete was employed as control. The mixing proportion and properties of the repair materials and the concrete substrate are the same as those listed in Table 5.2 and Table 5.3.

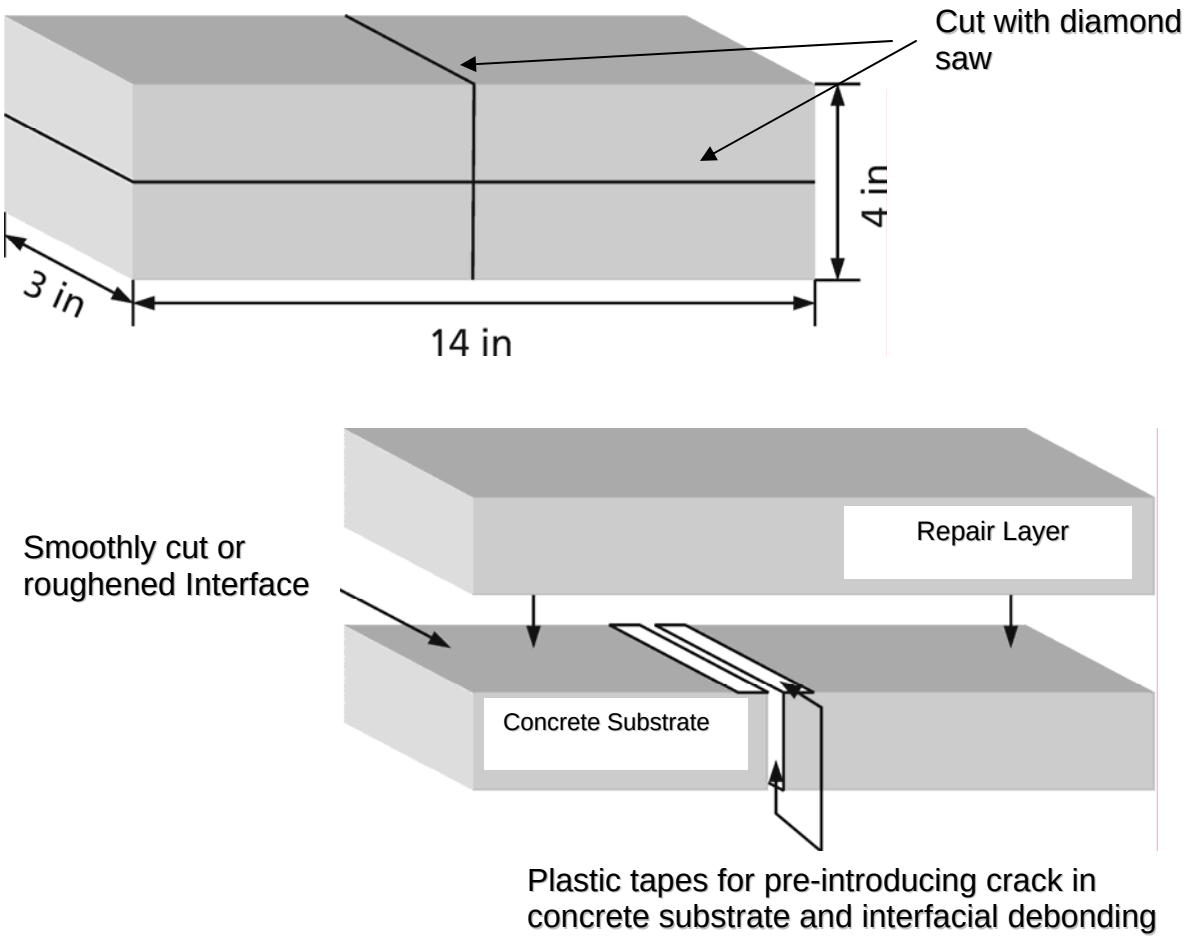

Figure 5.15: Layered repair specimen preparation

Concrete beams with dimensions of 14 in × 3 in × 4 in were first cast, and demolded after 24 hours. After demolding, the beams were cured in water at 60-70°F for 28 days. Then each beam was cut using a diamond saw into four concrete blocks with size of 7 in ×3 in × 2 in. The blocks were then stored in the laboratory condition for another week and then smooth plastic tape was used to form vertical cracking and interfacial debonding before the repair layer was cast. The vertical cracking was in the

middle of the concrete substrate, and the interfacial debonding length was 2 in. Each repair layer, made of either HES-ECC or HES-concrete, was cast on the top of two concrete blocks which formed the concrete substrate. The layered specimens were then demolded at 6 hours, air cured, and tested at 28 days. The specimen preparation is illustrated in Figure 5.15.

The contact surfaces of the concrete substrates were prepared in two different ways: smooth and rough (Figure 5.16). The smooth surfaces are diamond saw cut surfaces. The rough surfaces were roughened in the fresh state using a chisel to remove slurry cement from external surfaces of coarse aggregates. Before placing the repair layers, the substrate surfaces were recleaned with a brush and high-pressure air to ensure a clean bonding surface, and then they were dampened to achieve better bonding with the repair layers. After that, 2-in-thick repair layers made of each of the two repair materials were cast on the top of the concrete substrates.

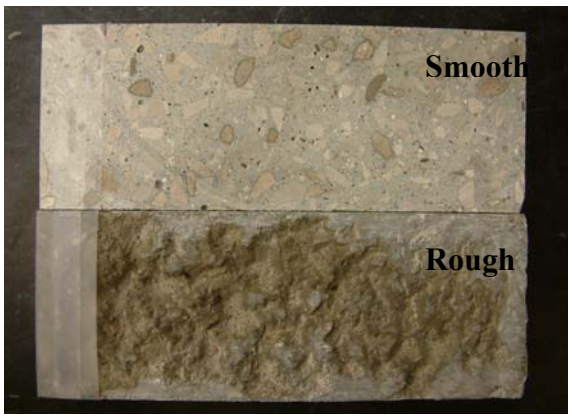

Figure 5.16: Concrete substrate surface preparation

5.2.3 Experimental Results

5.2.3.1 Monotonic Test

The flexural behavior of HES-ECC repair system compared with HES-Concrete repair system under monotonic loading is shown in Figure 5.17. The modulus of rupture (MOR) of the specimens were determined by

$$MOR = \frac{M}{bh^2/6}$$

where M is the bending moment at the center of the specimen, b is the width of the repair layer, and h is the thickness of the repair layer. The MOR, middle deflection at failure, and interface delamination length were summarized in Table 5.7 and Figure 5.18 to 5.20. The interface delamination length was measured including the initial 2-in interfacial debonding length.

HES-ECC layered repair system exhibited very ductile failure mode, as can be seen in Figure 5.17. This was in contrast with the sudden brittle failure mode of the HES-Concrete layered repair system. The flexural load carrying capacity of the HES-ECC repair system was significantly higher than HES-Concrete repair system. The MOR of the HES-ECC repair system was more than 100% higher than the HES-Concrete repair system. Similar results were obtained from the previous work by using PE-ECC and PVA-ECC M45 (Kamada and Li, 2000; Zhang, 1998). Furthermore, the deformation capacity of HES-ECC repaired system, represented by the specimen's center deflection at peak load, was 5 to 10 times higher than that of HES-Concrete repaired system. The greatly increased MOR and deformation capacity were contributed by the strain hardening behavior and high ductility of HES-ECC, which is in contrast with the tension softening behavior and brittle nature of HES-Concrete.

Comparing the flexural curves of HES-ECC repaired system with two differently prepared substrate surface, higher deformation capacity is noted when the surface is smooth (Figure 5.19). This was because smooth interface allowed for longer delamination between the HES-ECC repair layer and the concrete substrate. Therefore, longer zone of the HES-ECC repair layer (the delaminated part) was under the maximum bending stress and underwent multiple cracking, resulting in a higher deformation capacity. However for the HES-Concrete layered repair system, the influence of interface properties on the specimen's deformation capacity was negligible. Since the HES-Concrete layer had the single cracking behavior and low cracking resistance, it could not deform ductily so that interface delamination could not be further extended in spite of the interface bonding properties. The interface delamination of the different layered repair systems was measured including the initial delamination length, and is shown in Figure 5.20.

. Table 5.7: Flexural properties of different layered repair systems under monotonic loading

MOR (psi)	HES-ECC (Smooth)	2725.38	Average =2899.49
		3095.92	
		2877.19	
	HES-ECC (Rough)	2620.75	Average = 2751.95
		2861.51	
		2773.58	
	HES-Concrete (Smooth)	1370.99	Average = 1318.01
		1201.88	
		1381.16	
	HES-Concrete (Rough)	1391.18	Average = 1258.18
		1318.67	
		1064.69	
Deflection (in)	HES-ECC (Smooth)	0.138	Average = 0.147
		0.132	
		0.171	
	HES-ECC (Rough)	0.075	Average = 0.094
		0.112	
		0.095	
	HES-Concrete (Smooth)	0.017	Average = 0.017
		0.016	
		0.017	
	HES-Concrete (Rough)	0.015	Average = 0.016
		0.017	
		0.017	
Delamination (in)	HES-ECC (Smooth)	7.07	Average = 6.55
		6.45	
		6.12	
	HES-ECC (Rough)	4.20	Average = 3.92
		4.05	
		3.51	
	HES-Concrete (Smooth)	2.08	Average = 2.08
		2.12	
		2.05	
	HES-Concrete (Rough)	2.05	Average = 2.07
		2.10	
		2.06	

The cracking pattern of the different layered repair systems can be seen in Figure 5.21. The HES-Concrete / Concrete layered repair system had a sudden failure with one single crack formed in the repair layer. In contrast, the HES-ECC / Concrete layered repair system exhibited multiple micro-cracking behavior, with very tight crack width

below 0.36 × 10^{-3} in. When the concrete substrate surface was rough, fewer micro-cracks developed for the reason discussed above, so that its deformation capacity was lower than when the substrate surface is smooth. The significant difference of between the HES-ECC and HES-Concrete layered repair systems came from the kink-crack trapping mechanism: In the case of HES-Concrete repair, the initial interfacial crack always kinked into the repair layer and formed spalling. However for HES-ECC, the initial interfacial crack firstly kinked into the repair layer, and then trapped inside the HES-ECC because of the high toughness of the material. As the flexural load increased, the interfacial crack grew a little, and the kink-crack mechanism repeated till the final failure when the HES-ECC layer had its flexural strength exhausted. This kink-crack mechanism of HES-ECC repair helped to suppress repair spalling.

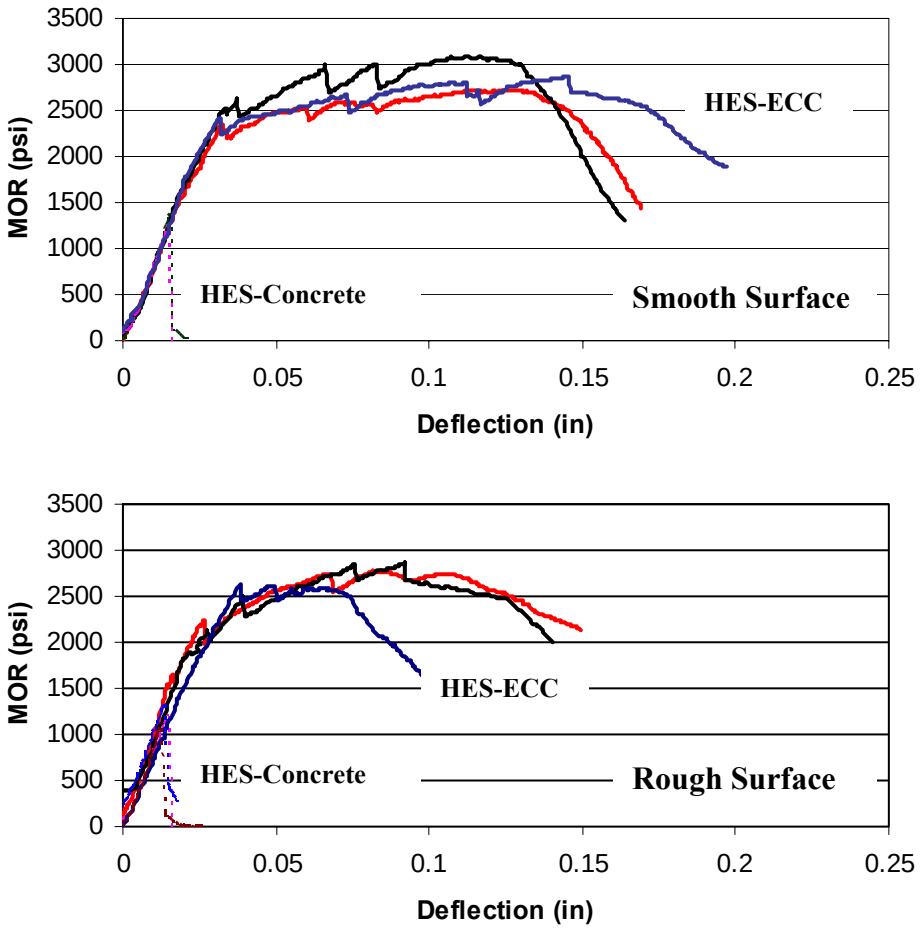

Figure 5.17: Flexural behavior of HES-ECC and HES-Concrete layered repair system under monotonic loading

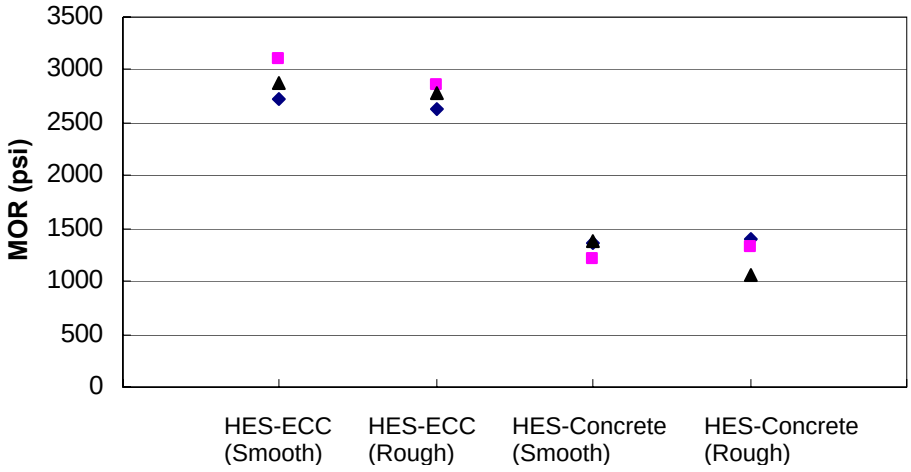

Figure 5.18: Modulus of rupture (MOR) of different layered repair systems under monotonic loading

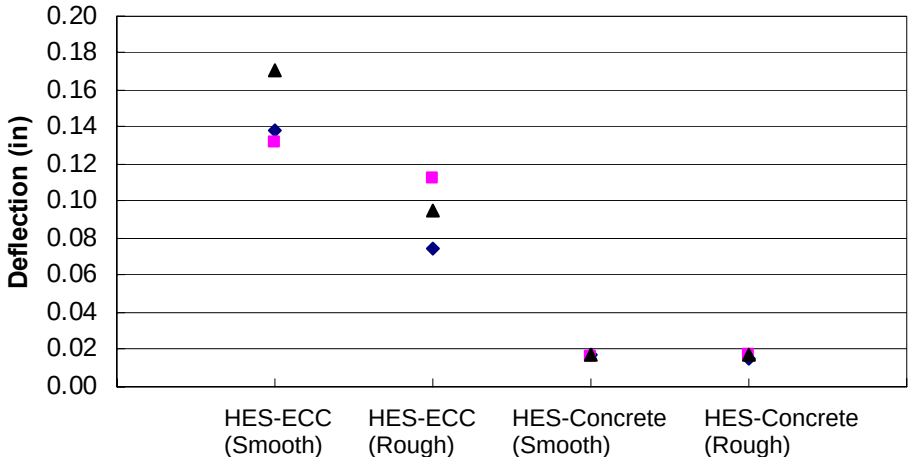

Figure 5.19: Deflection at failure of different layered repair systems under monotonic loading

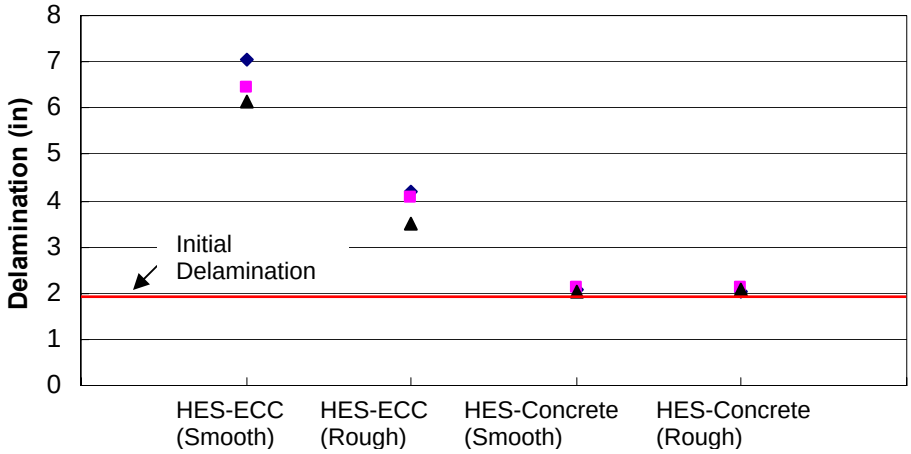

Figure 5.20: Interface delamination at failure of different layered repair systems under monotonic loading

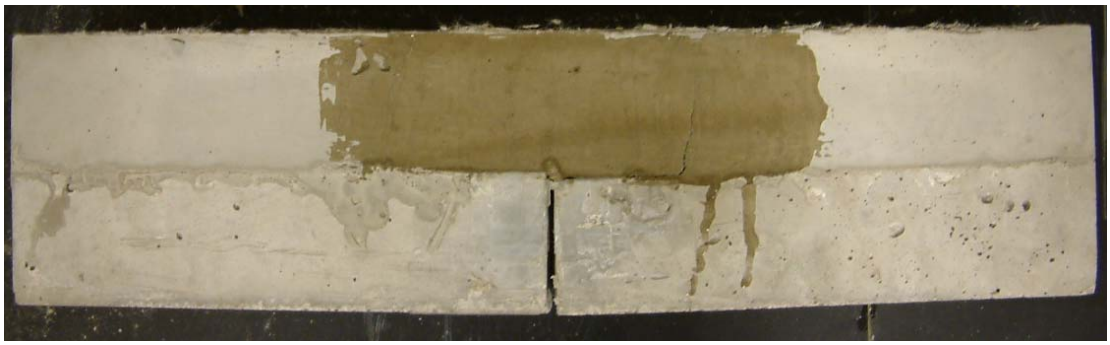

(a) HES-ECC / Concrete (Smooth Interface)

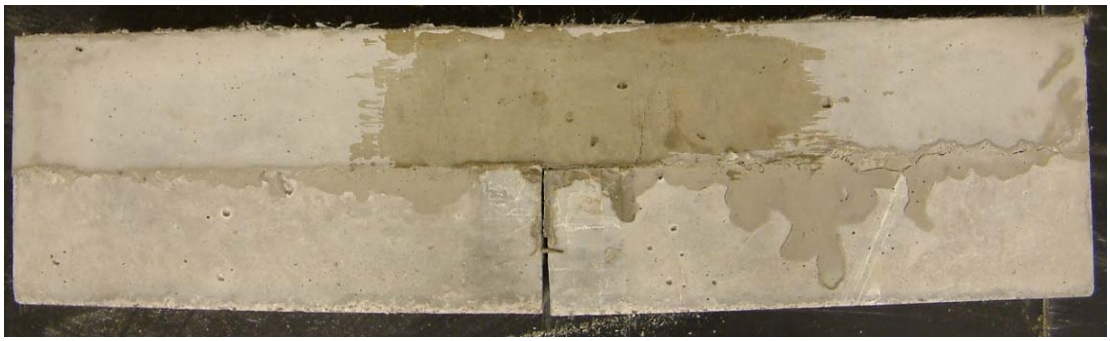

(b) HES-ECC / Concrete (Rough Interface)

(c) HES-Concrete / Concrete (Smooth Interface)

(d) HES-Concrete / Concrete (Rough Interface)

Figure 5.21: Cracking and interface delamination of different layered repair systems

5.2.3.2 Fatigue Test

The fatigue flexural performance of different layered repair systems is shown in Table 5.8 and Figure 5.22 in terms of MOR versus fatigue life (S-N). It is obvious that when the traffic loading is at the same level, the fatigue life of HES-ECC repair system is significantly longer than that of the HES-Concrete repair system. Different substrate surface preparation (smooth or rough) did not have significant effect on the fatigue life of HES-ECC and HES-Concrete layered repair systems. That was because the flexural fatigue life of a beam was dominated by a single crack propagation behavior under fatigue loading (Zhang, 1998; Zhang, Stang and Li, 1999). In other words, the HES-ECC repair's fatigue life until failure was likely governed by the fiber bridging properties under cyclic loading at the dominant single crack, no matter how many multiple micro-cracks were formed.

Similar to the monotonic flexural testing results, the maximum deflection at failure of HES-ECC repair system was larger when the concrete substrate is smooth. The reason was the same as discussed in section 5.2.3.1: Larger zone of HES-ECC repair layer was delaminated, and the whole delaminated portion of HES-ECC underwent multiple micro-cracking. There was no obvious difference on the crack patterns at failure between monotonic and fatigue flexural loading.

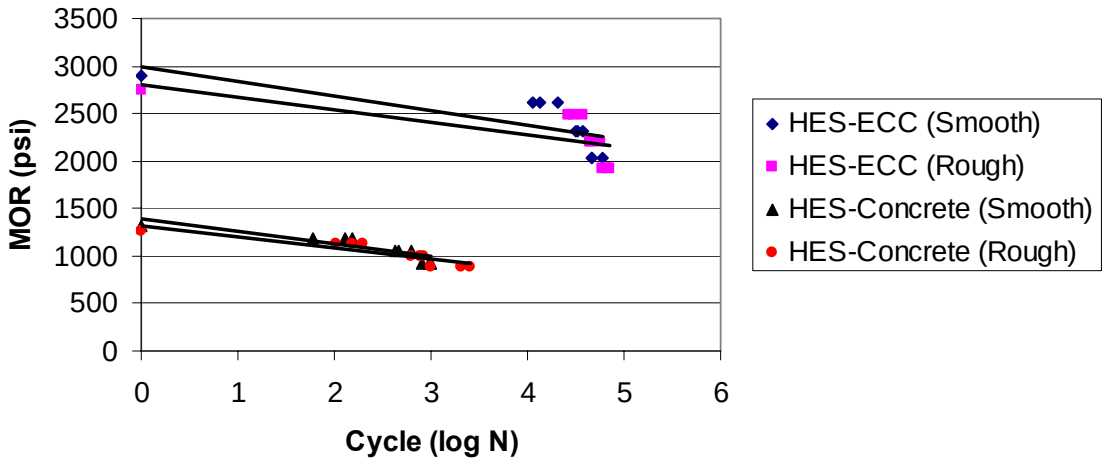

Figure 5.22: Fatigue life of different layered repair systems

Table 5.8: Fatigue life of different layered repair systems

	MOR (psi)		Cycle (N)	Cycle (Log N)
HES-ECC (Smooth)	MOR_{Max}	2899.49	1	0.0000
	$0.9 \times MOR_{Max}$	2609.54	11202	4.0493
		2609.54	20384	4.3093
		2609.54	13680	4.1361
	$0.8 \times MOR_{Max}$	2319.59	33654	4.5270
		2319.59	37382	4.5727
		2319.59	32216	4.5081
	$0.7 \times MOR_{Max}$	2029.64	46556	4.6680
		2029.64	58722	4.7688
		2029.64	47288	4.6748
HES-ECC (Rough)	MOR_{Max}	2751.95	1	0.0000
	$0.9 \times MOR_{Max}$	2476.75	37930	4.5790
		2476.75	29824	4.4746
		2476.75	26222	4.4187
	$0.8 \times MOR_{Max}$	2201.56	46120	4.6639
		2201.56	56826	4.7545
		2201.56	44002	4.6435
	$0.7 \times MOR_{Max}$	1926.36	59928	4.7776
		1926.36	70784	4.8499
		1926.36	68262	4.8342
HES-Concrete (Smooth)	MOR_{Max}	1318.01	1	0.0000
	$0.9 \times MOR_{Max}$	1186.21	60	1.7782
		1186.21	128	2.1072
		1186.21	152	2.1818
	$0.8 \times MOR_{Max}$	1054.41	464	2.6665
		1054.41	624	2.7952
		1054.41	426	2.6294
	$0.7 \times MOR_{Max}$	922.61	1012	3.0052
		922.61	962	2.9832
		922.61	806	2.9063
		1926.36	68262	4.8342
HES-Concrete (Rough)	MOR_{Max}	1258.18	1	0.0000
	$0.9 \times MOR_{Max}$	1132.36	104	2.0170
		1132.36	152	2.1818
		1132.36	202	2.3054
	$0.8 \times MOR_{Max}$	1006.54	764	2.8831
		1006.54	624	2.7952
		1006.54	826	2.9170
	$0.7 \times MOR_{Max}$	880.73	1012	3.0052
		880.73	2512	3.4000
		880.73	2088	3.3197

6. HES-ECC LARGER SCALE BATCHING (TASK 5)

Large scale mixing of ECC has been investigated in Japan and at the University of Michigan for the MDOT project "Field Demonstration of Durable Link Slabs for Jointless Bridge Decks Based on Strain-Hardening Cementitious Composites" (Li, Lepech and Li, 2005). These investigations, especially those done in Michigan, provide insight into large scale mixing processes for the newly developed HES-ECC material, and some information gained are directly applicable to this project.

Kanda et al (2003) investigated the tensile properties of ECC material in larger scale production using a 1.3 cubic yard omni-mixer. This mixer can be considered a type of force based mixer using external mixing paddles to deform a rubber drum containing the cementitious material. This mixing equipment is substantially different than gravity mixers which rely mainly on gravity to mix a viscous liquid (paddles within the rotating drum lift the material and agitate it by dropping the material inside the drum). Force based mixers are typically much more efficient in achieving homogeneity within concrete mixes because of the greater mixing agitation. However, force based mixers are very uncommon on construction sites where repair work is carried out, although they are common at precast concrete plants. Gravity mixers are more typical repair construction site equipment.

Kanda et al (2003) concluded that larger scale production of ECC is possible and the performance of the material is similar to that mixed in the lab. In addition to this study, work has been done by Kanda et al (2003) using both gravity and omni-mixers to process ECC material for spraying applications. The limited study concluded that mechanical performance of ECC processed using an ordinary concrete gravity mixer was similar with that using an omni-mixer.

For the MDOT project "Field Demonstration of Durable Link Slabs for Jointless Bridge Decks Based on Strain-Hardening Cementitious Composites" (Li, Lepech and Li, 2005), large scale mixing of ECC was carried out. Prior to concrete truck mixing of ECC, grain size distribution analysis was conducted, and preliminary test mixes in a gravity mixer with capacity of 9 cubic feet were completed. The length of PVA fiber was changed from 0.5", as used previously in ECC M45, to 0.33" to promote easier mixing and better fiber dispersion in a gravity mixer. A local concrete supplier was then

contracted to perform a series of trial mixes to process 1, 2 and 4 cubic yard trial batches of ECC material, which provided meaningful lessons on the mixing of large amount of ECC material in conventional concrete mixers.

Table 6.1: ECC material mixing proportions

Material	**Kanda et al**	**ECC – M45**	**HES-ECC**
Cement	1.0	1.0	1.0
Sand	0.91	0.8	1.0
Fly Ash	0.43	1.2	0.0
Water	0.65	0.53	0.33
PS Beads	0.0	0.0	0.064
High Range Water Reducer	0.0	0.03 Plastol 5000	0.0075 GL3200-HES
Accelerater	0.0	0.0	0.04
Anti-Shrinkage Agent	0.027	0.0	0.00
Fiber (vol %)	0.02	0.02	0.02

The large scale mixings ranging up from 1 cubic foot to 20 cubic yards concluded that large scale mixing of ECC can proceed quite smoothly and result in a fresh material, which is homogeneous, flowable and rheologically stable. Testing of mechanical properties of hardened material from the large scale batches has shown that the material compressive and tensile properties are similar to that of laboratory mixes.

Different from ECC M45, the developed HES-ECC material contains a much higher amount of cement without fly ash. In addition, the cement type is high early strength Portland cement type III instead of normal strength Portland cement type I, the former has finer particle size (Blaine Surface area 2637 ft^2/lb for type III versus 1806 ft^2/lb for type I). Furthermore, an accelerator is used in HES-ECC, which accelerates the strength development and processes of setting, resulting in shortened working time. Finally, polystyrene beads are included in HES-ECC mix which may affect on the flowability of the material. All of the four features of HES-ECC can have a great impact on its fresh properties.

6.1 Investigation of HES-ECC Mixing Procedure for Larger Scale Applications

6.1.1 Fiber Length Change

Prior to conducting larger scale HES-ECC batching, the fresh rheology of the HES-ECC mix was further optimized to adapt to large gravity mixers. To achieve good rheology and more homogeneous fiber distribution, a change of fiber length was examined. The standard poly-vinyl-alcohol (PVA) fiber, which is used in HES-ECC, is 0.5 inches long and 1.5 mils in diameter. After adding the fibers to the fresh HES-ECC matrix, a significant increase in viscosity of the material is observed. To improve the flowability of the fresh HES-ECC material, shorter PVA fibers with length of 0.33 inches and diameter of 1.5 mils were used and investigated. These fibers are identical with 0.5-inch-long fibers in aspects of fiber chemical composition, surface coating, strength and modulus, except shorter fiber length. The two types of fibers are shown in Figure 6.1.

The fresh state flowability and the hardened mechanical properties of HES-ECC material using shorter fibers were investigated. As expected, by using shorter fibers more homogeneous fiber distribution and an increase in the flowability of the fresh HES-ECC material were observed. A flowability test was performed on the fresh HES-ECC mix immediately after processing the material. The test is outlined in Kong et al (2003). To perform this test, a standard concrete slump cone was filled with fresh HES-ECC material and emptied onto a level Plexiglas or glass plate. The flowable HES-ECC material then flattened into a large pancake-shaped mass. Two orthogonal diameter of this "pancake" were measured and averaged, denoted as D_1, which captured the overall deformability, or flowability of the material in its fresh state. Flowability test showed that D_1 of HES-ECC was increased from 22 in to 24 in besides more homogeneous fiber distribution. This additional flowability of HES-ECC material should allow for easier mixing in large capacity gravity mixers and easier placement on the construction site.

Substituting 0.5-inch-long fibers with 0.33-inch-long fibers should not change the hardened mechanical properties of HES-ECC. The reason is that the micromechanical models used to develop HES-ECC material show that the critical fiber embedment length, which is necessary to allow for adequate fiber pullout and therefore composites strain

hardening behavior, is less than 0.165 in (half of short fiber length) (Kanda and Li, 1999). The tensile properties of HES-ECC with short fibers were evaluated using uniaxial tensile test. HES-ECC coupon specimen is 9" in length, 3" in width and 0.5" in thickness. Before testing, aluminum plates were glued to both ends of the coupon specimen to facilitate gripping. Tests were conducted on an MTS machine with 5.62kip capacity under displacement control at rate of 1.97×10^{-4}in/s. Specimens were demolded at 4h, cured in air, and tested at different ages from 4h to 28d. Three specimens were tested at each age.

Table 6.2 summarizes tensile properties of HES-ECC with 0.33 in fiber at different ages. Its typical stress-strain curves at different ages are plotted in Figure 6.2. It can be seen that HES-ECC with short fibers can still maintain tensile strain capacity of more than 3% at different ages. In conclusion, because of improved fresh properties and fiber distribution by using 0.33" fibers, and the similarity of the HES-ECC mechanical behavior between using 0.33" and 0.5" fibers, 0.33" fibers were decided to be used for the larger scale batching.

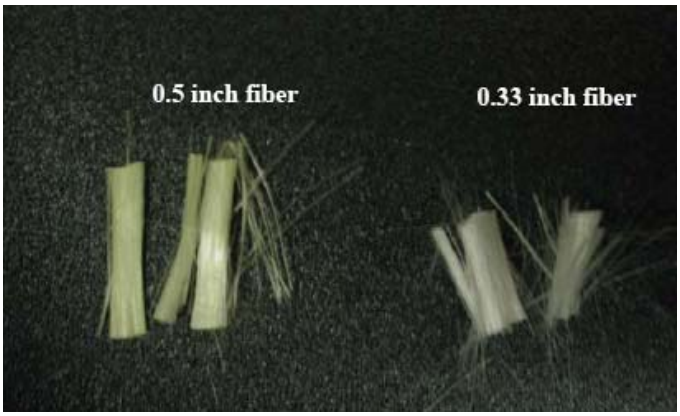

Figure 6.1: 0.5 inch and 0.33 inch PVA fiber

Table 6.2: Tensile properties of HES-ECC with 0.33 inch PVA fiber

Age	Young's Modulus (ksi)	Ultimate Strength (psi)	Strain Capacity (%)
4h	1728.26; 1913.22; 1997.68	511.54; 518.17; 525.73	4.21; 5.52; 5.66
24h	2553.43; 2596.56; 2687.32	679.11; 690.32; 702.12	3.95; 4.29; 4.43
7d	2901.12; 2987.55; 3102.28	820.33; 829.67; 851.52	3.36; 3.51; 3.64
28d	3245.42; 3376.51; 3401.63	811.67; 832.21; 908.82	3.28; 3.55; 3.57

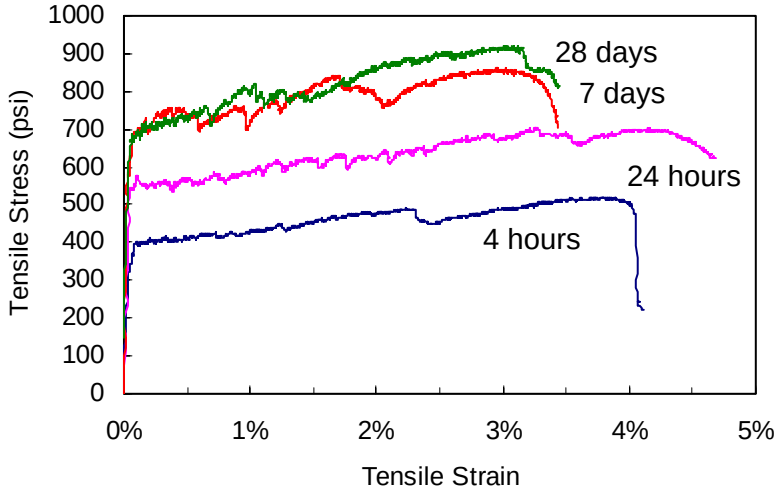

Figure 6.2: Tensile stress-strain curves of HES-ECC with 0.33 inch PVA fiber

6.1.2 Hydration Stabilizing Admixtures

A longer mixing time and working time were expected for the larger scale batching since a gravity mixer was to be used, which was less efficient in achieving homogeneity of HES-ECC material due to less powerful mixing agitation compared with force based mixers for laboratory investigation. In the laboratory situation, due to the very high amount of type III cement and use of an accelerator, the HES-ECC material set up very fast after finishing mixing. Furthermore, the HES-ECC material included Glenium 3200 HES admixture as the high-range water-reducing admixture, which was developed to provide extremely high early strength concrete. As a result, the slump retention of HES-ECC containing Glenium 3200 HES admixture was less than ECC treated with a conventional high-range water-reducing admixture. For all of the above reasons, the HES-ECC material began to lose the desired flowability and workability beyond the first 15-20 minutes after finishing mixing. This short setting time may be appropriate for preparing small scale specimens for laboratory test, but may not be adequate for larger scale repair applications on the construction site. Therefore, a retarding admixture is required to delay hydration and extend the time to setting when a longer working time is desirable.

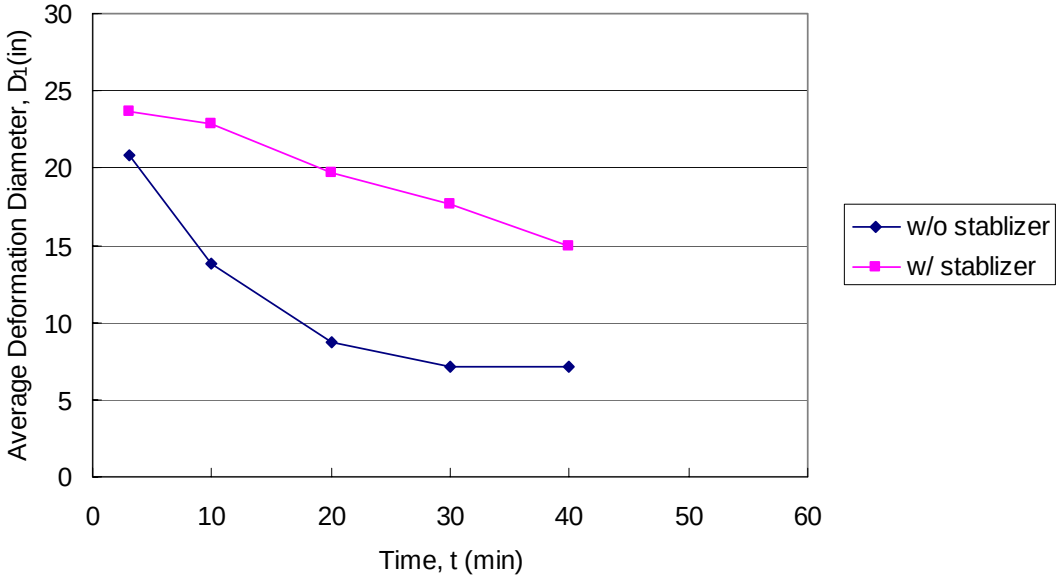

Figure 6.3: Loss of Deformability of HES-ECC without and with hydration stabilizer

A number of hydration retarders are commercially available, and for this project Delvo® Stabilizer from MasterBuilders was selected because it was from the same company as the accelerator Pozzolith® NC 534 and the HRWR Glenium® 3200HES used in HES-ECC. As recommended by MasterBuilders, the use of Delvo® extended set-controlling admixture can extend the slump retention of concrete containing Glenium 3200 HES admixture, and field trial mixture is recommended to ensure that the desired slump at a specific time period can be achieved. Besides retarding setting time, Delvo® Stabilizer can reduce water content required for a given workability and reduce segregation. Furthermore, it has been found that concrete produced with Delvo® Stabilizer will develop higher early (within 24 hours) and higher ultimate strengths than plain concrete when used within the recommended dosage range and under normal, comparable curing conditions.

Dosage for Delvo® Stabilizer in testing series followed the manufacturer's recommendation. The stabilizer is recommended for use at a dosage of 4±1 fl oz/cwt of cementitious materials for most concrete mixtures. Since HES-ECC has higher cement content compared with concrete, a high dosage rate within the specified range was used, which was 5 fl oz/cwt of the cementitious material. Experimental study

proved that the addition of hydration stabilizer significantly increased setting time and extended the fresh flowability of HES-ECC material. The development of flowability with respect to time is shown in Figure 6.3. The reported average deformation diameter is the average of two orthogonal diameter measurements of the "pancake" formed during flowability testing as described in section 6.1.1. The HES-ECC mixes tested contained 0.33 inch fibers. Obviously, HES-ECC without any stabilizer admixture exhibited rapid loss of flowability and became unworkable after 15-20 minutes. However, for HES-ECC containing stabilizer, a higher workability and prolonged setting time was exhibited. This will be validated in Section 6.2.2 through compressive testing of HES-ECC specimens from 6 cubic feet mixing.

6.1.3 Batching Sequence

To scale up the batching of HES-ECC from small laboratory mixers to large gravity mixers, the sequence of mixing must be optimized to promote the best homogeneity of the material. In a typical laboratory mixing, for which force-based mixer is used, all of the dry components of the HES-ECC matrix (cement and sand) were initially added and mixed together. Following a complete blending of cement and sand, water is slowly added to gradually turn the mixture into a liquid state. After the majority of the water is added, high range water reducer was added along the remaining water. Fibers were then slowly added and dispersed throughout the mixture. Normally half of the accelerator was added before fibers, and half after fibers. Finally PS beads was slowly added and mixed till well distributed. The overall mixing sequence lasted between 10 and 15 minutes.

For larger scale applications, however, the mixing sequence described above should not be applicable. Adding all of the dry components, including cement, followed by small amount of water can result in a large mass of very dry material which is extremely difficult for a gravity mixer to process. It is essential that the mixture remains as liquid as possible throughout the mixing process and attain its most viscous state at the very end of mixing. Li, Lepech and Li (2005) examined the effect of mixing sequence on the ECC material processing by using two gravity-based mixers. They concluded that the most successful mixing sequence was starting with adding all of the dry sand,

along with the addition all of the water and superplasticizer. Once these three components were well mixed, all other dry components (cement and fly ash) were added and mixed till the complete mortar matrix of ECC achieved homogenous liquid state. Then fibers were added gradually into the mixture and mixed till they were well dispersed. This mixing sequence took 9 ~ 12 minutes.

Since the newly developed HES-ECC contains similar components as ECC M45, except that it does not contain fly ash but PS beads and accelerator, the mixing sequence of HES-ECC will follow the above findings by Li, Lepech and Li (2005). This mixing sequence was first justified for its applicability in the one-cubic-foot mixing, as reported in the next section.

6.2 HES-ECC Larger Scale Batching

6.2.1 One Cubic Feet Batching

The target of this one cubic feet batching was to justify the applicability of the new mixing sequence of HES-ECC in a small gravity mixer, and to examine the material's fresh and hardened properties when including 0.33" fibers and hydration stabilizer. The mixing was carried out in a gravity mixer with the capacity of 2 cubic feet, as shown in Figure 6.4. The HES-ECC mixing proportions and batching weights are shown in Table 6.3. The batching sequence and time are listed in Table 6.4.

Figure 6.4: Gravity Mixer with Capacity of Two Cubic Feet

Table 6.3: Larger Scale HES-ECC Mixing Proportions and Batching Weights

Material	Proportion	Amount (lb/yard^3)
Cement	1.0	1547.37
Sand	1.0	1547.37
Water	0.33	507.54
PVA Fiber (vol %)	0.02	44.01
Polystyrene Beads	0.064	99.09
High Range Water Reducer	0.0075	11.61
Accelerator	0.04	61.83
Hydration Stablizer	0.0046	7.02

Table 6.4: Larger Scale HES-ECC Batching Sequence and Time

Activity	Elapsed Time including Mixing Time(min)
1. Charge all sand	2
2. Charge 3/4 amount of mixing water, all HRWR, and all hydration stabilizer	2
3. Charge all cement slowly	4
4. Charge remaining 1/4 amount of mixing water to wash drum	1
5. Charge 1/2 amount of accelerator, mix until the whole HES-ECC matrix material is homogenous	5
6. Charge PVA fibers slowly, mix until the fibers are well distributed	5
9. Charge PS beads slowly, mix until the beads are well distributed	4
10. Charge the remaining 1/2 amount of accelerator, mix until the complete material is homogenous and ready for placement	2
Total	25

Figure 6.5 illustrates the mixing procedure of HES-ECC in 1 cubic feet batch. Sand was firstly added, and most of water, all of HRWR and stabilizer were added and mixed with sand to achieve a liquid state as shown in Figure 6.5 (a). Cement was then slowly added and the remaining water was charged to wash the drum after adding cement. Since the matrix was a little dry at this stage, around 1/2 of accelerator was added, and the whole HES-ECC mortar matrix was mixed for around 5 minutes. After achieving a homogenous and creamy matrix (Figure 6.5 (b)), PVA fibers were slowly added and mixed for another 5 minutes until the fibers were well dispersed (Figure 6.5 (c)). Then PS beads were slowly charged and mixed until well distributed. The remaining 1/2 amount of accelerator was finally added and mixed until the complete HES-ECC mix was ready for casting (Figure 6.5 (d)). The whole mixing process went on smoothly, validating the applicability of the suggested batching sequence for larger scale (3 and 6 cubic feet) mixing of HES-ECC.

Flowability test was conducted on the HES-ECC processed in this one cubic feet batching, and the results were shown in Table 6.5 and Figure 6.6, which is similar to Figure 6.3.

HES-ECC compressive cylinder specimens and tensile coupon specimens were cast from the one cubic feet batch and tested for hardened mechanical properties at different ages. Compressive testing was done according to ASTM C39 “Standard Test Method for Compressive Strength of Cylindrical Concrete Specimens” on standard 4” × 8” cylinders. Three specimens were tested for each test series. The compressive test results are summarized in Table 6.6 and Figure 6.7. It can be seen that HES-ECC processed from one cubic feet batching can achieve the target compressive strength at both early and late ages.

Uniaxial tensile tests were conducted on HES-ECC tensile plate specimens cast from the one cubic feet batch, with the same specimen size and test setup as shown in Figure 4.3. Three specimens were tested for each test series and their tensile properties were summarized in Table 6.7. Figure 6.8 shows representative tensile stress-strain curves of HES-ECC mix at different ages. It can be seen that HES-ECC processed from one cubic feet batching can achieve the target >2% tensile strain capacity at both early and late ages.

a) After adding sand, water, HRWR and hydration stabilizer

b) After adding cement (homogenous and creamy HES-ECC mortar matrix)

c) After adding PVA fibers

d) After adding PS beads

Figure 6.5: HES-ECC one cubic feet mixing

Table 6.5: Flowability test results from one & six cubic feet batching

Minute	Average Deformation Diameter, D_1(in)	
	One Cubic Feet	Six Cubic Feet
3	22.83	24.02
10	21.26	
20	18.50	20.47
30	17.72	17.72
40	15.75	15.35

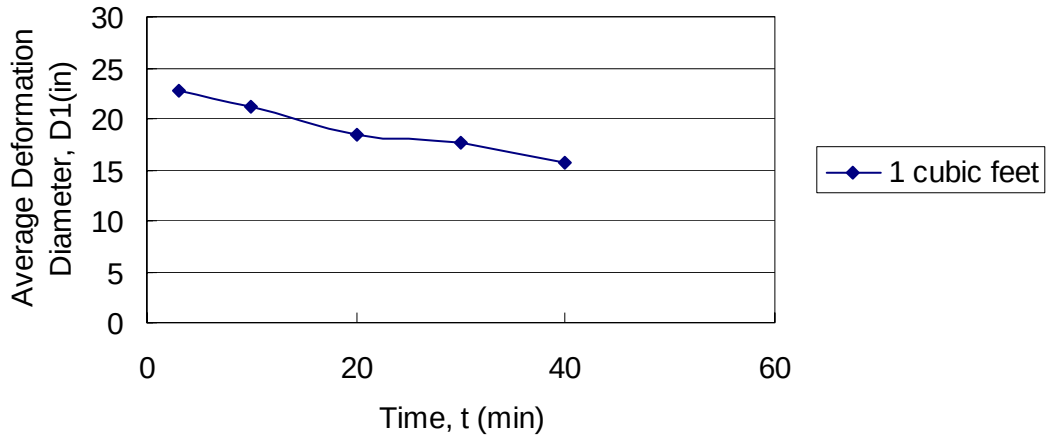

Figure 6.6: Loss of deformability of HES-ECC processed in one cubic feet batching

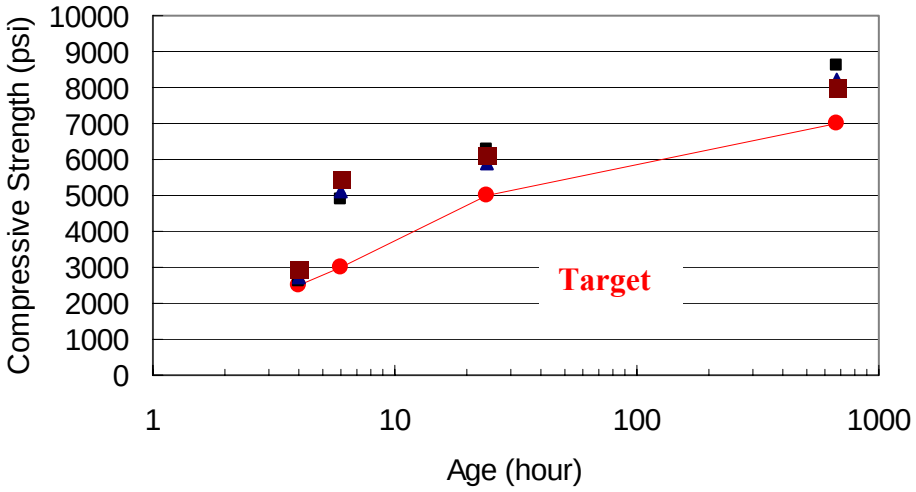

Figure 6.7: Compressive strength development of HES-ECC from one cubic feet batching

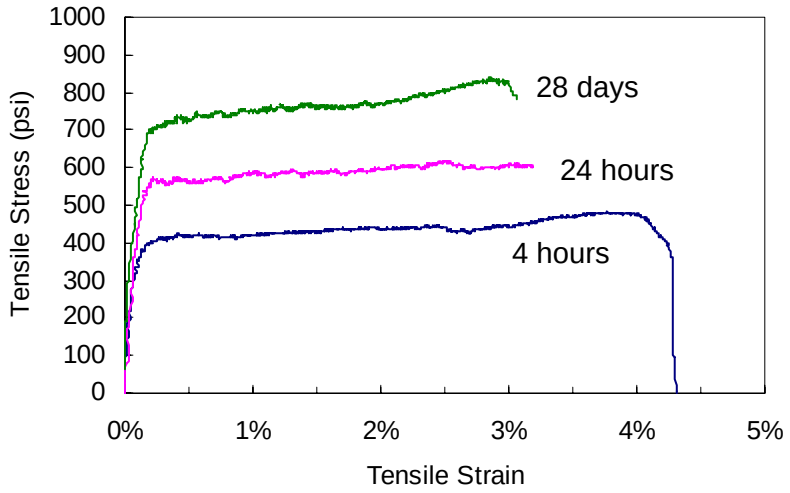

Figure 6.8: Tensile stress-strain curves of HES-ECC from one cubic feet batching

Table 6.6: Compressive Strength development of HES-ECC from one & six cubic feet batching

Age	Compressive Strength (psi)						
	Target	One Cubic Feet			Six Cubic Feet		
4 h	2500	2623	2718	2932	3012	2511	2732
6 h	3000	4876	5113	5428	5526	4722	5209
24 h	5000	6258	5873	6115	6211	5977	6289
28 d	7000	8621	8209	8012	8701	8454	8500

Table 6.7: Tensile properties of HES-ECC from one & six cubic feet batching

Age		Young's Modulus (ksi)	Ultimate Strength (psi)	Strain Capacity (%)
One Cubic Feet	4h	1728; 1913; 1998	512; 518; 526	4.21; 5.52; 5.66
	24h	2553; 2597; 2687	679; 690; 702	3.95; 4.29; 4.43
	28d	3245; 3377; 3402	812; 832; 909	3.28; 3.55; 3.57
Six Cubic Feet	4h	1812; 1901; 1979	497; 522; 533	4.05; 4.53; 4.68
	6h	2000; 2103; 2210	601; 619; 629	4.34; 4.52; 5.01
	24h	2499; 2587; 2713	678; 689; 695	3.43; 3.55; 3.87
	28d	3302; 3421; 3499	813; 826; 851	3.02; 3.26; 3.62

6.2.2 Three Cubic Feet Batching and Six Cubic Feet Batching

Three and six cubic feet batching of HES-ECC were conducted using a larger gravity mixer with capacity of 9 cubic feet, as shown in Figure 6.9. The batching process is illustrated in Figure 6.10. The mixer was firstly pre-wetted (Figure 6.10 (a)). Similar to the one cubic feet batching, the sand, most of water, all of HRWR and stabilizer were firstly added and mixed achieve a liquid state as shown in Figure 6.10 (b). Then cement was slowly added and the remaining water was charged to wash the drum. After adding around 1/3 of accelerator, the whole HES-ECC mortar matrix was mixed until a homogenous and creamy matrix was achieved (Figure 6.10 (c)). PVA fibers were slowly added and mixed for another 5 minutes (Figure 6.10 (d)). After the fibers were well dispersed, PS beads were slowly charged and mixed until well distributed. The remaining 2/3 amount of accelerator was finally added and mixed until the complete HES-ECC mix was ready for casting (Figure 6.10 (e)).

Figure 6.9: Gravity mixer with capacity of 9 cubic feet

The HES-ECC material for the both batchings was evaluated for fiber distribution, flowability and mixture rheology upon completion of the mixing. Fiber dispersion was evaluated through visual inspection and random sampling of the material to look for pockets or conglomerates of unmixed matrix materias or fiber bundles. In both cases the texture of HES-ECC material had a flowable, smooth, creamy viscosity. No segregation was found.

For the three cubic feet batching, after achieving a homogenous HES-ECC material, small additional amount of superplasticizer was added to evaluate the possibility of further increasing the material's flowability. However, segregation was observed after adding the extra amount of superplasticizer. Therefore, the mixed HES-ECC material was disposed of and was not evaluated for its compressive and tensile properties. We concluded that higher flowability than D_1=30in of HES-ECC could be hardly achieved, and the following six cubic feet batching strictly followed the mixing proportion specified in Table 6.2.

Evaluation of the fresh HES-ECC from six cubic feet batching was done through flowability testing of the material. This test utilized a standard concrete slump cone which was filled with fresh HES-ECC. Once the cone was removed, the flowable material formed a "pancake", as shown in Figure 6.10 (f). The average deformation diameter D_1 was 24 in. The flowability test results were summarized in Table 6.5. The loss of deformability of HES-ECC processed in six cubic feet batching was shown in Figure 6.11.

Similar to the one cubic feet batching, HES-ECC compressive cylinder specimens and tensile coupon specimens were cast from six cubic feet batch and tested for hardened mechanical properties at different ages. Three specimens were tested for each test series. The compressive test results were summarized in Table 6.6, and Figure 6.12. The tensile test results were summarized in Table 6.7 and Figure 6.13. It can be seen that HES-ECC processed from six cubic feet batching can achieve the target compressive strength and tensile strain capacity at both early and late ages.

a) Pre-wetting the mixer

b) After adding sand, water, HRWR and hydration stablizer

c) After adding cement (homogenous and creamy HES-ECC mortar matrix)

d) After adding PVA fibers

e) After adding PS beads

f) Flowability test (5 minutes)

Figure 6.10: HES-ECC six cubic feet mixing

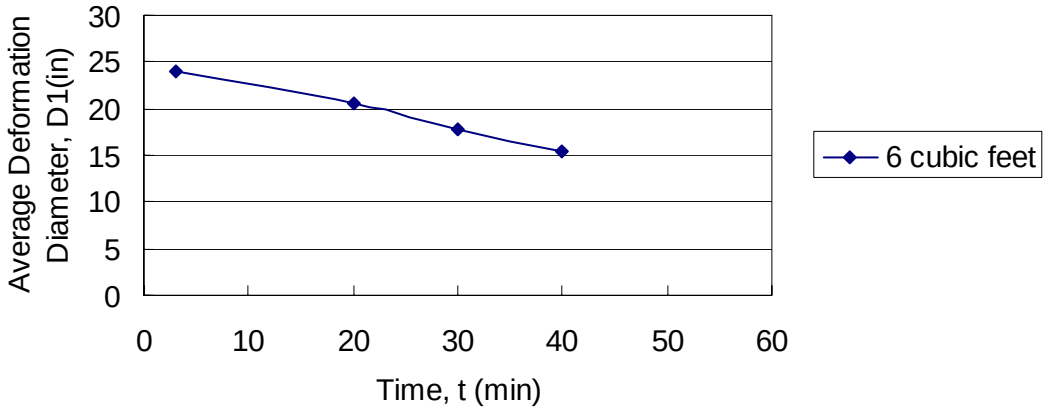

Figure 6.11: Loss of deformability of HES-ECC processed in six cubic feet batching

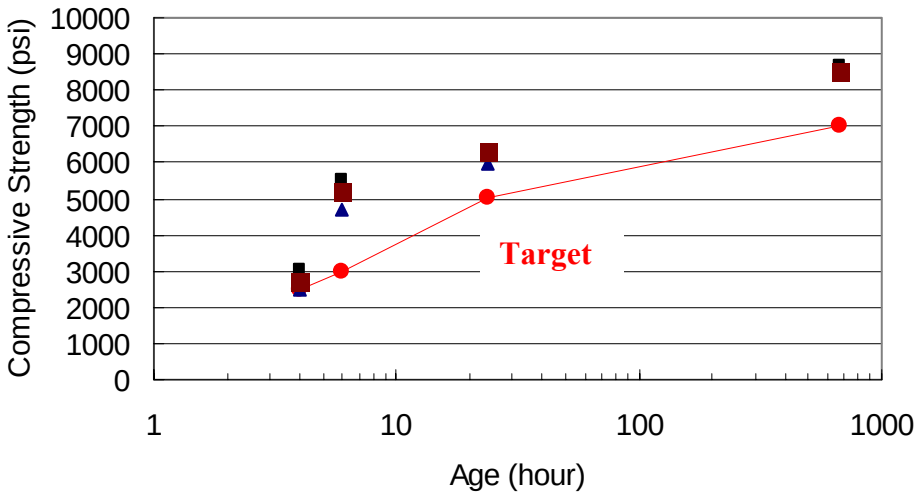

Figure 6.12: Compressive strength development of HES-ECC from 6 cubic feet batching

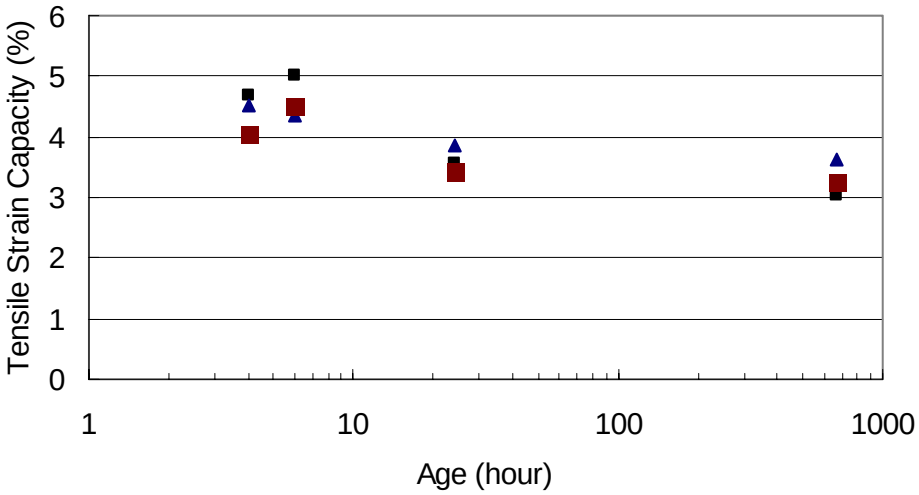

Figure 6.13: Tensile strain capacity development of HES-ECC from 6 cubic feet batching

7. HES-ECC REPAIR QUALITY CONTROL

This section provides specifications on quality control of constructing a HES-ECC repair. Except as modified by this special provision, all work is to be in accordance with the 2003 Standard Specifications for Construction.

7.1 Materials

Cement used for HES-ECC material must be Type III Portland cement, which is a finely ground Ordinary Portland Cement (OPC) with Blaine surface area of 2637 ft^2/lb. Type III Portland cement is available from the following contact.

Barry Descheneaux
Manager-Product Support & Development
Holcim (cement)
Telephone: (734) 347-8070
Barry.Descheneaux@Holcim.com

Fine aggregates used for HES-ECC material must be virgin silica sand consisting of a gradation curve with 50% particles finer than 0.04 mils and a maximum grain size of 12 mils. Fine aggregates meeting this requirement are available from the following manufacturer under the trade name "F-110 Foundry Silica Sand." Approved equal will be accepted.

US Silica Corporation
701 Boyce Memorial Drive
Ottawa, Illinois 61350
Telephone: (800) 635-7263

Fibers to be used for HES-ECC material must be manufactured of poly-vinyl-alcohol (PVA) with a fiber diameter of 1.5 mils and a length between 0.3 inch and 0.5 inch. The surface of the fiber must be oiled by the manufacturer with 1.2% (by weight) hydrophobic oiling compound along the length of the fiber. Fiber strength shall be a minimum of 232 ksi with a tensile elastic modulus of at least 5,800 ksi. Fibers meeting this requirement are available from the following manufacturer under the trade name REC-15. Approved equal will be accepted.

Kuraray America
101 East 52nd Street, 26th Floor
New York, New York 10022
Telephone: (212) 986-2230

The high-range water-reducing admixture used for HES-ECC material is Glenium® 3200 HES complying with ASTM C 494/C 494M requirements for Type A, water-reducing, and Type F, high-range water-reducing, admixture. Glenium® 3200 HES is a new generation of admixture based on polycarboxylate chemistry, and is very effective in producing concrete mixtures with different levels of workability including applications that require the use of self-consolidating concrete. Glenium® 3200 HES admixture is also very effective in producing concrete mixtures with very high early strength requirements. Glenium® 3200 HES is available from the following manufacturer.

Armand Atienza
BASF (Degussa) Admixtures, Inc.
armand.atienza@degussa.com
Telephone: (248) 867-2901

The accelerating admixture used for HES-ECC material is Pozzolith® NC 534 which is formulated to accelerate time of setting and to increase early concrete strengths. Pozzolith NC 534 admixture does not contain calcium chloride and is formulated to comply with ASTM C 494/C 494M Type C, accelerating, admixture requirements. Pozzolith® NC 534 is available from the following manufacturer.

Armand Atienza
BASF (Degussa) Admixtures, Inc.
armand.atienza@degussa.com
Telephone: (248) 867-2901

The hydration stabilizing admixture used for HES-ECC material is Delvo® Stabilizer. Delvo® Stabilizer retards setting time by controlling the hydration of portland cement and other cementitious materials while facilitating placing and finishing operations. Delvo® Stabilizer admixture meets ASTM C 494/C 494M requirements for Type B, retarding, and Type D, water-reducing and retarding, admixtures. Delvo®

Stabilizer is available from the following manufacturer.

Armand Atienza

BASF (Degussa) Admixtures, Inc.

armand.atienza@degussa.com

Telephone: (248) 867-2901

The polystyrene (PS) beads used for HES-ECC material has a size of 0.157 in. Having cylinder shape with sharp edges and extremely weak bond with the surrounding cement binder, these PS beads serve as crack initiators. The polystyrene beads are available from the following manufacturer under the trade name Styron™.

The Dow Chemical Company

2030 Dow Center

Midland, MI 48674

Telephone: (800) 441-4369

7.2 HES-ECC Mix Design

The HES-ECC mixture requirements are shown in Table 7.1.

Table 7.1: HES-ECC mix design

Material	Proportion	Amount (lb/yard^3)
Cement	1.0	1547.37
Sand	1.0	1547.37
Water	0.33	507.54
PVA Fiber (vol %)	0.02	44.01
Polystyrene Beads	0.064	99.09
High Range Water Reducer	0.0075	11.61
Accelerator	0.04	61.83
Hydration Stablizer	0.0046	7.02

The mixing and batching sequence and time of HES-ECC mixture should follow those specified in Table 7.2. Strength requirements for HES-ECC material are shown in Table 7.3.

Table 7.2: HES-ECC batching sequence and time

Activity	Elapsed Time including Mixing Time (min)
1. Charge all sand	2
2. Charge 3/4 amount of mixing water, all HRWR, and all hydration stabilizer	2
3. Charge all cement slowly	4
4. Charge remaining 1/4 amount of mixing water to wash drum	1
5. Charge 1/2 amount of accelerator, mix until the whole HES-ECC matrix material is homogenous	5
6. Charge PVA fibers slowly, mix until the fibers are well distributed	5
9. Charge PS beads slowly, mix untill the beads are well distributed	4
10. Charge the remaining 1/2 amount of accelerator, mix until the complete material is homogenous and ready for placement	2
Total	25

Table 7.3: Minimum requirements of HES-ECC material

Minimum Requirements of HES-ECC Material	4 hour	6 hour	24 day	28 day
Compressive Strength (psi)	2500	3000	5000	7000
Tensile Strength (Uniaxial) (psi)	400	500	600	700
Ultimate Tensile Strain Capacity (uniaxial)	2%			

Adequate workability of the HES-ECC mixture shall be verified using a standard slump cone. Workability testing should be performed on a flat Plexiglas or glass surface upon completing mixing. Upon removal of the cone, the resulting pancake of ECC material that is formed must be greater than 22 inches in average diameter and no material segregation shall be observed.

7.3 Preparation, Placement, and Cure of HES-ECC Material

The HES-ECC material can be mixed on the repair site, and placement of the material must be completed within 30 minutes after finishing mixing. Prior to the placement of the HES-ECC repair material, all concrete/HES-ECC interfaces shall be cleaned and wetted with a uniform spray application of water so that the surfaces are moist at the time of placement. Water collecting in depressions shall be blown out with clean, oil free, compressed air.

Finishing of the surface shall follow subsection 706.03M. Special care must be taken to ensure that creation of transverse surface grooves does not disturb fiber distribution on the finished surface. Light texturing with a rake can achieve this result. If this is not possible, texturing of the hardened surface must be undertaken to achieve an acceptable riding surface. The careful use of a tining rake shortly after initial setting of the HES-ECC material is allowed to produce a surface texture resulting in acceptable ride performance. When using the rake, care must be taken not to remove fibers from the top layer of HES-ECC material.

Application of curing compound and curing of the HES-ECC material shall follow section 706.03N. If necessary, the removal of the continuous wet curing system within the ECC portion of the construction is permitted after 6 hours provided that the 6 hour compressive and tensile strengths and tensile strain capacity have reached the target properties specified in section Table 7.3.

If the workability limits outlined within section 7.2 of this provision cannot be met, or due to other site circumstances, the Contractor may be allowed to use hand held vibration equipment to aid in placement and consolidation of the ECC material. Vibration should be used judiciously to promote proper consolidation and only as a final measure in guaranteeing the quality of the construction. Care must be taken during vibration to not affect proper dispersion of the fibers within the fresh composite.

7.4 Quality Assurance

Quality assurance of ECC materials will be consistent with section 701.03.G.2. In addition to standard compressive cylinders, sets of four uniaxial tensile test plates will be cast on site at identical intervals to casting of compressive cylinders. Dimensions for

uniaxial specimens are shown in Figure 7.1 and are to be cast by a concrete testing technician approved or designated by the Engineer. Tolerances for these plates are ±0.05" for all dimensions and tensile forms should be properly treated with form oil or other approved releasing agent to facilitate easy form stripping. Uniaxial tension tests are to be performed by a testing organization or research facility designated by the Engineer and is experienced and familiar with conducting uniaxial tension testing of strain hardening cementitious composites. Scheduling, completion, and reporting of all material testing is the responsibility of the Contractor. Uniaxial tension tests are to be run on a servo-hydraulic testing system under displacement control using a test speed of 0.1mil/sec. Testing of this type may be conducted at the following location. Advanced Civil Engineering Materials Research Laboratory University of Michigan

2326 George G. Brown Laboratory

2350 Hayward Street

Ann Arbor, Michigan 48109-2125

Telephone (734) 764-3368

Under the direction of Professor Victor C. Li

Other testing laboratories must be approved by the Engineer prior to testing.

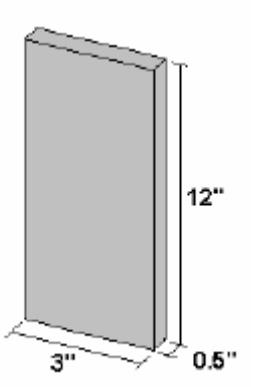

Figure 7.1: Uniaxial tensile test plate dimensions

8. HES-ECC MATERIAL COST EFFECTIVENESS

Below are estimated material cost (not including installation cost) of HES-ECC compared with various materials that have been used in repair jobs:

Portland cement concrete:	$80/cu yard
Steel fiber reinforced concrete:	$195/cu yard
High strength concrete:	$200/cu yard
Latex modified concrete	$275-$300/cu yard
Gypsum based patching material	$415/cu yard
Normal PVA-ECC:	$220/cu yard
Thoroc 10-60	$595 /cu yard
HES-ECC	$615/cu yard
Polymer concrete/mortar:	$2700/cu yard
Ductal:	$3000/cu yard

The higher cost of HES-ECC mainly comes from the large amount of fine silica sand, fibers, and accelerators used in the mixture. However, HES-ECC repair is still expected to be cost effective compared with other repair materials, from the viewpoint of service life cost, and in some cases even first cost. First cost can be assumed to include both material cost and installation cost. It may also include crack sealing cost for concrete deck repairs, which appears to be an accepted practice. The HES-ECC material cost is $615/cu yard currently, which is higher than Portland cement concrete ($80/cu yard), high strength concrete ($200/cu yard), Steel Fiber Reinforced Concrete (SFRC) ($195/cu yard), and Gypsum based patching material ($415/cu yard). However, it is similar as Thoroc 10-60, which is a very rapid-setting one-componet cement mortar, and much cheaper than many other currently used “high performance” repair material, such as Ductal ($3000/cu yard, marketed by LaFarge), and Polymer Concrete/Mortar ($2700/cu yard). It should be noted that repair material cost may only occupy a small portion of the repair first cost. Research work done by the Virginia Department of Transportation [Spinkel, 2000a, 2000b] concluded that the major cost of current repair overlay construction derives from costs associated with labor, equipment, mobilization, and traffic control. Material cost is generally less than 10% of the total repair overlay cost. In addition, the construction of the composite steel/ECC deck of a cable-stayed

bridge in Hokkaido, Japan cites the reduction of installed cost (construction speed and lower labor cost) as one reason behind the choice of ECC over other cementitious materials. Other reasons cited included durability (estimated 100 years service life) and light-weight (40% reduction compared with normal concrete with thicker section). Therefore, even though the material cost of HES-ECC is higher than concrete, high strength concrete, and SFRC, the great saving in labor and equipment cost related to decreased traffic control and congestion during shortened construction and curing time, can minimize the first cost of HES-ECC repairs.

From the service life cost point of view, HES-ECC repairs are expected to be significantly more durable, compared with other mortar or concrete type materials. As has been justified in this research project, the ductility of HES-ECC can effectively suppress repair surface cracking and repair/concrete interface delamination, resulting in a greatly prolonged repair service life compared with other repair materials which generally have brittle nature. The HES-ECC repair has also been demonstrated to have significantly longer fatigue life because of its high ductility. These expectations are at least partially supported by the experience of the durability of ECC (not HES-ECC version) placed on Curtis Road over I-14 in Ann Arbor, MI in 2002. The patch repair with a concrete material used by the MDOT maintenance crew at that time was already re-patched after 3 years, while the ECC placed at the same time remains in service today. Therefore, the great savings from reduced maintenance and future repairs, retrofits and rehabilitations should make this material very competitive economically.

A preliminary life cycle cost (LCC) analysis was conducted based on the following assumptions:

a) Deck patch repair incurs the following costs: material, chipping, traffic control and mobilization

b) Other than deck repair (e.g. pier repair) incurs the following costs: material, chipping, forming, and mobilization

c) Repair depth = 4 in; each cubic yard of material converts to 9 sq yd patch area, or 81 sq ft patch area.

d) Discount factor I=3%

e) All numbers below are based on MDOT document http://www.michigan.gov/documents/MDOT_14aCSM_Workbook05_126884_7.xls

Materials:

Concrete patch material cost = $115/cyd (concrete material) + $685/cyd (repair premium charge) = $800/cyd

HES-ECC patch material cost = $615/cyd (HES-ECC material) + $685 /cyd (repair premium charge) = $1300/cyd

Chipping:

Deck: $125/syd = $1125/cyd (for 4inch-deep repair)

Pier: $65/cft = $1755/cyd (for 4inch-deep repair)

Forming:

$28/sft = $2268/cyd (for 4 inch-deep repair)

Traffic control:

Assuming traffic control related cost is $3000/day; patch repair typically use 2 days, therefore, traffic control related cost = $6000

Mobilization:

5% of all other cost

Based on the assumptions a) – e), we can do the following calculations:

i) Deck patch repair cost per cubic yard:

Normal concrete patch repair:

$800/cyd (material) + $1125/cyd (chipping) + $6000/cyd (traffic) + 396/cyd (mobilization) = $8320/cyd

HES-ECC patch repair:

$1300/cyd (material) + $1125/cyd (chipping) + $6000/cyd (traffic) + $421/cyd (mobilization) = $8846/cyd

ii) Other than deck patch repair cost per cubic yard:

Normal concrete patch repair:

$800/cyd (material) + $1755/cyd (chipping) + $2268/cyd (forming) + $241/cyd (mobilization) = $5064/cyd

HES-ECC patch repair:

$1300/cyd (material) + $1755/cyd (chipping) + $2268/cyd (forming) + $266/cyd (mobilization) = $5589/cyd

The question to be discussed here is: Assuming the life of a normal concrete patch is 3 or 10 years, how long must HES-ECC patch last for its life cycle cost to equal to that of normal concrete patch?

i) Deck patch repair

(a) Normal concrete patch life = 3 years

Assuming the present value of LCC of a normal concrete deck patch with life of 3 years equals to the present value of LCC of a HES-ECC deck patch with life of x years:

$$\$8320 + \frac{\$8320}{(1+3\%)^3} + \frac{\$8320}{(1+3\%)^6} + \frac{\$8320}{(1+3\%)^9} + \frac{\$8320}{(1+3\%)^{12}} + \frac{\$8320}{(1+3\%)^{15}} + ...$$

$$= \$8846 + \frac{\$8846}{(1+3\%)^x} + \frac{\$8846}{(1+3\%)^{2x}} + \frac{\$8846}{(1+3\%)^{3x}} + \frac{\$8846}{(1+3\%)^{4x}} + \frac{\$8846}{(1+3\%)^{5x}} + ...$$

By solving this equation we get x = 3.2 years

Therefore, the HES-ECC deck patch must last at least 3.2 years for its LCC to equal or be less than that of a normal concrete deck patch with life of 3 years.

(b) Normal concrete patch life = 10 years

Assuming the present value of LCC of a normal concrete deck patch with life of 10 years equals to the present value of LCC of a HES-ECC deck patch with life of y years:

$$\$8320 + \frac{\$8320}{(1+3\%)^{10}} + \frac{\$8320}{(1+3\%)^{20}} + \frac{\$8320}{(1+3\%)^{30}} + \frac{\$8320}{(1+3\%)^{40}} + \frac{\$8320}{(1+3\%)^{50}} + ...$$

$$= \$8846 + \frac{\$8846}{(1+3\%)^y} + \frac{\$8846}{(1+3\%)^{2y}} + \frac{\$8846}{(1+3\%)^{3y}} + \frac{\$8846}{(1+3\%)^{4y}} + \frac{\$8846}{(1+3\%)^{5y}} + ...$$

By solving this equation we get y = 10.5 years

Therefore, the HES-ECC deck patch must last at least 10.5 years for its LCC to equal or be less than that of a normal concrete deck patch with life of 10 years.

ii) Non-deck patch repair

(a) Normal concrete patch life = 3 years

Assuming the present value of LCC of a normal concrete non-deck patch with life of 3 years equals to the present value of LCC of a HES-ECC non-deck patch with life of x years:

$$\$5064 + \frac{\$5064}{(1+3\%)^3} + \frac{\$5064}{(1+3\%)^6} + \frac{\$5064}{(1+3\%)^9} + \frac{\$5064}{(1+3\%)^{12}} + \frac{\$5064}{(1+3\%)^{15}} + ...$$

$$= \$5589 + \frac{\$5589}{(1+3\%)^x} + \frac{\$5589}{(1+3\%)^{2x}} + \frac{\$5589}{(1+3\%)^{3x}} + \frac{\$5589}{(1+3\%)^{4x}} + \frac{\$5589}{(1+3\%)^{5x}} + ...$$

By solving this equation we get y = 3.3 years

Therefore, the HES-ECC non-deck patch must last at least 3.3 years for its LCC to equal or be less than that of a normal concrete non-deck patch with life of 3 years.

(b) Normal concrete patch life = 10 years

Assuming the present value of LCC of a normal concrete non-deck patch with life of 10 years equals to the present value of LCC of a HES-ECC non-deck patch with life of y years:

$$\$5064 + \frac{\$5064}{(1+3\%)^{10}} + \frac{\$5064}{(1+3\%)^{20}} + \frac{\$5064}{(1+3\%)^{30}} + \frac{\$5064}{(1+3\%)^{40}} + \frac{\$5064}{(1+3\%)^{50}} + ...$$

$$= \$5589 + \frac{\$5589}{(1+3\%)^y} + \frac{\$5589}{(1+3\%)^{2y}} + \frac{\$5589}{(1+3\%)^{3y}} + \frac{\$5589}{(1+3\%)^{4y}} + \frac{\$5589}{(1+3\%)^{5y}} + ...$$

By solving this equation we get y = 10.9 years

Therefore, the HES-ECC non-deck patch must last at least 10.5 years for its LCC to equal or be less than that of a normal concrete non-deck patch with life of 10 years.

The Thoroc 10-60 Rapid Mortar is a patch repair material MDOT has been using. It is a very rapid-setting cement mortar containing crystalline silica, Portland cement, hydraulic cement and lithium carbonate. During the HES-ECC patch repair demonstration project (Section 9), patch repairs made of Thoroc 10-60 and HES-ECC were poured side by side to compare their early-age and long-term performance. The material cost of Thoroc 10-60 is $595 /cu yard, which is similar as the $615/cu yard material cost for HES-ECC. Assuming the installation costs for HES-ECC and Thoroc 10-60 are the same, the preliminary LCC analysis show that both the Thoroc 10-60 patch and the HES-ECC patch must last at least 3.2 years (deck patch) or 3.3 years (non-deck patch) for their LCC to equal or be less than that of a normal concrete patch with life of 3

years; both the Thoroc 10-60 patch and the HES-ECC patch must last at least 10.5 years (deck patch) or 10.9 (non-deck patch) for its LCC to equal or be less than that of a normal concrete patch with life of 10 years.

The above LCC calculations suggest that from an economics point of view, the use of HES-ECC is preferable to other repair materials if the repair service life can be extended by about 10%. The experimental findings detailed in this report, however, indicate that service life of patch repair can be enhanced substantially above 10%. Thus the application of HES-ECC is fully justified. This conclusion results from the fact that while HES-ECC is more expensive than normal repair concrete, material cost occupies only a fraction of the total cost when chipping, forming, traffic control and mobilization costs are accounted for.

9. HES-ECC PATCH REPAIR DEMONSTRATION

Construction of patch repair on the Ellsworth Road Bridge over US-23 (S07 of 81074) began at 9am on Tuesday, November 28, 2006 with placement of traffic control devices. Photographs of the construction process are shown in Figures 9.1 – 9.14 below. The MDOT repair personnel conducted partial depth concrete removal, sandblasted the patch area, replaced damaged reinforcement, and completed patch preparation. Before pouring the patch material, water fog was sprayed onto the concrete substrate to enhance repair bonding.

HES-ECC mixing materials were pre-batched in the laboratory for easy field processing, and were transported to the repair site. A 7-cubic foot HES-ECC batch was mixed by the research personnel using a 12-cubic foot capacity concrete gas mixer provided by MDOT (Figure 9.8). The mixing time lasted around 30 minutes. The mixed HES-ECC exhibited desirable creamy viscosity, good fiber distribution and good flowability (Figure 9.11). Flowability test using a slump cone was conducted right after finishing the mixing. The 25.6" slump diameter indicated that the mixed HES-ECC had self-compacting property (Figure 9.11). The HES-ECC material was then poured into a wheelbarrow, transported to the patch area, and poured into the patch. The self-compacting property of HES-ECC allowed itself to easily flow into the corners of the patch area without any vibration. The surface of the HES-ECC patch was finished by hand using steel trowel.

The Thoroc 10-60 Rapid Mortar is a patch repair material MDOT has been using. It is a very rapid-setting cement mortar containing crystalline silica, Portland cement, hydraulic cement and lithium carbonate. Mixing of Thoroc 10-60 was performed using the same mixer as HES-ECC. It can be seen from Figure 9.12 that the flowability of Thoroc 10-60 was not high as HES-ECC, and therefore its placement and finishing involved more effort. The patch repairs using both HES-ECC and Thoroc 10-60 were placed side by side, as shown in Figure 9.13. Latex-based curing compound was sprayed onto both patches to reduce evaporation and shrinkage.

The patch repair on the Ellsworth Road Bridge was completed at around 1pm on Tuesday, November 28, 2006, as shown in Figure 9.14. Traffic reopened at 9am on Wednesday, November 29, 2006.

Figure 9.1: Ellsworth Road Bridge over US-23 (S07 of 81074)

Figure 9.2: Bridge deck cracking

Figure 9.3: Partial depth removal

Figure 9.4: Sandblasting of patch area

Figure 9.5: Replacement of damaged reinforcement

Figure 9.6: Completed patch repair preparation

Figure 9.7: Separated patch areas for HES-ECC repair and Thoroc 10-60 repair

Figure 9.8: 12-Cubic-Foot Capacity Gas Mixer

Figure 9.9: Pouring HES-ECC into wheelbarrow for transporation

Figure 9.10: HES-ECC was poured into patch

Figure 9.11: HES-ECC show self-compacting property

(Flowability test slump diameter = 25.6")

Figure 9.12: Placement of Thoroc 10-60

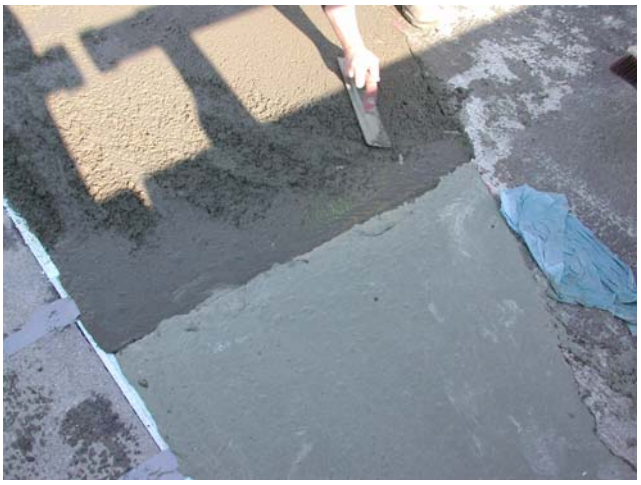

Figure 9.13: Comparison of HES-ECC patch repair and Thoroc 10-60 patch repair

Figure 9.14: Completed patch repair work

10. CONCLUSIONS

Within this project, a newer version of ECC, High Early Strength ECC (HES-ECC) has been successfully developed under the guidance of micromechanical models. The material design began from matrix screening for strength requirements, and the initially selected mixing proportion was further tailored to achieve the target tensile strain capacity.

After HES-ECC was developed, extensive experimental work was conducted to document the developed HES-ECC material tensile, compressive, flexural, free shrinkage and restrained shrinkage properties at different ages. The developed HES-ECC can achieve high early compressive strength more than 3000 psi and modulus of rupture (MOR) more than 1400 psi at age of 4h. Furthermore, HES-ECC is a very ductile material with tensile strain capacity averaging 3.5% at both early and late ages. This material exhibits significant strain hardening behavior under tensile loading and deformation hardening behavior under flexural loading. The high tensile strain capacity and low values of Young's modulus of HES-ECC enable the material to deform compatibly with concrete substrate structure when used as a repair material. Drying shrinkage deformation of HES-ECC is high due to the very high cement content and lack of coarse aggregates in its mix. However, under restrained drying shrinkage, HES-ECC can develop multiple micro-cracks with average crack width as low as 1.97×10^{-3} in. The high early age and late age compressive/flexural strength, high tensile strain capacity, low Young's Modulus as well as tight width of its multiple micro-cracks suggest HES-ECC material as a durable material for concrete structure repair applications.

HES-ECC is a specialized version of ECC material designed based on micromechanical models and Integrated Structures and Materials Design Approach (ISMD) (Li & Fisher, 2002). Different from ECC M45, HES-ECC features high early strength properties besides tensile ductility. The high early strength was achieved by using Portland cement type III instead of Portland cement type I, adding accelerator, and eliminating fly ash from the HES-ECC mix. Meanwhile, introduction of artificial flaws (PS beads) into the HES-ECC mix enables the material to retain its high tensile strain capacity after alteration of matrix and fiber/matrix interface properties. Furthermore, the free shrinkage deformation of HES-ECC is higher than ECC M45 because of the

absence of fly ash and therefore even higher cement content in its mix. However, similar as ECC M45, the high tensile strain capacity of HES-ECC and tight crack width during strain hardening stage make the material exhibit sound performance under restrained drying shrinkage conditions.

Besides HES-ECC material properties, research was also carried out to verify the durability of a layered repair system with the fresh HES-ECC repair material bonded to the old concrete substrate. The interaction between the repair material and the old concrete when subjected to environmental and mechanical loading was investigated.

When subject to restrained drying shrinkage, the high ductility of the HES-ECC repair layer could accommodate the shrinkage deformation by forming multiple micro-cracks with tight crack width. By this means, tensile and shear stresses at the interface was released, so that both repair cracking and interface delamination could be suppressed. For the traditional HES-Concrete repair, several localized cracks normally formed in the repair layer with large crack width. For the HES-SFRC repair, still several localized cracks formed, but the cracks were bridged by steel fibers. Since the cracks could not open freely to accommodate the repair layer's shrinkage deformation, the interface delamination was much larger than HES-Concrete and HES-ECC repairs.

When subject to monotonic loading, the HES-ECC layered repair system exhibited 100% increased load carrying capacity, and 10 times the deformation capacity of HES-Concrete layered repair system. Instead of forming one single crack in the HES-Concrete repair layer, the initial interfacial crack would kink into the HES-ECC repair layer, and then trapped there without reflected to the repair surface. Upon additional loading, delamination resumes at the interface. The unique kink-trap-cracking behavior repeated itself with increasing flexural loading till the flexural strength of HES-ECC was exhausted. In this way, repair spalling was successfully suppressed by using HES-ECC.

When under the same level of fatigue loading, HES-ECC layered repair system showed significantly longer service life than HES-Concrete layered repair system. The interface properties did not exhibit an effect on the cycles experienced before failure. Like the monotonic flexural test, the deformation capacity of the HES-ECC layered repair system was much larger than the HES-Concrete layered repair system, and the

maximum deflection before failure was bigger when the interface was smooth. There was no evident difference on the layered repair specimen's cracking pattern under the monotonic and the fatigue loading conditions.

The above experimental results suggest that HES-ECC can be a very durable repair material with prolonged service life, no matter under environmental loading or mechanical loading. The common failure modes such as large surface cracking, spalling and interface delamination can be successfully suppressed by the uniquely large tensile strain capacity of HES-ECC material.

Workability of HES-ECC was evaluated with larger batching sizes. Gravity mixers were used to process HES-ECC with batch sizes of 1, 3 and 6 cubic feet. These batch sizes are chosen for repair operations of limited dimensions such as those used on the Curtis Road Bridge in October, 2002. Prior to the larger scale batching, preliminary tests in laboratory were carried out to improve flowability and workability of the material. The 0.5" long PVA fiber used previously in HES-ECC was changed to 0.33" long PVA fiber to promote easy mixing and better fiber distribution in gravity mixer, and improve flowability of the material. Effect of hydration stabilizer on the flowability, initial setting time, and hardened mechanical properties of HES-ECC was evaluated. Batching sequence of this material was also optimized to facilitate mixing based on larger scale gravity mixers.

Based on the 1, 3 and 6 cubic feet batching experiments, it was concluded that larger scale mixing of HES-ECC material approaching those in field conditions was applicable. Using the batching sequence described in section 6.2.1, the overall mixing of HES-ECC material can proceed very smoothly and result in a fresh material which is homogeneous, flowable, and rheologically stable. Testing of hardened mechanical properties of HES-ECC processed in 1, 3 and 6 cubic feet larger scale batching, showed that the early age and late age compressive strength and tensile strain capacity were similar to those mixes made in a laboratory size Hobart mixer, and continued to meet all of the targets set forth when developing this material.

The final mix design, which satisfies all requirements including batching, is given in Table 6.2. The recommended mix procedure is summarized in Table 6.3. The construction specification and quality control of HES-ECC material are identified in

section 7. The estimated material cost and cost effectiveness of HES-ECC are discussed in section 8.

Overall, this project successfully developed a high early strength engineered cementitious composite (HES-ECC), which features high early strength, high late age strength, high ductility, high material durability, significantly improved repair system durability, and can be easily mixed in large scale on repair construction site using traditional concrete gravity mixers. This HES-ECC material can be suitable for a wide range of concrete repair applications in transportation infrastructures with significantly shortened down time, while greatly improving durability and reducing future maintenance requirements.

11. REFERENCES

ACI Committee 212 (2001), "Admixtures for Concrete (ACI 212.3R-91)", ACI Manual of Concrete Practice, Part 1, American Concrete Institute, Detroit, MI

Ahlborn, T. M., Kasper, J. M., Altan, H., Koyuncu, Y., and Rutyna, J. (2002), "Causes and Cures for Prestressed Concrete I-Beam End Deterioration", MDOT report, August 2002

American **S**ociety for **T**esting and **M**aterials (U.S. Code Organization)

American Concrete Institute, Building Code Requirements for Structural Concrete (ACI 318-02) and Commentary (ACI 318R-02), American Concrete Institute. Farmington Hills, MI. 2002

Baraguru, P. D., and Bhatt, D., "Rapid Hardening Concrete", Report No. FHWA NJ 2001-3, New Jersey Department of Transportation, Trenton, New Jersey, 22 pages, 2000

Collepardi, M., "Water Rducers/Retarders", in Concrete Admixtures Handbook, ed. V. S. Ramachandran, Noyes Publications, Park Ridge, NJ, pp. 116-210, 1984

Concrete Construction (2001), "Paving Repair Finds a Four-hour Champion," Vol. 46, No. 12, pp. 69-70, 2001

Edmeades, R. M. and Hewlett, P. C., "Cement Admixtures", Lea's Chemistry of Cement and Concrete, 4th ed., ed. P. C. Hewlett, Arnold, London, pp. 837-902, 1998

mmons, P. H., "Concrete Repair and Maintenance Illustrated", American Society for Testing and Materials (U.S. Code Organization), pp. 155-164, 1994

Federal Highway Administration (FHWA), Manual of Practice: Materials and Procedures for Rapid Repair of Partial-Depth Spalls in Concrete Pavements, Federal Highway Administration (FHWA), 135 pages, 1999

Fischer, G., and Li, V. C., "Effect Of Matrix Ductility On Deformation Behavior Of Steel Reinforced ECC Flexural Members Under Reversed Cyclic Loading Conditions", ACI Structural Journal, Vol. 99, No. 6, pp. 781-790, 2002.

Hewlett, P. C., and Young, J. F., "Physico-chemical Interactions between Chemical Admixtures and Portland Cement", Journal of Materials Education, Vol. 9, No. 4, pp. 389-433, 1989

Kanda, T. and V.C. Li, "Effect of Apparent Fiber Strength and Fiber-Matrix Interface on Crack Bridging in Cement Composites," ASCE J. of Engineering Mechanics, Vol. 125, No. 3, pp. 290-299, 1999.

Kanda, T., and Li, V. C., “Interface Property and Apparent Strength of a High Strength Hydrophilic Fiber in Cement Matrix”, ASCE J. Materials in Civil Engineering, Vol. 10, No. 1, pp. 5-13, 1998

Kabele, P., “Assessment of Structural Performance of Engineered Cementitious Composites by Computer Simulation”, CTU Report 4, V.5, Czech Technical University, Prague, 2001

Kamada, T. and Li, V. C., "The Effects of Surface Preparation on the Fracture Behavior of ECC/Concrete Repair System," J. of Cement and Concrete Composites, Vol. 22, No. 6, pp.423-431, 2000.

Knofel, D., and Wang, J. F., “Properties of Three Newly Developed Quick Cements”, Cement and Concrete Research, Vol. 24, No. 5, pp. 801-812, 1994

Kong, J.H., Bike, S. and Li, V.C., “Development of a Self-Consolidating Engineered Cementitious Composite Employing Electrosteric Dispersion/Stabilization,” Journal of Cement and Concrete Composites, Vol. 25, No.3, pp. 301-309, 2003

Kriviak, G. W., Skeet, J. A., and Carter, P. D., “Service Life Prediction of Protective Systems for Concrete Bridge Decks in Alberta,” International Association of Bridges and Structural Engineers Symposium, San Francisco, Calif., pp. 469-474, 1995.

Kurtz, S., Blaguru, P., Consolazio, G., and Maher, A., “Fast Track Concrete for Construction Repair”, Report No. FHWA 2001-015, New Jersey Department of Transportation, Trenton, New Jersey, 67 pages, 1997

Leung, C. K. Y., and Li, V. C. (1990). ‘‘Strength-based and fracture based approaches in the analysis of fibre debonding.’’ J. Mat. Sci. Letter, 9, 1140–1142.

Li, V. C., “Engineered Cementitous Composties (ECC) – Tailored Composites Through Micromechanical Modeling”, Fiber Reinforced Concrete: Present and the Future, Eds: N. Banthia, A. Bentur, and A. Mufti, Canadian Society of Civil Engineers, pp. 64-97, 1990

Li, V. C., “High Performance Fiber Reinforced Cementitious Composites as Durable Material for Concrete Structure Repair”, Int’l J. for Restoration of Buildings and Monuments, Vol. 10, No 2, 163–180, 2004

Li, V. C., and Fischer, G., “Reinforced ECC - An Evolution from Materials to Structures”, Proceedings of the First FIB Congress, Osaka, Japan, pp.105-122, Oct. 2002.

Li, V. C., “Performance Driven Design of Fiber Reinforced Cementitious Composites”, in Proceeding of 4th RILEM International Symposium on Fiber Reinforced Concrete, Ed. R. N. Swamy, pp. 12-30, Chapman and Hall, 1992

Li, V. C., and Leung, C. K. Y., "Theory of Steady State and Multiple Cracking of Random Discontinuous Fiber Reinforced Brittle Matrix Composites", ASCE Journal of Engineering Mechanics, Vol.118, No.11, pp. 2246-2264, 1992

Li, V. C., Lepech, M. and Li, M., "Final Report on Field Demonstration of Durable Link Slab for Jointless Bridge Decks Based on Strain-Hardening Cementitious Composites," submitted to Michigan Department of Transportation, 2005

Li, V. C., and Stang, H. (1997). ''Interface property characterization and strengthening mechanisms in fiber reinforced cement based composites.'' J. Advanced Cement Based Mat., 6(1), 1–20.

Li, V. C., and Wu, H. C., "Conditions for Pseudo Strain Hardening in Fiber Reinforced Brittle Matrix Composites", Journal of Applied Mechanics Review, Vol.45, No.8, pp. 390-398, 1992

Li, V. C., "High Performance Fiber Reinforced Cementitious Composites as Durable Material for Concrete Structure Repair," Int'l J. for Restoration of Buildings and Monuments, Vol. 10, No 2, pp 163–180, 2004

Lin, Z., Kanda, T., Li, V. C., "On Interface Property Characterization and Performance of Fiber-reinforced Cementitious Composites", Journal of Concrete Science and Engineering, RILEM, No.1, pp. 173-184, 1999

Lin, Z., and Li, V. C. (1997). ''Crack bridging in fiber reinforced cementitious composites with slip-hardening interfaces.'' J. Mech. Phys. Solids, 45(5), 763–787.

Lim, Y. M. and Li, V. C., "Durable Repair of Aged Infrastructures Using Trapping Mechanism of Engineered Cementitious Composites," J. Cement and Concrete Composites, Vol. 19, No. 4, pp. 373-385, 1997.

Lim, Y. M., and Li, V. C., "Characterization of Interface Fracture Behavior in Repaired Concrete Infrastructures", in Fracture Mechanics of Concrete Structures Proceedings FRAMCOS-3, AEDIFICATIO Publishers, D-79014 Freiburg, Germany, pp. 1817-1828, 1998

Malhotra, V. M., Berry, E. E., and Wheat, T. A., "Superplasticizers in Concrete", Proceedings of International Symposium, Ottawa, 1988 (2 vols.), CANMET, Department of Energy, Mines and Resources, Ottawa, Canada, also published in part as ACI SP-62, American Concrete Institute, Detroit, MI, 1989.

Marshall, D. B., Cox, B. N., "A J-integral Method for Calculating Steady-state Matrix Cracking Stresses in Composites", Mechanics of Materials, No.8, pp. 127-133, 1988

Mather, B., and Warner, J., "Why do Concrete Repairs Fail", Interview held at Univ. of Wisconsin, Dept. of Engineering Professional Development, MD, WI, ,http://aec.engr.wisc.edu/resources/rsrc07.html>, accessed, Dec., 2003

Michigan Department of Transportation (MDOT) (2003), “Qualification Procedure For Prepackaged Hydraulic Fast-Set Materials for Patching Structural Concrete”, MDOT Quality Assurance and Quality Control (QA/QC)

Mindess, S., Young, J. F., and Darwin, D. (2003), Concrete 2nd Ed.

Neville, A. M., and Brooks, J. J., Concrete Technology, Longman Scientific and Technical, 438 pages, 1987

Nmai, C. K., Schlagbaum, T., and Violetta, B., “A History of Mid-Range Water Reducing Admixtures”, Concrete International, Vol. 20, No.4, pp. 45-50, 1998

Parker, F., and Shoemaker, M. L., “PCC Pavement Patching Materials and Procedures”, ASCE Journal or Materials in Civil Engineeringg, Vol. 3, No.1, pp. 29-47, 1991

Ramachandran, V. S., Concrete Admixtures handbook, Noyes Publications, Park Ridge, NJ, 1984

Ramachandran, V. S., Calcium Chloride in Concrete Science and Technology, Applied Science Publishers, London, 1986

Ramachandran, V. S., Malhotra, V. M., Jolicoeur, C. and Spriato, N., Superplasticizer: Properties and Applications in Concrete. Publ. No. MTL-14 (TR), CANMET National Resources Canada, Ottawa, Canada, 1998

Rear, K., and Chin, D., “Non-Chloride, Accelerating Admixtures for Early Compressive Stength”, Concrete International, Vol. 12, No.10, pp. 55-58, 1990

Redon, C., V.C. Li, C. Wu, H. Hoshiro, T. Saito, and A. Ogawa, "Measuring and Modifying Interface Properties of PVA Fibers in ECC Matrix," ASCE J. Materials in Civil Engineering, Vol. 13, No. 6, Nov./Dec., 2001, pp399-406.

Rixom, M. R., and Mailvaganam, N. P., Chemical Admixtures for Concrete, 2d ed., E & FN Spon, London, 1986

Seehra, S.S., Gupta, S., Kumar, S., “Rapid Setting Magnesium Phosphate Cement for Quick Repair of Concrete Pavements – Characterization and Durability Aspects”, Cement and Concrete Research, Vol. 23, No. 2, pp. 254-266, 1993

Smith, K. L., Peshkin, D.G., Rmeili, E. H., Dam, T. V., Smith, K. D., Darter, M. I., “Innovative materials and Equipment for Pavement Surface Repairs”, Strategic Highway Research Program (SHRP), National Highway research Council, Washington D.C. 205 pages, 1991

Soroushian, P. and Ravanbakhsh, S., "High-early-strength concrete: Mixture proportioning with processed cellulose fibers for durability", ACI Materials Journal, Vol. 96, No. 5, pp. 593-599, 1999

Sprinkel, M. M., "Very-Early-Strength latex-modified Concrete Overlay", Report No. VTRC99-TAR3, Virginia Department of Transportation, Richmond, Virginia, 11 pages, 1998

Sprinkel, M., "Evaluation of Latex-Modified and Silica Concrete Overlays Placed on Six Bridges in Virginia", Virginia DOT Final Report, 2000.

Sprinkel, M., "Evaluation of High Performance Concrete Overlays Placed on Route 60 Over Lynnhaven Inlet in Virginia", Virginia DOT Final Report, 2000.

Stang, H., "Scale Effects in FRC and HPRFCC Structural Elements," in High Performance Fiber Reinforced Cementitious Composites, RILEM Proceedings Pro 30, Eds. Naaman, A.E. and Reinhardt, H.W., pp. 245-258, 2003

Stingley, W. M., NCHRP Synthesis of Highway Practice No. 45: Rapid Setting Materials for Patching of Concrete, National Cooperative Highway research Program (NCHRP), Transportation Research Board, Washington D.C. 13 pages, 1977

Vaysburd, A. M., Brown, C. D., Bissonnette, B, and Emmons, P. H., ""Realcrete" versus "Labcrete"", Concrete International, Vol. 26 No.2, pp 90-94, 2004

Wang, K., Jansen, D. C. and Shah, S. P., "Permeability Study of Cracked Concrete", Cement and Concrete Research, 27, 3, pp. 381-393, 1997

Wang, S. and Li, V. C., "Tailoring of Pre-existing Flaws in ECC Matrix for Saturated Strain Hardening," Proceedings of FRAMCOS-5, Vail, Colorado, U S A, April 2004, pp. 1005-1012, 2004

Weimann, M. B. and Li, V. C., "Hygral Behavior of Engineered Cementitious Composites (ECC)", International Journal for Restoration of Buildings and Monuments,Vol. 9, No 5, pp513-534, 2003

Whiting, D., and Nagi, M., "Strength and Durability of Rapid Highway Repair Concretes", Concrete International, Vol. 16, No.9, pp. 36-41, 1994

Wittmann, F. H., and Martinola, G., "Decisive Properties of Durable Cement-Based Coatings for Reinforced Concrete Structures," International Journal for Restoration of Buildings and Monuments, Vol. 9, No 3, pp 235-264, 2003.

Zhang, J., Fatigue fracture of fiber reinforced concrete—an experimental and theoretical study. PhD thesis, Department of Structural Engineering and Materials, Technical University of Denmark, Serie R, 41, 1998.

Zhang, J., Stang, H., Li, V. C., Fatigue life prediction of fibre reinforced concrete under flexure load, Int. J. Fatigue 21 (10), 1999

Zhang J., Li, V.C., "Monotonic and Fatigue Performance in Bending of Fiber Reinforced Engineered Cementitious Composite in Overlay System ," J. of Cement and Concrete Research, Vol. 32, No.3, pp. 415-423, 2002

Zia, P., Leming, M. L., and Ahmad, S. H., “High Performance Concretes, a State-of-the-Art Report”, Report No. SHRP-C/FR-91-103, Strategic Highway Research Program, National Research Program, Washington, DC